AN ABSTRACT OF THE DISSERTATION OF

Defne Çakın for the degree of Doctor of Philosophy in Chemistry presented on January 9, 2008.

Title: Design, Characterization, and Application of Spectrometers for Determination of Low-Level Dissolved Oxygen with Small-Volume Sampling Methodology

Abstract approved: _____
James D. Ingle, Jr.

New analytical methods and instrumentation were developed for the determination of dissolved oxygen (DO) at low concentrations in water. The methods were based on monitoring the absorbance increase due to the oxidation of reduced indigo carmine (IC) by oxygen in the sample in different types of spectrometer cells. Spectrophotometer cells included a 1.2-cm vial cell and liquid core waveguide (LCW) cells with path lengths from 20 to 100 cm. The LCW based spectrophotometer consisted of a miniature peristaltic pump, a multi-port reactor, and a LCW cell (24-cm, Teflon-AF tubing) which were connected together in a flow loop and enclosed in a unique housing filled with a reductant solution. This configuration allows double containment of the components and purging of the solutions to reduce the oxygen contamination. Unique sampling methodology based on syringes or a unique micro-pump sampler and on double-septum caps enabled transferring of small-volume samples (1 mL or less) from septum-sealed bottles into

the spectrometer cells containing IC with minimal atmospheric contamination. The new methodology was applied for the determination of low DO concentrations in prepared standards and anaerobic cultures under Fe(III)-reducing, sulfate-reducing and methanogenic conditions. A detection limit of 0.03 mg/L (1 μM) DO for a 0.5-mL sample was achieved with the 1.2-cm vial and N_2 purging of the headspace in the cell. The novel use of H_2 purging of the solution circulating through the LCW cell for continual reduction of IC with a Pt catalyst was demonstrated. This purging made it possible to negate the effects of oxygen diffusing into the reagent and oxidizing IC, to keep the absorbance on scale with the long pathlength, and to achieve a DL for DO of 0.03 mg/L with a 0.1-mL sample volume.

Design, Characterization, and Application of Spectrometers for Determination of Low-Level Dissolved Oxygen with Small-Volume Sampling Methodology

by
Defne Çakın

A DISSERTATION

submitted to

Oregon State University

in partial fulfillment of
the requirements for the
degree of

Doctor of Philosophy

Presented January 9, 2008
Commencement June 2008

Doctor of Philosophy dissertation of Defne Çakın presented on January 9, 2008

APPROVED:

Major Professor, representing Chemistry

Chair of the Department of Chemistry

Dean of the Graduate School

I understand that my dissertation will become part of the permanent collection of Oregon State University libraries. My signature below authorizes release of my dissertation to any reader upon request.

Defne Çakın, Author

ACKNOWLEDGEMENTS

I would like to thank James Ingle for his mentorship throughout my career at Oregon State University. I greatly appreciate his wisdom, experience, and most of all his effort in my scientific and personal education.

I would also like to acknowledge:

Göksel Akçin who introduced me to research in chemistry and encouraged me to pursue higher education in science,

US Environmental Protection Agency for providing financial support,

My committee members, Vincent Remcho, Staci Simonich, Michael Lerner, and Fredrick Prahl for their guidance and interest,

Peter Ruiz Haas for his helpful discussions and technical assistance,

Ted Hinke and Joe Magner without whose expertise the construction of the instrumentation would not have been possible,

Fellow graduate students and friends overseas for their moral support,

My family and Corey Koch for their encouragement, patience, and understanding.

CONTRIBUTION OF AUTHORS

James D. Ingle has provided major assistance in editing this dissertation.

TABLE OF CONTENTS

TABLE OF CONTENTS (Continued)

Page

TABLE OF CONTENTS (Continued)

Page

LIST OF FIGURES

LIST OF FIGURES (Continued)

LIST OF FIGURES (Continued)

LIST OF TABLES

LIST OF APPENDICES

LIST OF APPENDICES

LIST OF APPENDIX FIGURES

LIST OF APPENDIX TABLES

CHAPTER 1:

Introduction

Measurement of dissolved oxygen (DO) has been, and will continue to be, of great interest in science. Oxygen is significant because it is involved in numerous processes in the environment and it is the most abundant chemically and biologically active, strong oxidant (Stumm and Morgan, 1981). The abundance and oxidant properties of oxygen are also responsible for the challenges of quantification of dissolved oxygen, particularly at low levels.

On a global scale, O_2 is produced via photosynthesis and it cycles back to the atmosphere after consumption by various pathways. The atmosphere contains 21% oxygen and the DO concentration in air-saturated water is 8 mg/L (at 25 ºC and with no salinity). In equilibrium models, the oxygen-water couple appears to dominate the redox level relative to other less abundant redox couples and thus, the redox level of the sea (Stumm and Morgan, 1981). When consumption and production of oxygen is not in balance, oxygen concentrations in a particular environmental compartment may vary to the extreme. For example, in the absence of photosynthesis or sunlight, the DO concentration can become limited due to the respiration of microorganisms and the slow transport of oxygen. When O_2 is depleted in the sub-surface by processes such as microbial reduction, aquatic or aquifer systems can become sub-oxic or anoxic (Chapelle, 2001).

Anaerobic microorganisms play an important role in bioremediation of halogenated organic pollutants in ground water systems primarily because, unlike aerobic organisms, they are able to attack carbon-halogen bonds (Ritmann et al., 2001). Molecular oxygen is toxic to all obligate anaerobes. Thus, anaerobic

biodegradation rates and pathways of organic compounds are known to depend strongly on environmental conditions such as DO concentration (Chapelle, 2001). However, the measurement of DO at low levels (below 1 mg/L DO) is a challenging task in the field and laboratory, particularly for studies with laboratory-scale bioreactors, columns and microcosms. With any DO measurement technique, keeping the analytical device (the parts that are in contact with the sample), the reagents for some of the methods, and the sample free of contamination from atmospheric oxygen is the key to a reliable DO quantitation. In this thesis, issues regarding contamination were evaluated extensively for each instrument built and specific methodology such as sampling procedures.

In chapter 2, conventional methods for the determination of DO are reviewed. The primary focus is on environmental applications with aqueous samples although some methods had been used interchangeably in bioanalytical and medicinal studies. Winkler titrations, and its modifications, have been favored in environmental DO applications (ASTM, 2004). Electrochemical sensors such as membrane-covered, amperometric and polarographic DO probes (Clark-type electrodes) are highly robust, portable, and widely used in environmental monitoring and in bio-analytical studies. Luminescent oxygen sensors have been introduced more recently and are frequently used in the food packaging industry, bio-medical research, and recently for environmental monitoring. Determination of DO with redox indicators is another widely used approach which includes the standard method for low level DO

measurements (ASTM, 2005). Advantages and disadvantages of the standard methods are discussed including the typical detection limits, accuracy and precision.

Many of the standard methods for low-level DO measurements (i.e., in boilers and ground water) rely on continuous flow of the sample through the sampling cell or chamber to purge out the residual oxygen to minimize O_2 contamination. This is achieved with large volumes (more than 300 mL) of the sample. Hence, methods that require this purging approach are not applicable for closed systems with a limited volume of sample such as anaerobic microcosms and packed columns.

In Chapter 3, the design and application of a portable flow sampler and analysis system to determine DO at low levels with small sample volumes (1 mL or less) are presented. This method based on oxidation of reduced indigo carmine (IC). The absorbance of IC was monitored with miniature spectrophotometers. The primary goal was to design and build an instrument that can be used to sample different experimental systems such as septum bottles, bioreactors, columns, and ground water sampling pumps. Unique double-septum caps were developed to minimize the O_2 contamination of samples, standards and reduced indicator solutions. Sample introduction was performed with two different devices: a gas-tight syringe, and a micro pump that was directly connected to the sample with tubing and controlled via laptop computer with a microcontroller module.

Calibration data were obtained with different sample volumes. Low DO samples and anaerobic cultures under Fe(III)-reducing, sulfate-reducing and

methanogenic conditions were sampled and analyzed for DO to evaluate the reliability of the analytical method and the ability to sample an enclosed anaerobic culture with minimal contamination of the transferred sample with oxygen.

In Chapter 4, the determination of DO with a liquid core waveguide (LCW) based spectrometer that is useful for anoxic samples is reported for the first time. A liquid core waveguide is capillary tubing that propagates light through its liquid core by total internal reflection. For absorbance measurements, it serves as a long-path flow cell. With a long-path cell, the calibration sensitivity of the absorption measurement is increased relative to conventional 1-cm cells. LCW cells have internal volumes less than 1 mL providing very low detection limits without pre-concentration or the requirement for large sample volumes.

A major section of chapter 4 deals with the progressive development of several versions of LCW flow spectrometers with pathlengths from 20 to 100 cm to establish and optimize design criteria for optical and flow system components. Because the LCW cells were made of a special type of Teflon tubing, the cells were porous to O_2. Methods to minimize O_2 diffusion into the LCW cell and other flow components, such as double-containment, were investigated for later versions of the spectrometer. The performance of earlier versions of the spectrometer was evaluated by obtaining calibration data and detection limits for determining Fe(III) at nanomolar and micromolar concentrations. Different approaches for cleaning the LCW cells and compensating for baseline shifts during absorbance measurements were explored.

The final version of the LCW spectrometer was used to obtain calibration data for DO at low levels (below 1 mg/L) based on the oxidation of reduced IC and some of sampling methodology described in Chapter 3. The continuous reduction of the redox indicator (IC), during the analysis with H_2 and a Pt catalyst to compensate for O_2 diffusing into the flow system, was investigated.

References

Annu. Book ASTM Stand. **2004,** *11.01,* D888-03, 59-67.

Annu. Book ASTM Stand. **2005,** *11.01,* D888-05, 60 -70.

Annu. Book ASTM Stand. **2005,** *11.02,* D5543-94, 759 -765.

Chapelle, F. H. *Ground-water Microbiology and Geochemistry*, Wiley & Sons: Canada; 2001.

Rittmann, B. E.; McCarty, P. L. *Environmental Biotechnology: Principles and Applications*; McGraw-Hill: New York; 2001; pp 639.

Stumm, W.; Morgan, J. J. *Aquatic Chemistry*, 2nd ed.; Wiley-Interscience: New York; 1981; pp 780.

CHAPTER 2:

Review of Determination Methods for Dissolved Oxygen in Environmental Samples

2.1. Overview

The primary focus of this review is the determination of dissolved oxygen (DO) in aqueous environmental samples. Oxygen determination is important for many types of samples and in many fields outside of environmental applications. Some of the new or improved methods which have been developed and applied to biological samples and may be applicable to the environmental sciences are also discussed.

The ideal characteristics of an analytical method for measuring DO is dependent on the application. The desired attributes of DO methods or equipment for environmental analysis include portability, large dynamic range, robustness, operational simplicity, low detection limit, good precision, low maintenance, low calibration frequency, low expense and long lifetime of the equipment. In particular for measuring low DO in subsurface samples or laboratory samples, critical performance or instrumental characteristics include lower detection limits (at nanomolar concentrations), miniaturization, shorter response times (minutes), and the ability to monitor temporal or spatial changes within a system over a long period.

2.2. Analytical Methods for Determination of Dissolved Oxygen

2.2.1. Winkler (Iodometric) Titration and its Modifications

The Winkler titration (Winkler, 1988) and its modifications had been favored in environmental applications due to its accuracy (0.1%) and precision (0.6 % RSD) for concentrations higher than 1 mg/L (31 μM) DO (ASTM, 2004). The principle of the method is that oxygen in the water sample oxidizes iodide ion (I^-) to iodine (I_2) quantitatively. The amount of iodine generated is then determined by titration with a standard thiosulfate ($S_2O_3^{2-}$) solution with a visual indicator (APHA, AWWA and WEF, 1989). The Winkler titration has been automated to improve precision (0.04% RSD) and used mainly for oceanographic studies (Furuya and Harada, 1995) for concentrations in the range of 70 to 250 μM. Furuya and Harada determined the end-point with potentiometric detection. Other automated studies have reported end-point detection with amperometric or photometric methods and resulted in 0.03 - 0.1 %RSD (Furuya and Harada, 1995).

The classical procedure of Winkler titration consist of 4 steps and in each step, different reagents are added to the sample bottle/flask. Usually, the samples are collected into 125-300-mL bottles with ground-glass stoppers and the bottle is washed out with the sample at least three times. First, $MnSO_4$ solution is added to the aliquot of a sample, and without any delay, alkaline KI solution is added. Under alkaline conditions, DO in the sample oxidizes Mn^{2+} to Mn^{3+} and $Mn(OH)_3$ precipitates. As soon as the medium is acidified, Mn^{3+} oxidizes I^- to I_2. Up to this

step, the sample is considered "fixed" and storage of 6-8 hr is possible but not preferred. Later, I_2 in the sample is titrated with a standardized thiosulfate solution using starch indicator. Overall, 2 moles of I_2 is produced per one mole of O_2.

The Pomeroy-Kirshman modification (Golterman, 1983) of the Winkler titration prevents loss of I_2 by using a higher concentration of I^- solution and formation of the I_3^- complex. Also eliminating the transfer of the sample and titrating directly in the sample bottle can minimize errors. Other significant modifications of Winkler's method are employed to eliminate possible interferences. The azide modification (Alsterberg, 1925) and the permanganate modification (Rideal et al., 1901) are applied to minimize nitrite and ferrous ion interferences, respectively.

The Winkler titration and its modifications are often denoted as the "gold standard" of DO measurements and newer DO methods are usually validated by comparing results between the accepted and new methods (Glazer et al., 2004, Wilkin et al., 2001). For groundwater, in which majority of the samples are expected to have less than 0.5 mg/L DO, manual Winkler titrations should not be used for validation of newer methods because the detection limit (DL) is ~0.2 mg/L DO and too close to these low DO levels (APHA, AWWA and WEF, 1989).

Disadvantages of Winkler titrations include usage of toxic chemicals (e.g., sodium azide) for some modifications and the requirement of tedious wet chemistry techniques with multiple steps. Large sample (125-300 mL) volumes are needed and the apparatus is not very portable.

2.2.2. Amperometric and Voltammetric Oxygen Sensors

The Clark DO electrode (membrane covered polarographic electrode) (Clark et al., 1953) is the basis for the most favored method in electrochemical sensing of O_2. Numerous variations of the Clark DO have been developed and applied in different scientific fields (USGS, 2005; Johnson, 2005).

Clark-type amperometric, DO probes rely on measuring the change in current due to O_2 being reduced at the working electrode when a fixed potential is applied. Commonly, two noble electrodes, such as Au and Pt, and the electrolyte are separated from the sample with a membrane film. The electrodes, the electrolyte (i.e., KCl based) and the O_2 permeable membrane are all enclosed in a probe which is normally lowered into a sample solution. The DO in the sample solution diffuses through the membrane and then into the electrolyte and reaches to the cathode surface. When a sufficient potential difference (>600 mV) is applied to the system, O_2 is reduced irreversibly to water at the cathode. The increase in the current is proportional to the partial pressure of O_2 in the sample. The working range of Clark-type electrodes is typically 0.15-20 mg/L DO with the accuracy of 0.1 mg/L and a DL of 0.15 mg/L (4.8 μM).

The membrane barrier (i.e., Teflon) between the sample and the electrochemical cell provides separation of DO from most electrochemically-active species. Poisoning of the cathode is somewhat minimized unless the sample contains gaseous interferents such as H_2S. The response time of the sensor highly depends on the thickness and the chemical composition of the membrane and the electrolyte. In

practice, sufficient time and stirring are required for partial pressure of O_2 to be the same in the internal electrolyte solution and the sample solution. Another disadvantage of the membranes is the deposition of particles or debris onto the membrane. Over time, the effective surface area of the membrane for O_2 diffusion can decrease and affect the calibration. For smaller-volume samples, the consumption of DO in the measurement is a concern because the DO concentration can decrease significantly over time.

Temperature correction is necessary because as the sensor output and the solubility of the O_2 depend on temperature. The current of the amperometric DO-probe changes by 3 - 4 % per ºC (Hale, 1983). Also, the permeability of O_2 in the membrane and the properties of diffusion boundary layer at the electrodes are affected by temperature changes. For most commercially available DO probes, temperature is measured with a thermistor that is incorporated into the probe and the signal processor automatically displays a temperature-corrected result.

Electrochemical methods measure the activity of DO rather than its concentration in a sample. The effect of salinity on activity must be taken into consideration when comparing measurements made with electrochemical DO probes to other DO methods. Analytical DO methods that rely on stoichiometric reactions, such as Winkler titrations, estimate the concentration of DO rather than its activity.

Solid-state voltammetric microelectrodes where the applied potential is scanned allow detection of other species along with O_2. Consumption of DO in the sample is less because the applied potential is not fixed for constant O_2 reduction.

Membrane-free microelectrodes (Sosna et al., 2007) with a DL of ~0.04 mg/L (1 μM) DO have been developed as in-situ marine sensors.

Other electrochemical methods such as potentiometric, coulometric and conductometric DO sensors have been reported (Hitchman, 1978) but were not favored as voltammetric and amperometric methods.

2.2.3. Absorbance-based Oxygen Sensors

Oxygen is commonly measured in a quantitative or a semi-quantitative manner upon its reaction with indicators. Normally, the reaction product formed is colored or is different in color from the reagent. The amount of O_2 can be estimated visually or quantitatively determined by measuring the absorbance of the product.

Oxygen-sensitive indicators are used in different forms such as dissolved in a solution or immobilized onto a thin polymer film. Immobilized oxygen indicators are mostly used in food packaging for the determination of atmospheric oxygen.

Absorbance-based sensors are also classified in two groups in terms of the nature of the reaction between oxygen and the indicator (Eaton, 2002). These types of reactions are oxidation-reduction (redox) reactions of dyes and complexation of oxygen with biological or synthetic binders.

Complex-forming sensors with biological binders are reversible, but often require competitive binders to remove oxygen for regeneration of the reagents (Eaton, 2002). Measurement of dissolved oxygen in water using glass-encapsulated myoglobin was demonstrated for the DO range of 2 - 8 mg/L (63 – 250 μM) (Chung et al., 1995).

Most colorimetric or spectrophotometric oxygen sensors are based on redox indicators. Oxidation of the reduced form of the indicator (leuco form) with dissolved oxygen is monitored visually or spectrophometrically. Although there are a vast number of redox indicators available, indicators with low redox potential (typically a formal potential at pH 7 of 0 V or below) are more sensitive to oxygen. In general, the analytical procedure starts with the removal of oxygen from reagent indicator solutions by purging with an inert gas (commonly N_2). Next, the indicator is partially or totally reduced with a reductant so that it is ready for the addition of the sample. In some cases, excess reductant is used to remove the DO in reagent solutions.

Determination of DO using photoreduced leuco phenothiazine dyes in solution was studied (Hamlin et al., 1971). In the presence of aminopolycarboxylate salts (e.g., EDTA) and ambient light, N_2-purged solutions of phenothiazine dyes (e.g. thionine, methylene blue) were photoreduced. The disadvantage of this kind of reduction is that continuous monitoring of the absorbance is not possible because exposure to light might enhance the reduction due to excess aminopolycarboxylate in the solution. Different volumes of air-saturated water (8 mg/L at 25ºC) were tested as standards in this study. No detection limit was reported.

Spectrophotometric determination of DO with indigo carmine (indigo disulfonate) is a well established method (Loomis, 1954 and Buchoff, et al., 1955). Indigo carmine (IC) is easily reduced by soluble reductants such as dithionite or base-catalyzed fructose. Loomis used a gas-tight syringe as the spectrophotometric

cell after sampling and mixing of reagents within the same syringe. The lowest DO standard concentration was measured as 0.97 mg/L (30 μM).

Commercial kits are normally used in which IC is provided in a vacuum-sealed ampoule with fructose so that the dye is already completely reduced. For analysis, the ampoule is submerged in the sample and the tip of the ampoule is broken which allows the sample to be drawn into the ampoule. The sample and reagent are mixed by shaking and the vial that becomes the cell for visual or spectrophotometric measurement of the absorbance of the oxidized indicator. Measurements must be made within 1 min to minimize significant contamination by O_2 in the air entering the vial and reacting with the remaining reduced indicator.

The IC method has been successfully applied to field measurements of DO in ground water (Wilkin et al., 2001). In this study, commercial DO kits for the high range (1 – 12 mg/L) were used. Ground water was sampled by placing the ampoules inside an overflow cell that had been washed out more than 30 min for other analyses (with a flow rate of 300 mL/min). The precision of duplicate or triplicate measurements were reported as 0.3 – 0.5 mg/L (9 – 15 μM) O_2 for samples with DO above 1 mg/L.

The lowest method detection limit of indigo carmine methods reported by the manufacturer (CHEMets, Vacu-vial test kit K-7503) is 0.05 mg/L (2 μM) O_2. CHEMetrics also markets DO measurement kits based on another redox indicator with the trade name Rhodazine-D (which has a higher molar absorptivity than indigo

carmine) that is reported to provide detection limits down to 1 μg/L (31 nM) DO with a pathlength of 25 cm (CHEMetrics, 2007).

2.2.4. Fluorescent Oxygen Sensors (oxygen optrodes)

Fluorescent oxygen sensors are frequently used in food packaging industry, bio-medical research and recently environmental monitoring. They are often packaged in a probe form and based on measuring the degree of quenching of the fluorescence of a fluorophore that is incorporated into a membrane at the tip of the probe and in contact with the sample.

Quenching of the fluorescence occurs due to collisions or via formation of a charge transfer complex of the fluorophore and oxygen (Peterson et al., 1984). During this process, the energy is transferred from the photo-activated fluorophore to oxygen and the decrease in fluorescence is related to the concentration of oxygen. Quantitative basis of quenching is based on Stern-Volmer equation (Ingle and Crouch, 1988).

Favored fluorophores are mostly organometallic complexes of ruthenium and platinum due to their high quantum yield, longer excited state lifetimes and better quenchability with oxygen. These properties of the fluorophore are highly affected by the membrane matrix. Various polymers had been successfully used to improve fluorescence sensors such as sol-gel derived glass matrix, plasticized poly(vinyl chloride), silicone rubber, and class II organically modified silicate membranes (Tao et al., 2006).

The main disadvantage of fluorescent oxygen sensors is that the quenching process and the diffusion of oxygen through the membrane depend on temperature. Temperature correction is commonly achieved by including a thermistor or another luminophore that is sensitive to only temperature changes in the sensor unit. Then a second-order polynomial algorithm is used as the calibration function (Palma et al., 2007).

Fluorescent oxygen sensors have a relatively fast response time which depends on the oxygen permeability of membrane used and is typically less than a minute. Also the consumption of O_2 is insignificant in comparison to Clark-type electrodes.

Recent studies are mostly about improving membrane matrices (Hartmann et al., 1996), methodology of temperature correction (Palma et al., 2007) and probes at submicron dimensions (Kopelman et al., 1995). Commercial fluorescent oxygen sensors are claimed to provide a detection limit of 0.05 - 0.03 mg/L (2 - 0.9 μM) DO (websites of Hach Company and Ocean Optics Inc.). Sub-micrometer fiber optic sensors were developed for the detection of intra-cellular DO with a detection limit of 0.014 mg/L (0.44 μM) DO (Park et al., 2005).

Optical sensors (optrodes) that can function under “extreme” environmental conditions were studied. Respiration rates of yeast cultures were measured at 275 atm with a fluorescent oxygen sensor incorporated into a high pressure reactor (Stokes et al., 1999). Oxygen optrodes withstanding sterilization were evaluated for bioreactor monitoring during fermentation (Voraberger et al., 2001).

2.3. Summary of Analytical Methods for Dissolved Oxygen and Field Studies

Field comparison of a DO optrode and a Clark DO electrode in the Tualatin River, Oregon (Johnston et al., 2005) showed that optrodes suffered less fouling and calibration drift over three weeks of deployment. In this study, the drift of the optrodes ranged from -0.09 – 0.02 mg/L DO for high levels of oxygen.

Low DO concentrations were measured in ground water with Rhodazine D colorimetric method (White et al., 1990). They reported a detection limit of 6 μg/L (0.2 μM) with prepared standard solutions in the range of 0 – 8.0 μM (0 - 0.3 mg/L). Detected chemical interferences were Fe^{3+}, Cu^{2+} and CrO_4^{2-}. Rhodazine D vials were snapped at different well depths with a down-hole wire line tool which also minimized the sample contamination.

Wilkin et al. (2001) determined low DO concentrations in ground water with different methods. They used two field standards of 1 and 8 mg/L (31 and 248 μM) DO although majority of the samples were determined as below 1 mg/L. Results of Winkler titrations and membrane covered electrodes showed poor correlation at low DO levels. Best correlation with the Winkler titration was obtained using visual colorimetric methods.

CHEMets methods based on spectrophotometric measurement of indigo carmine and visual Rhodazine D detection are the only approved methods for the range of 0 – 100 μg/L (0 – 3.12 μM) DO in ASTM (2005). Recently, the luminescence-based sensor was approved (ASTM D888-05, 2005) for the range of 0.05 to 20 mg/L (2 – 625 μM) DO and became the third method for DO

measurements. Previously, Clark-type electrodes and Winkler titrations (only for concentrations above 1 mg/L) were certified.

The detection limits of the Winkler titration and the Clark-type DO probe (~0.2 mg/L and ~0.15 mg/L (~6 μM), respectively) are reasonably well established. In practice, these detections limits can only be achieved if the sample is transferred without significant O_2 contamination to the titration vessel or electrode cell.

Absorbance measurements with redox indicators yield the best reported detection limits and lowest detection limit (~1 μg/L (~0.03 μM)) is reported with spectrophotometric measurement of Rhodazine D with a path length of ~25 cm. In ASTM (2005) studies, the blank standard deviation was not directly reported. It is strange that the reported SD is 0.4 μg/L for a range of samples from 0 to 4.9 μg/L but is 4 μg/L for samples in the range of 5 to 20 μg/L and higher DO ranges. The SD for measurements within a factor of 10 of the detection limit does not normally vary by a factor of 10 with any technique.

Reported detection limits for fluorescent optrodes are near 0.02 mg/L (0.6 μM) DO and hence near the best spectrophotometric methods. There appears to be little data in the reviewed literature documenting the performance of this probe including standard deviations for DO levels below 1 mg/L or for blanks. In an inter-laboratory validation study (Hach Company, 2004), the detection limit is reported to be ~0.05 mg/L (2 μM) based on the standard deviation of measurements of a DO standard of 0.07 mg/L. The procedure for preparing the standard or means to put the probe in contact with the standard were not described.

2.4. References

Alsterberg, G.; *Biochem. Z.*, **1925**, *159,* 36-47.

Annu. Book ASTM Stand. **2004,** *11.01,* D888-03, 59-67.

Annu. Book ASTM Stand. **2005,** *11.01,* D888-05, 60 -70.

Annu. Book ASTM Stand. **2005,** *11.02,* D5543-94, 759 -765.

Buchoff, L. S.; Ingber, N. M.; Brady, J. H. *Anal. Chem.*, **1955,** *27*, 1401-1404.

CHEMetrics product specifications in www.chemetrics.com, 2007.

Chung, K. E.; Lan, E. H.; Davidson, M. S.; Dunn, B. S.; Valentine, J. S.; Zink, J. I. *Anal. Chem.*, **1995,** *67*, 1505-1509.

Clark, L. C. Jr.; Wolf, R.; Granger, D.; Taylor, Z. *J. of Appl. Physiol.,* **1953,** *6(3),* 189-193.

Eaton, K. *Sens. Actuators B: Chem.,* **2002**, 85*,* 42-51.

Furuya, K.; Harada, K. *J. Oceanogr.*, **1995,** *51*, 375-383.

Glazer, B. T.; Marsh, A. G.; Stierhoff, K.; Luther, G. W. III. *Anal. Chim. Acta,* **2004,** *518,* 93-100.

Golterman, H. L. In *Polarographic Oxygen Sensors* (ed. by Gnaiger/Forstner) Springer-Verlag: Berlin, Heidelberg, 1983; pp 346-351.

Hach Company, Luminescent Dissolved Oxygen Probe; www.hach.com

Hach Company, Report on the Validation of Proposed EPA Method 360.3 (Luminescence) for the measurement of Dissolved Oxygen in Water and Wastewater, 2004

Hamlin, P. A.; Lambert, J. L. *Anal. Chem.*, **1971,** *43*, 618-620.

Hartmann, P.; Trettnak, W. *Anal. Chem.*, **1996,** *68*, 2615-2620.

Hale, M. J. In *Polarographic Oxygen Sensors* (ed. by Gnaiger/Forstner) Springer-Verlag: Berlin, Heidelberg, 1983; pp 3-17.

Hitchman, M. L. Measurement of Dissolved Oxygen, In *Chemical Analysis, v. 49* (ed. by Elving, P. J.; Winefordner, J. D.; Kolthoff, I. M.), Wiley-Interscience: New York, 1978; pp. 130-159.

Ingle, J. D. Jr.; Crouch, S. R. *Spectrochemical Analysis*; Prentice-Hall: New Jersey; 1988.

Johnson, C. D.; Paul, D. W. *Sens. Actuators B: Chem.,* **2005,** *105,* 322-328.

Johnston, M. W.; Williams, J. S. In *U. S. Geological Survey Open-File Report 2006-1047,* 2006; pp 11.

Kopelman, R.; Rosenzweig, Z. *Anal. Chem.*, **1995,** *67*, 2650-2654.

Loomis, W. F. *Anal. Chem.*, **1954,** *26*, 402-404.

Ocean Optics Inc., FOXY Fiber Optic Oxygen Sensor; www.oceanoptics.com

Palma, A. J.; Lopez-Gonzales, J.; Asensio, L. J.; Fernandez-Ramos, M. D.; Capitan-Vallvey, L. F. *Anal. Chem.*, **2007,** *79*, 3173-3179.

Park, E. J.; Reid, K. R.; Tang, W.; Kennedy, R. T.; Kopelman, R. *J. Mater. Chem.,* **2005,** *15*, 2913-2919.

Peterson, J. I.; Fitzgerald, R. V. *Anal. Chem.*, **1984,** 56, 62-67.

Rideal, S.; Stewart, G. G. *Analyst,* **1901,** *26,* 141b-148.

Sosna, M.; Denuault, G.; Pascal, R.W.; Prien, R.D.; Mowlem, M. *Sens. Actuators B: Chem.,* **2007**, *123,* 344-351.

Standard Methods for the Examination of Water and Wastewater, 17th Ed.; 4500-O Oxygen (Dissolved), APHA, AWWA and WEF, 1989.

Stokes, M. D.; Somero, G. N. *Limnol. Oceanogr.*, **1999**, *44(1),* 189-195.

Tao, Z.; Tehan, E. C.; Tang, Y.; Bright, F. V. *Anal. Chem.*, **2006,** *78*, 1939-1945.

Voraberger, H. S.; Kreimaier, H.; Biebernik, K.; Kern, W. *Sens. Actuators B: Chem.,* **2001**, *74,* 179-185.

White, A. F.; Peterson, M. L.; Solbau, R. D. *Ground Water,* **1990**, *28*, 584-590.

Wilkin, R. T.; McNeil, M. S.; Adair, C. J.; Wilson, J. T. *Ground Water Monit. Rem.,* **2001,** *21(4),* 124-132.

Winkler, L. W. *Ber. Dtsche. Chem. Ges*., **1988**, *21*, 2843-2855.

CHAPTER 3:

Methodology for Low-Volume Sampling and Determination of Low Dissolved Oxygen Concentrations by Spectrophotometric Monitoring of the Oxidation of Reduced Indigo Carmine

ABSTRACT:

The determination of dissolved oxygen (DO) at low concentrations is based on monitoring the absorbance of reduced indigo carmine (IC) upon its oxidation in a double-septum spectrometer vial. A new sampling methodology was developed for transferring small volume samples (1 mL or less) from enclosed anaerobic or anoxic systems with minimal atmospheric contamination. The O_2 contamination of samples, standards, and reduced IC solutions was minimized with unique double-septum caps. The portable flow sampler can be connected to different experimental systems such as septum bottles, bioreactors, columns, and ground water sampling pumps. The reliability of the analytical methods was demonstrated with analysis of prepared DO samples and anaerobic cultures under Fe(III)-reducing, sulfate-reducing and methanogenic conditions. Detection limits were 0.04 mg/L (1 μM) and 0.07 mg/L (2 μM) DO with the syringe sampling and the flow sampler, respectively. The relative standard deviation was 4% or less for standard solutions near 1 mg/L DO.

3.1. Introduction

Oxygen is one of the most significant chemical species in nature because it is connected with numerous biological and abiotic processes and the most abundant chemically and biologically-active, strong oxidant (Stumm and Morgan, 1981). When O_2 is depleted in the sub-surface by processes such as microbial reduction, aquatic or aquifer systems can become anoxic. There appears to be no strict definitions for the term “low O_2 concentration". However, the term hypoxia is referred to as O_2 concentrations below 2 mg/L (63 μM) in oceanography by the U.S. Geological Survey (USGS, 2006). Sub-oxic zones have been defined as zones with O_2 concentrations below 0.32 mg/L (10 μM) (Murray et al., 1995).

Determination of dissolved oxygen (DO) below 1 mg/L (or 31 μM) in a reliable manner is still a challenge in many fields such as geochemistry, oceanography, microbiology, medicine and biochemistry. Winkler titrations and its modifications have been favored in environmental applications due to its accuracy (0.1%) and precision (0.6% RSD) (ASTM, 2004). Automation of the Winkler titration method has increased its precision to 0.04% RSD for the DO range of 70 - 250 μM and it has been used mainly for oceanographic studies (Furuya and Harada, 1995). However, this method is normally recommended for applications with higher DO values (> 1 mg/L DO) (ASTM, 2004), requires toxic chemicals (i.e., Na azide) for the modifications, consumes large sample volumes (>300 mL), and is tedious for field work. The DO detection limit is normally reported as 0.2 mg/L (6.3 μM) for a 300 mL sample (APHA, AWWA and WEF, 1989).

Electrochemical sensors such as membrane-covered, amperometric and polarographic DO probes (Clark-type electrodes) are highly robust, portable, and widely used in environmental monitoring and in bio-analytical studies. It is possible to place a DO probe in a flow-cell in-line with water pumped from a ground water well to minimize O_2 contamination of the sample (Garner, 1988). The primary disadvantages are membrane fouling, the requirement of frequent calibration, and a detection limit too high for samples with very low DO levels. The detection limit is normally reported in the range of 0.05 - 0.2 mg/L (2– 6 μM) DO with an accuracy of 0.1 mg/L DO (APHA, AWWA and WEF, 1989) for commercially available membrane electrodes with sample volumes of 200 mL or greater. Also, microelectrodes with or without membrane coverage have been developed as marine sensors with a DL of ~0.04 mg/L (0.9 μM) DO (Sosna et al., 2006).

Luminescent oxygen sensors are frequently used in food packaging industry, bio-medical research and recently environmental monitoring. They are often packaged in a probe form and based on measuring the degree of quenching of the fluorescence of a fluorophore that is incorporated into a membrane or crystal at the tip of the probe and in contact with the sample. Detection limits as low as 14 ppb (0.44 μM) have been reported (Park et al., 2005).

Determination of DO with redox indicators is another widely used approach. These methods rely on measuring the increase in absorbance when a reduced indicator is mixed with an aqueous sample. The absorbance of the oxidized indicator is monitored with a spectrometer or the change in color is detected visually and

compared to standards. Correction for salinity or temperature is not necessary as it is for electrochemical or luminescent sensors.

A vast number of redox indicators are commercially available that change color when exposed to oxygen such as resazurin and thionine (Bishop, 1972). Indigo carmine is used in commercial products for DO measurement and is favored over other reduced indicators because it is sulfonated and adsorbs less readily to surfaces and reacts faster with DO. The indigo carmine method has been studied and applied in groundwater studies (White et al., 1990). Detection limits are typically in the range of 0.05 - 1 mg/L (1.6 – 31 μM) for spectrophotometric and visual detection (CHEMetrics, 2006). CHEMetrics also markets DO measurement kits based on another redox indicator with the trade name Rhodazine-D (which has a higher molar absorptivity than indigo carmine) that is reported to provide detection limits down to 1 μg/L (31 nM) DO with a pathlength of 25 cm (CHEMetrics, 2007).

With any DO method, keeping the analytical device (the parts that are in contact with the sample), the reagents for some of the methods, and the sample free of contamination from atmospheric oxygen are the keys to a reliable detection, particularly when measuring trace levels of O_2. The difficulty of sampling anoxic waters was investigated in lake sediments (Carignan et al., 1994) and in ground water (Rose et al., 1988). Similar issues are discussed for an application involving measurement of nanomolar levels of oxygen in solid and liquid biological samples by HPLC with electrochemical detection (Seppi et al., 1997). They successfully monitored the change in low levels of O_2 due to respiratory activity of a conifer

needle and the corrosion effects of a paper clip with a detection limit of 4.9 nM (in-chamber concentration). For both of these samples, the sample was originally in equilibrium with air before it was placed in the sample chamber. The sample chamber was evacuated before starting to measure the change in O_2 concentration due to O_2 diffusing out of the sample.

The sample transfer and detection of low levels of DO becomes more challenging if the sample has very low DO, such as below 1 mg/L, and especially below 0.1 mg/L. Under these conditions, the O_2 gradient between air and the sample is high and a small absolute O_2 contamination has a large relative effect on the accuracy of the DO measurement. Without adequate protection, the DO concentration in a sample can increase rapidly and significantly as it is transferred from its original location (down a well or in a bottle or bioreactor) into a measurement cell where the sample contacts a probe or is mixed with a reagent. Many of the standard methods for low level DO environments (i.e., boilers and ground water) rely on continuous flow (before and during sampling) of the sample through the sampling cell or chamber to purge out the residual oxygen before the measurement is made and sometimes to minimize O_2 contamination while the DO measurement is being made. Often more than 300 mL of the sample is required to purge the sampling cell or chamber. Hence, methods that require this purging approach are not applicable for closed systems with a limited volume of sample.

We present the design and application of a portable flow sampler and analysis system to determine low DO levels with small sample volumes (1 mL or

less) based on oxidation of reduced indigo carmine. This apparatus can be connected to different experimental systems such as septum bottles, bioreactors, columns, and ground water sampling pumps. Unique double-septum caps were developed to minimize the O_2 contamination of samples, standards and reduced indicator solutions during piercing of the vial or bottle septa with syringes. Low DO samples and anaerobic cultures under Fe(III)-reducing, sulfate-reducing and methanogenic conditions were sampled and analyzed for DO to evaluate the reliability of the analytical method and the ability to sample an enclosed anaerobic culture with minimal contamination of the transferred sample with oxygen.

3.2. Experimental Section

3.2.1. Chemicals and Solution Preparation

Indigo carmine (IC) was obtained from Aldrich with 92% purity. Structures of the oxidized form and the reduced form are given in Figure 3.1 along with the absorption spectra in Figure 3.2. IC is electrochemically reversible, reacts rapidly with dissolved oxygen, and has a formal redox potential of -0.125 V at pH 7 (Bishop, 1972). In addition, IC is highly soluble in water (3 mg/mL) (Green, 1990) and its adsorption onto surfaces is insignificant.

An IC stock solution (2 mM) was prepared in deionized water. An IC reagent solution (0.5 mM) was prepared weekly by dilution of the stock solution in 0.1 M pH 7 buffer (TRIZMA hydrochloride, Sigma Aldrich) and was reduced with 10 mL/min H_2 (100%, BOC Gases) in the presence of coiled Pt wire (gauge 31, length 10-30 cm) as the catalyst in a 20-mL vial with a double-septum cap (details about the cap are presented in the instrumentation section). Photo-degradation of the indicator with the tungsten lamp was not observed during the analysis period but stock solutions were stored at 4°C and in the dark to avoid daylight for longer periods.

Ti(III) citrate was used as a soluble reductant for initial experiments (Jones, 1999, Zehnder and Whurmann, 1976). A stock solution of ~80 mM Ti(III) citrate was prepared by dissolving 4 g of TRIZMA·HCl and 7.4 g of sodium citrate

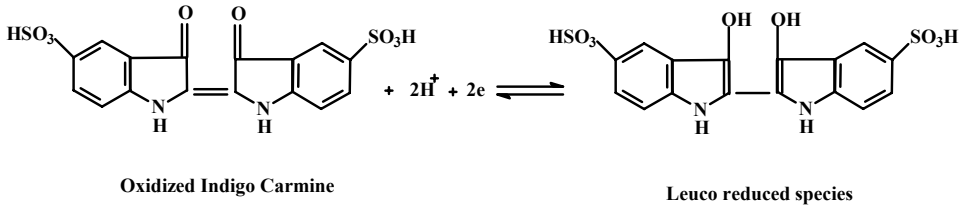

Figure 3.1 Chemical structures of oxidized and reduced indigo carmine (IC).

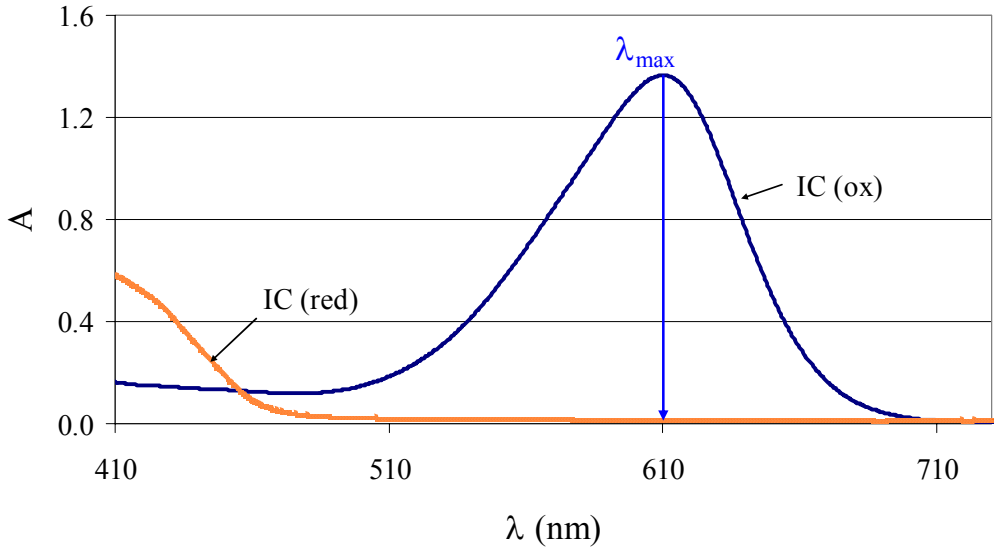

Figure 3.2 Absorption spectrum of oxidized and reduced indigo carmine. IC (40 μM) was reduced with H_2 in the presence of Pt wire.

monohydrate (Sigma Aldrich) in 20 mL of deionized water, followed by the addition of 5 mL of $TiCl_3$ (13 % w/w in 20 % v/v HCl, Fluka). While the solution was continuously purged with N_2, the pH was adjusted to 7 with concentrated NaOH and the volume was brought to 50 mL with deionized water in a volumetric flask. Then the solution was transferred into a septum vial (I-CHEM Vials) and stored at 4°C. More dilute Ti(III) citrate solutions were prepared by diluting ~80 mM stock and keeping the citrate and buffer concentrations constant. As the concentration of Ti(III) citrate solutions decrease quickly overtime, multiple additions were required for reduction of indicators.

DO standard solutions with concentrations of 0 – 1 ppm (mg/L) were prepared by purging deionized water in septum bottles with mixtures of N_2 and O_2/air (BOC gases) for 2 hr. Individual gas flow rates were adjusted with a Tylan RO-28 electronic flow rate controller/readout and mass flow controllers (FC-280 and FC-260) and the outlet flows were mixed within a tee. Mass flow controllers were calibrated with a solid state flowmeter (Restek Flowmeter 6000) and the accuracy of the DO standards was verified with a Clark-type DO probe (Hach, DO175 Dissolved Oxygen-meter Model 50175). Prepure N_2 was further purified with Restek heated purifier unit (Model 21496).

Standard solutions and culture media was prepared in 125-mL septum media bottles (Wheaton) and capped with butyl rubber locking flange septa (Wheaton). Hypodermic needles (gauge 22, Popper and Sons) were used for the gas inlet and vent. Gas inlet and vent needles were connected to PEEK™ tubing (Upchurch Sci.)

via ¼-28 fittings and unions. The distal end of the vent tubing was submerged in a flask or a beaker that contained water to prevent back diffusion of O_2. All solutions were prepared with deionized water obtained from a Millipore Milli-Q water purifying system.

The analytical results of the proposed method to determine O_2 were compared to the DO values evaluated with "Oxygen CHEMets®" which is listed as a standard method for low-level dissolved oxygen in ASTM (2005). Oxygen CHEMets (Calverton, VA) colorimetric test kits consist of vacuum sealed ampoules that contain the reduced indicator Rhodazine D™. The working concentration range of the kits is given as 0 - 40 μg/L (K-7540) and 0 - 1 mg/L (K-7501). with the method detection limits (MDL) of 2.5 μg/L and 25 μg/L, respectively.

Rhodazine D methodology (ASTM, 2005) relies on large volume samples (200 mL or more) to flush the sampling lines and continuous flow of the sample through the sampling tube is necessary during sampling. The ampoule is inserted (tip facing down) into a vertical sampling tube which is open to air. Then the tip of the ampoule is snapped manually by tilting the upper part. After inversion of the ampoule once, the color is compared visually with the standards in 30 s for the closest match. The liquid color standards are in sealed ampoules that are in the concentration range of the kits and are provided by the manufacturer. This procedure is not applicable for laboratory anaerobic cultures in a bottle, a bioreactor, or a column where the total sample volume is normally limited (e.g., 100 mL - 1 L) and the system is closed to minimize O_2 contamination. For example, insertion of an

ampoule into a 125-mL sample bottle would clearly result in the diffusion of excess O_2 and so the damage of the anaerobic culture and further studies of the sample would not be possible.

The DO concentration in the standards prepared in this study was evaluated with CHEMets kits. They are applicable because a fresh standard can be prepared for every ampoule in a 125-mL septum bottle and an ampoule tip can be snapped in a short amount of time (15 s) before the excess O_2 diffuses into the bottom of the solution. An ampoule was placed (tip facing down) into a septum bottle that contained 125 mL of deionized water. The bottle was capped with a single septum and it was purged for 2 h. Then, the cap of the bottle was removed and the ampoule was snapped by applying pressure manually towards the middle part.

Rhodazine D (4 mL from Oxygen CHEMets K-7540) was reduced with 10 mL/min H_2 (100 %, BOC Gases) in the presence of coiled Pt wire (gauge 31, length ~10 cm) as the catalyst in a 4-mL vial with a double-septum cap.

3.2.2. Anaerobic Wastewater Samples

Microcosms dominated by Fe(III)-reducing, sulfate-reducing or methanogenic conditions were prepared by seeding appropriate media with wastewater sludge (Chapelle, 2001). Sludge was obtained from the anaerobic digester of City of Corvallis Wastewater Reclamation Plant and let settle in a 1-L glass bottle.

Media compositions were modified from Chapelle (2001). For Fe(III)-reducing conditions, 0.68 g of sodium acetate, 1 g of $FeCl_3$, 0.2 g of NH_3Cl, 0.02 g of KCl, 0.25 g of $NaHCO_3$, 0.06 g of NaH_2PO_4 and 0.1 g of NaCl were transferred into a 125-mL septum bottle and were dissolved in 90 mL of deionized water. For sulfate-reducing conditions, 0.68 g of sodium acetate, 0.1 g of Na_2SO_4 sulfate, 0.2 g of $MgSO_4$, 0.1 g of NH_3Cl, 0.1 g of $CaCl_2$, 0.05 g of KH_2PO_4 and 0.35 g of yeast extract and 0.1 g of L-ascorbic acid were transferred into a 125-mL septum bottle and dissolved in 90 mL of deionized water.

The media for methanogenic bacteria was modified from Mah et al. (1981) and 0.8 g of sodium acetate, 0.1 g of NH_3Cl, 0.1 g of $MgCl_2$, 0.04 g of K_2HPO_4, 0.5 g of $NaHCO_3$, 0.05 g of L-cysteine, 0.2 g of yeast extract, 0.04 g of $CaCl_2$ and 0.1 g of L-ascorbic acid were transferred into a 125-mL septum bottle and dissolved in 90 mL of deionized water. All of these chemicals were obtained from Mallinckrodt Chemicals excluding the yeast extract and L-cysteine which were obtained from EMD Chemicals Inc. and Sigma, respectively.

Before the addition of wastewater sludge, the pH of all media was adjusted to 6.5 - 7.0 by adding drop-wise concentrated HCl or NaOH while monitoring the pH with glass electrode and purged with N_2 for 30 min. With a 25-mL syringe, 20 mL of the supernatant of the wastewater sludge was transferred into the septum bottle. Bottles were stored at room temperature and upside down to minimize the headspace and contamination from O_2.

Microorganism growth was visually observed at the inner walls of the sample bottles and as increased turbidity. Specific products of microbial reduction (e.g. Fe(II), S(-II), CH_4) were measured in each bottle to verify anaerobic conditions.

Fe(II) measurements were performed over the course of a month for samples under Fe(III)-reducing conditions. Fe(II) was determined using the 1,10 phenanthroline method (Jones, 2000; APHA, 1994) by withdrawing 1-mL of sample through the bottle septum with a gas-tight syringe. The sample was injected into a spectrophotometric cell with the reagent and the absorbance was determined with a spectrometer.

To test the Fe(III) interference on the O_2 measurements, a deaerated Fe(III)-hydroxide solution was prepared in a septum vial by adjusting a 1% (w/v) $FeCl_3$ solution to pH 7 followed by N_2 purge. Samples were taken from this anoxic solution and injected into spectrometer vial.

Microcosm bottles with sulfate-reducing bacteria became turbid overnight, possibly due to high production rate of sulfide and resulting polysulfide species. Sulfide was determined in these samples with a CHEMetrics Vacuette Sulfide monitoring kit (Chemetrics, Calverton, VA) which employs the methylene blue method. The procedure was modified to use 1.5 mL of sample (withdrawn with a syringe) and keeping the ratio of sample to reagent volumes the same as in the original procedure for all reagents. The absorbance of the final solution was measured in a 1-cm cuvette at 670 nm with a spectrometer (Ocean Optics Inc.) and

compared to CHEMetrics' sulfide calibration table to determine the sulfide concentration.

Methanogenic cultures were not sampled for the first two weeks after inoculation of the media. Methane was determined by headspace analysis with an HP 5890 GC (30-m GS-Q column and flame ionization detection) which was located in Merryfield Hall (Department of Civil, Construction and Environmental Engineering), OSU. Suitable temperatures (250 ºC, 50 ºC, 250 ºC for the detector, the oven and the inlet, respectively) were set. A sample of 10 μL was injected into GC with a gas-tight syringe (Precision Sampling). A three-point calibration curve was constructed by dilution of 100% CH_4 with air in 125-mL media bottles.

3.2.3. Instrumentation

3.2.3.1. Experimental Apparatus

A diagram of the experimental apparatus developed for O_2 determination is shown in Figure 3.3. The absorbance of the solution in the double-septum vial (DSV) was monitored with a spectrometer (S2000 FL, Ocean Optics) that has a 200-μm entrance slit and a grating of 600 lines/mm blazed at 500 nm. The light source and the spectrometer were interfaced to a laptop computer with a data acquisition card (DAQ-700Card, National Instruments). The S2000-FL provides multi-wavelength monitoring with a 2048-element charged coupled device (CCD) as the detector and with OOIBase32^{TM} (Ocean Optics) as the operating software. The advantage of

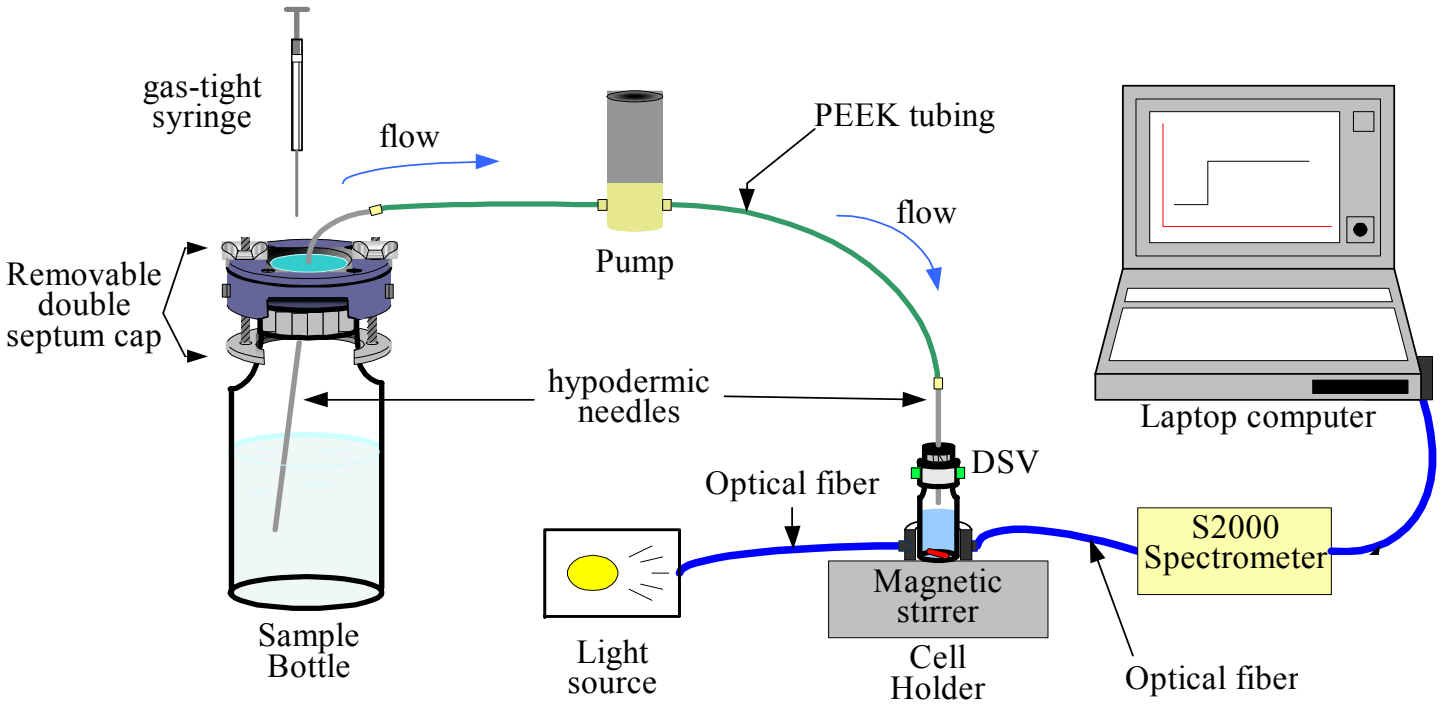

Figure 3.3 The experimental apparatus for low-volume sampling from closed-anoxic systems and the determination of DO. The transfer of the sample into spectrometer cell (DSV) was performed with a micropump or a gas-tight syringe.

multi-wavelength monitoring is that it allows baseline correction at a wavelength where IC does not absorb light. Thus, the effects of sudden disturbances such as syringe needle blocking the light or bubbles forming during injection can be minimized. Commercial multimode fiber optic cables (Ocean Optics) with 200-600 μm core size were used to transmit the light from the tungsten light source (Analytical Instrument Systems, Model DT 1000) to the cell holder and then to the spectrometer.

Glass cylindrical vials (4 mL, Fisher Scientific) and conventional 1-cm cuvettes (from Spectrocell, Oreland, PA) were initially evaluated as the spectrophotometric cell. Vials were chosen for further studies. Each vial had a 1.2-cm pathlength and the cylindrical shape of the vial provided efficient mixing because a 10-mm Teflon stir bar (VWR) driven and spin rapidly and consistently by a HANNA Instruments (HI 190M) magnetic stirrer. Continuous stirring was maintained throughout a run.

To minimize O_2 contamination of the samples, standards, or blanks in the septum bottles, the sample or reagent in the spectrophotometer cell, the reduced reagent in the reagent vial, or the syringe, unique caps were designed and machined for the measurement cuvettes or vials and sample bottles. Schematics of the two different configurations are given in Figure 3.4 and 3.5. The vial double-septum cap has been discussed previously (Haas, 2006). As seen in the Figure 3.4, the vial screw cap has a female threaded bottom and a male threaded top (13-425 GPI size for both). The gap between two septa (gray butyl rubber stoppers with a 12-mm

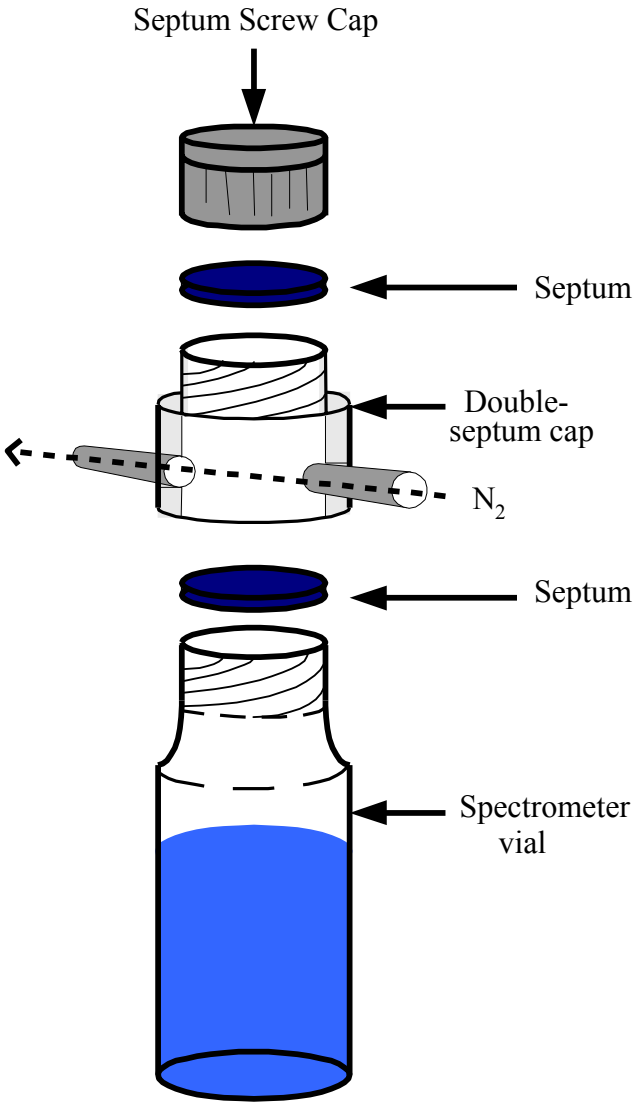

Figure 3.4 Details of the double-septum vial (DSV) which serves as the spectrometer cell. The space in between the septa is purged with N_2 through the PEEK tubing attached to the cap.

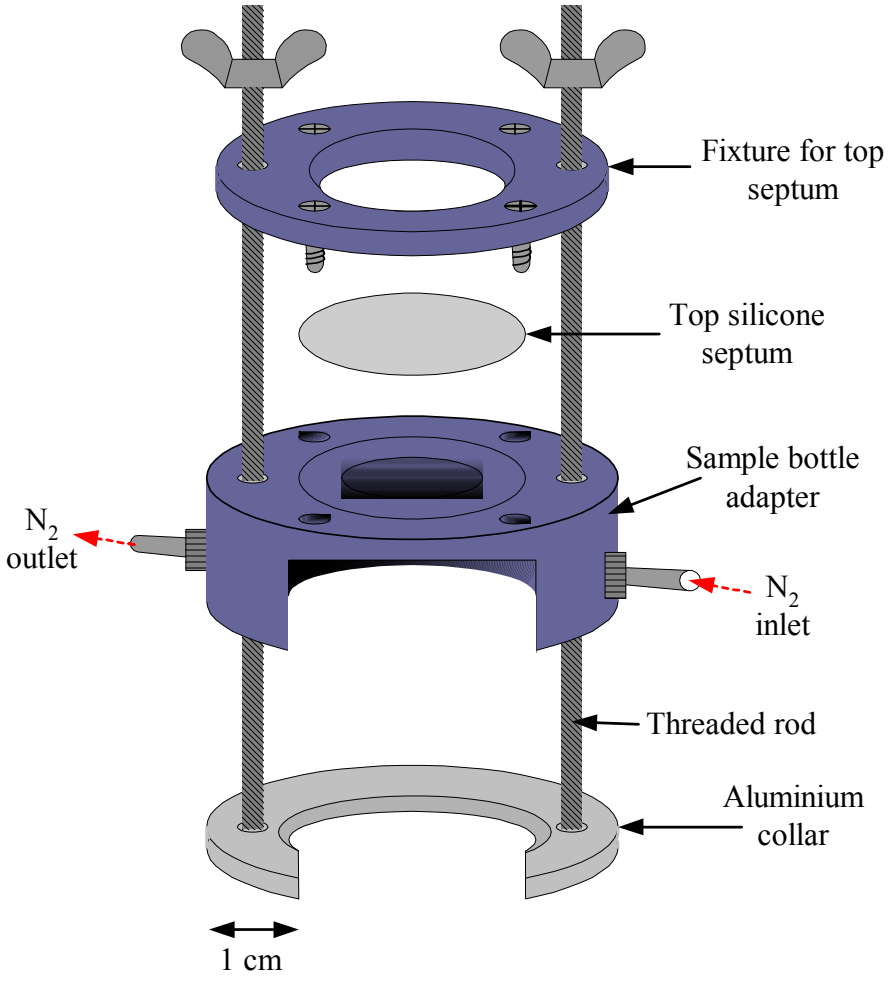

Figure 3.5 Removable septum cap for sample bottles. The sample bottle adaptor and the fixture for the top septum are made of Delrin. The bottom septum is normal septum in the bottle cap. Nitrogen flow between the septa is provided through PEEK tubing which is connected to the cap via ¼-28 fittings.

diameter, Kimble) was continuously purged with N_2 (~30 mL/min) to minimize permeation of air into the vial during piercing action. The cap of the double-septum vial (DSV) was kept on the vial until a run was completed.

A similar double-septum cap was made for the 20-mL vial used to prepare and store reduced IC. This cap is similar in design to the cap depicted in Figure 3.4, but it has a larger diameter and fits the larger size threading (22-400 GPI size). Two 20-mm butyl rubber septa (Agilent Tech.) were used.

The removable bottle cap, which has a single septum, was attached onto sample bottle's septum cap before sampling to form a gap that was purged with N_2 during sampling (Figure 3.5). The bottle cap was removed after sampling was complete. The N_2 flow rate between septa was set to 30-100 mL/min. This cap was designed to fit Wheaton media bottles with a GPI size of 33-430 as shown in Figure 3.6. The single septum on top was a 22-mm diameter Teflon-faced silicon septum (Supelco). Using Teflon material, instead of butyl rubber as top septum, enabled easy piercing of both septa at the same time.

Figure 3.6 Photograph of the removable septum cap on a septum bottle.

3.2.3.2. Sample Introduction

Sample introduction into the vial was performed with two different devices: a 1-mL gas-tight syringe with a fixed needle (SGE Analytical Science), and a solenoid actuated diaphragm pump (Bio-chem Valve Inc.) with a preset volume of 50 µL. A Lee solenoid actuated diaphragm pump (the Lee Co., LPLA 1230350L) was used for initial studies. The total volume of the sample delivered to the sample cell by the pump is the product of the preset volume and the number of strokes. The micro pump was controlled via a home-made circuit (Appendix A) interfaced to the laptop computer with a microcontroller module. The number of strokes is controlled by the number of pulses sent to the pump (up to 2 per second). The BS1USB module (Parallax, Inc.) consists of a BASIC Stamp®-1 microcontroller, an on-board USB interface and a USB-A connector. A short basic stamp-1 program (Appendix A) was created with "the BASIC Stamp Editor for Windows version 2.2" for different commands such as start pumping, pump until stopped, deliver a set volume of sample and stop pumping.

A stainless steel frit with 20-µm pore size (Upchurch Scientific) was placed at the inlet of the pump to prevent clogging and damage. PEEK^{TM} 1.57-mm (1/16-in) OD tubing and ¼-28 flangeless fittings (Upchurch Scientific) were used as components of the sampling pump and also for N_2 flow through double-septum caps. Stainless steel hypodermic needles (20 and 22 gauge, Popper and Sons) were connected at both ends of the pump PEEK tubing with epoxy glue (60-s system, VersaChem) for easy piercing of the septum. The total internal volume of sampling

pump, tubing and needles was ~350 μL. The precision, accuracy and working range of the pump was evaluated for different sample headspace pressures (Appendix B).

The headspace of the septum bottle with sample or standards was pressurized to 1 psi during sampling with the aid of pressure gauge. The headspace was purged with purified N_2 (~100 mL/min) to provide the positive pressure as discussed in more detail in Appendix B. The magnitude of the gas pressure was adjusted with a needle valve (Upchurch Scientific) until the analog pressure gauge (Matheson Co. Rutherford, N.J.), which was connected to the headspace via a hypodermic needle, registered 1 psi.

3.2.4. Analytical Procedure

With an electronic digital pipette (Rainin), 2 mL of pH 7 buffer (0.1 M TRIZMA) were transferred into spectrometer double-septum vial (DSV) and purged with N_2 for 30 min to remove the dissolved oxygen. The absorbance was set to zero with this solution. With a gas-tight syringe, 1 mL of reduced IC was transferred into the spectrometer vial. First, the syringe needle was inserted so that the needle tip was in between the septa of the 25-mL vial with reduced IC. After flushing the syringe (filling and emptying) 10 times with the N_2 flowing in between the septa, the syringe needle was inserted through the lower septum into the IC solution followed by an immediate withdrawal and transfer into the spectrometer vial The time acquisition of OOIBase32 software was initiated for monitoring the absorbance of the reagent

solution at 610 nm and 700 nm. The data acquisition rate was typically 1 data point every 4 s.

When sampling from the 125-mL septum bottle with a gas-tight syringe, the syringe was first flushed with N_2 to remove air before filling the syringe with sample. First, the top septum of the sample bottle was pierced with the syringe needle and it was flushed 10 times with N_2 as described for transfer of the IC. The needle was pushed through the lower septum and into the sample solution. The sample (0.5 mL) was drawn into the syringe, the needle was removed and immediately inserted through both septa of the DSV, and the sample was injected into the IC solution. The N_2 purge needles were removed from the bottle just before sampling so that the bottle could be tilted sideways and the syringe needle reached the sample solution.

In a similar way, when sampling with the pump, the tubing and pump were purged for 10 min by pumping N_2 from the sample bottle cap to the spectrometer vial. To implement the purging, the pump inlet needle was inserted in between septa of the sample bottle and the outlet needle was inserted in between septa of the spectrometer vial. After 10 min of N_2 flushing, the inlet needle was inserted into the sample solution and 1.5 mL of sample was pumped to the spectrometer vial into the gap of the DSV cap. Due to continuous N_2 flow in between septa of the cap, this portion of the sample was easily pushed out from the purge outlet tube and directed towards the waste. Then, the outlet needle of the pump was immediately inserted through the bottom septum and into the reagent solution and 0.5 mL of the sample

was pumped into the spectrometer vial. The needle was left in place until the reaction reached completion and the regular baseline slope was observed.

After the completion of the first reaction, normally another 0.5-mL sample was injected on top of the same reagent solution. Before the second injection, the pump sampling lines were flushed with 1.5 mL of fresh sample again as described above. In the case of a larger sample volume such as 1 mL, only one injection per vial was performed. Also, multiple small volume (5 - 100 μL) syringe injections (per one spectrometer vial) were performed for concentrated standards such as air-saturated water.

Gaseous standards (air) were introduced into spectrometer vial via gas-tight syringes. After drawing air into the syringe, the needle of the syringe was inserted into the reduced IC solution (contained in spectrometer vial) and the air standard was injected without delay.

Another type of air introduction into reagent solution was as trapped bubbles. Bubble-trapping experiments were developed to increase the time that an injected air bubble spends in the IC solution before it rises into the headspace. The needle was inserted into the solution towards the center of folded Pt wire. The air standard was injected very slowly (over ~10 s) such that an air bubble formed and was trapped inside the folded wire more that a couple of minutes. The syringe needle was removed from the DSV after the injection. For very small volume of air standards (1 - 3 μL), the syringe needle was not removed because it was possible to trap small bubbles in solution only when they kept contact with the needle.

Sampling from an anaerobic waste water bottle was conducted every other day to provide recovery time for microorganisms in case the sample was contaminated with oxygen. The background scattering was significant for some samples with particles smaller than 20 μm. To measure the background scattering signal, these cultures were sampled for a second time into 3-mL of a pH 7 buffer solution. To keep the total solution volume the same as before, 1 mL of extra buffer solution was used instead of reduced IC.

3.2.5. Calculations

During a run, the absorbance of the solution in the spectrometer vial was monitored with a data acquisition period of 4 s, which was continuously streamed to a data file as absorbance vs. time. Later, the data points were smoothed by averaging every 6 consecutive points. As seen in Figure 3.7, the observed absorbance change between times t_1 and t_2 after the injection of the sample has three components:

a) The dilution of the reagent with the sample (A_d)

c) The reaction of reduced IC with O_2 in the sample (A_{ox})

b) The baseline slope (A_b)

The absorbance of the reagent solution before the sample injection is A_1 at an initial time of t_1 with an initial volume of V_1 (3 mL). According to Beer's Law (6):

$$A_1 = \varepsilon b c_1 \quad \text{or} \quad A_1 = \varepsilon b \left(n_1 / V_1 \right) \tag{3.1}$$

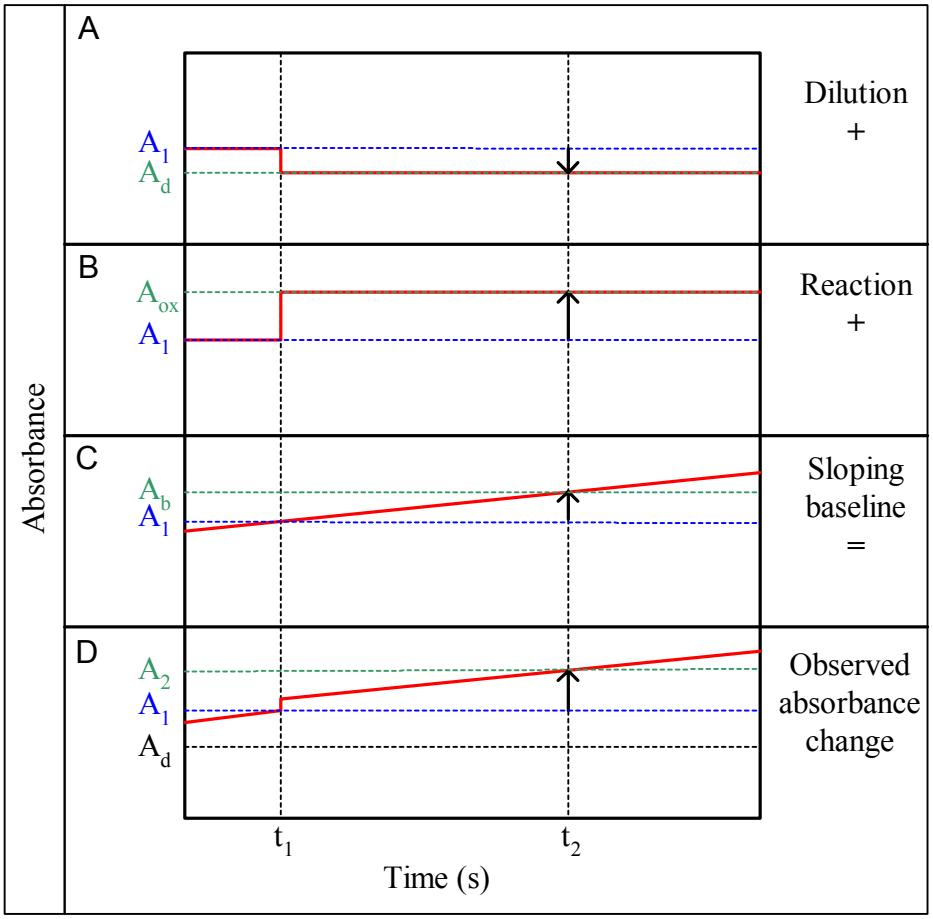

Figure 3.7 Schematic representation of the observed absorbance change of indigo carmine overtime and its significant components. A) Stepwise decrease in absorbance due to dilution of the reagent. B) Stepwise increase in absorbance due to dissolved oxygen in the sample. C) Continuous increase in absorbance due to contamination. D) Total observed absorbance change.

where n_1 is the initial number of moles of oxidized IC, b is the pathlength and ε is the molar absorptivity of IC (ox). After sample injection, the volume of solution in the cell increases to V_2 (3.5 mL) resulting in dilution and a decrease of the observed absorbance to A_d. To calculate only the effect of the dilution on initial absorbance, n_1 and the final volume (V_2) are considered:

$$A_d = \varepsilon b \left(n_1 / V_2 \right) \tag{3.2}$$

Substitution of equation 3.1 into equation 3.2 yields;

$$A_d = A_1 \left(V_1 / V_2 \right) \tag{3.3}$$

The baseline slope is due to slow oxidation of IC (red) with residual O_2 already in the spectrometer cell or continual O_2 contamination entering through the cap and the N_2 lines. This increase in absorbance (A_b) between t_1 and t_2 is calculated by multiplying the slope of the baseline (S) by the reaction period ($\Delta t_{ox} = t_2 - t_1$). In practice, the slope of the baseline was calculated over a period of 50 - 100 s after the reaction reached completion.

$$S = \Delta A / \Delta t \tag{3.4}$$

The estimated absorbance increase at t_2 (A_b) is calculated from equation 3.5,

$$A_b = S(\Delta t_{ox}) \tag{3.5}$$

The absorbance change due to the reaction of reduced IC and DO in the sample (A_{ox}) is calculated by subtracting other absorbances from the final observed absorbance (A_2);

$$A_{ox} = A_2 - (A_d + A_b) \quad (3.6)$$

In the case of sampling twice (each 0.5 mL) during the same run, the ratio of the initial and final volume of the solution (V_1/V_2) was different for each injection. Thus, A_{ox} for the second injection was multiplied by a correction factor (final volume for the 2nd injection divided by final volume of the 1st injection = 4/3.5) to enable the comparison of A_{ox} for the first and second injections.

For the measurements of blank solutions, the blank signal was denoted as $A_{bk.}$ The blank signal (A_{bk}) is the absorbance change due to the reaction of reduced IC and DO in the blank and is calculated with the same procedure as A_{ox}.

Concentrations of the standard solutions were calculated according to American Society for Testing and Materials' (ASTM) publications (2005). With the known fraction of O_2 in the gas mixture, barometric pressure and temperature, the concentration of dissolved oxygen in water could be calculated. Sample calculations are given in Appendix C.

The net absorbance change due to scattering (A_{sc}) was calculated with the same procedure that was used to calculate A_{ox} for a regular sample. The net absorbance change represents only the absorbance change due to scattering because without IC there was no reaction and no sloping baseline during these measurements. Then, the absorbance due to background scattering (A_{sc}) was subtracted from the blank-corrected absorbance (A_{ox}) obtained with the initial measurement with reduced IC.

3.3. Results and Discussion

3.3.1. Initial Studies

3.3.1.1. Choice of the Reduction Method

Pre-reduction of IC with a soluble reductant such as Ti(III) citrate or sulfide and H_2 were compared. The reduction of IC with H_2 (100%) in the presence of Pt wire catalyst was chosen as the method for further studies.

In the case of a soluble reductant, the reductant solution (deaerated with N_2) was injected into the N_2-purged double-septum vial (DSV) that contained the oxidized indicator solution. Because the exact concentration of an oxygen-sensitive reductant such as Ti(III) is difficult to know due to continued slow oxidation in its container, an excess of reductant was usually injected. As seen Figure 3.8, there is a significant re-oxidation of IC after reductant injection in the first couple hundred seconds and the rate of re-oxidation slows and eventually a constant positive slope is observed.

This initial relatively rapid re-oxidation after the rapid reduction may be due to the kinetics involved in the reactions between the redox indicator, O_2 and Ti(III). It appears that Ti(III) citrate reduces the indicator rapidly, but then some of the reduced IC is re-oxidized within minutes by some other undefined oxidant (see Appendix I for details). Once the majority of the oxidant is removed from the solution, the rate of re-oxidation decreases to the point that a relatively constant

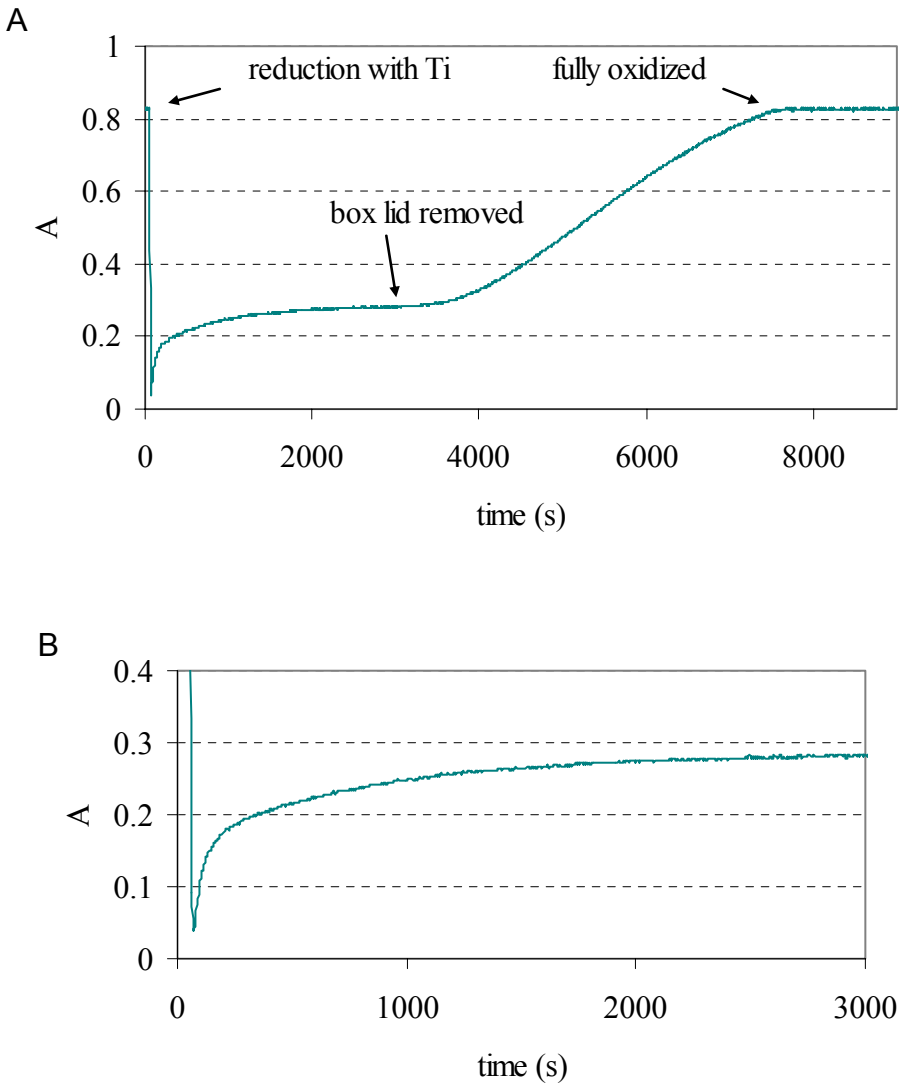

Figure 3.8 Reduction of IC with Ti(III) and the change in baseline slope with and without double containment of a single septum cuvette. A) The lid of the protective box was removed at 2936 s. B) A closer look at the equilibration time after the injection of Ti(III) citrate.

positive slope is observed at times typically longer than 2 min (3-40 min) after the Ti(III) citrate injection. The slow oxidation is attributed to O_2 diffusing from the headspace or the stirbar into the solution.

The response to injection of 25 μL of air-saturated water was not reproducible upon reduction with Ti(III) citrate. The imprecision may be due to variable amounts of unconsumed soluble reductant.

Other soluble reducing agents such as sulfide and DTT (dithiotreitol) solutions were tested for the reduction of IC. Even with excess amounts of sulfide or DTT (i.e., 10 times the number of moles of IC in the cell), the reduction was kinetically slow (15-33 min for ~90% reduction of IC) compared to Ti(III) citrate reduction of IC.

For further experiments, IC solution was reduced in a separate vial when H_2 was used as the reductant with Pt wire. Then, the appropriate volume of reduced IC solution was injected into the DSV. This procedure separates the reductant from the catalyst, and thus, eliminates the possibility of excess reductant in the sample vial. Sample throughput is also increased because it does not take 5 to 15 min for the baseline slope to stabilize as is does with Ti(III) injection.

Pt wire was preferred over Pt-coated alumina pellets (Aldrich). Disadvantages of pellets were sorption of the indicator onto the pellets and disintegration of the pellets over time. Upon disintegration, Pt powder could be transferred during the injection of reduced IC into the cell causing further reduction of the indicator during a sample run (Appendix D).

3.3.1.2 Minimization of Contamination with Double Containment

Contamination of the reagent solution by air leakage into the sample vial through the normal septum cap was evaluated. Methodology was developed to minimize the large positive baseline slope due to re-oxidation of reduced indicator. The effect of the double containment on a single-septum vial was tested by placing the cell holder into a polypropylene box that was purged continuously with N_2. As shown in Figure 3.8A, IC was partially reduced with Ti(III) citrate while in the box. After the rapid reduction and slower re-oxidation of the IC in the first 1000 s, an increasing baseline with constant slope (1×10^{-5} AU/s) was observed. When the lid of the box was removed, the only barrier left to the cell solution was the single-septum cap. Within 8 min after removing the lid, oxidation of the indicator occurred at an increased rate (1×10^{-4} AU/s). Double containment reduced the magnitude of the baseline slope by a factor of 10. Lower baseline slope is preferred because it makes it easier to detect small changes in absorbance due to O_2 in samples and it maximizes the time before the reagent must be changed because the absorbance goes off scale.

Initially rectangular and cylindrical vials with and without a double-septum cap were compared and the results are shown in Table 3.1. The type of septum cap used with a given type of cell did not significantly affect the initial slope. However, the baseline slopes with the vial were ~5 times greater than the baseline slopes using the cuvette regardless of the type of cap. This behavior is attributed to more efficient stirring and a higher transfer rate of oxygen from the headspace into the solution

Table 3.1 Comparison of baseline slopes for different cell and cap combinations. [a]

Type of cell	Type of septum cap	Initial baseline slope [b]		
		μAU/s (%RSD)	pmol O_2/min	nM O_2/min
Rectangular cuvette	Single septum	18 (44)	75	25
Rectangular cuvette	Double septum	22 (31)	91	30
Cylindrical Vial	Single septum	95	329	110
Cylindrical Vial	Double septum	130 (46)	450	150

[a] The reductant was H_2 with Pt as the catalyst. The vial contained a larger stir-bar (3 mm wide × 10 mm long) than the cuvette (1.5 mm wide × 8 mm long). Visually no surface turbulence in the cuvette was observed when filled with 3 mL of solution. The septum material was butyl rubber. The baseline slope in terms of pmol/min is calculated from the following formula S (pmol O_2/min) = [S (AU/s) x 10^{12} x 60 s/min x 0.003 L] / [2 x 21647 (AU/ M cm) x pathlength (cm)]. It is assumed that 1 mol of oxygen reacts with 2 mol of IC. The baseline slope in terms of nM/min is calculated from S (nM O_2/min) = [S (AU/s) x 10^9 x 60 s/min] / [2 x 21647 (AU/ M cm) x pathlength (cm)]. Pathlengths were 1 cm for the cuvette and 1.2 cm for the vial.

[b] The means and RSD are based on three measurements (n = 3) except for the cylindrical vial with the single septum for which n = 1.

when the larger stir-bar (3 mm x 10 mm) was used with the cylindrical vial. The cuvette only accommodated a rice size stir-bar (1.5 mm x 8 mm) and visually no surface turbulence was observed if filled with more than 2 mL of solution. The mixing speed of the rice size stir-bar was not reproducible and highly dependent on the alignment of the cuvette with the magnetic stirrer.

The vial was used instead of the rectangular cuvette for further experiments even though the baseline slope due to O_2 contamination is higher by a factor of 4 to 5. Reproducible mixing ensures more consistent results and rapid mixing of the reagent and added sample is essential to observed rapid oxidation of the indicator by the O_2 in the sample.

The rates of O_2 contamination shown in Table 3.1 are somewhat comparable with previous studies. Harbury (1953) measured the rate of oxidation of 10-mL of deaerated leuco indigo carmine solution (0.1 μM, 50% reduced dye) under a static atmosphere of helium. The estimated O_2 consumption due to O_2 in an inert gas tank (helium tank supplied by the United States Bureau of Mines) was reported as 1×10^{-8} equivalents of oxygen per hour (or 40 pmol O_2/min). This rate is within a factor of 2 observed in this thesis research with the cuvette where the stirring was inefficient.

During the previous research in this laboratory at OSU, Ruiz-Haas (2006) reported an oxygen permeation rate of 716 pmol/min (with continuous re-circulation but no mechanical stirring) into a microcosm bottle (250 mL). This rate was measured with thionine as the redox indicator, continuous N_2-purging of the headspace, and a flow loop with the microcosm bottle, a spectrometer flow cell, and

a peristaltic pump. The pump tubing was protected by enclosure in a chamber with ascorbic acid solution. The oxygen permeation rate with the microcosm bottle (716 pmol/min) is ~2 times the rate of oxidation (329-450 pmol/min) observed with the cylindrical vial (see Table 3.1). Comparing results of the two studies is difficult because the indicators, the reductants, the sample volumes, and the sample surface areas are different. Ruiz-Hass demonstrated that most of the contamination in the recirculating system occurred through the tubing and connectors of the solution loop outside of the microcosm bottle.

Artificial injections without sample delivery were performed to demonstrate the effect of piercing a single-septum vial and a double-septum vial without injecting solutions. As observed in Figure 3.9, the baseline slope increased about a factor of 10 after the single-septum vial was pierced 2 times. In contrast, the slope increased only with a factor of 2 after piercing the double-septum vial 3 times.

It is hypothesized that atmospheric O_2 passes through the septum into the headspace during the piercing action of a conventional septum cap vial and that the rate of oxidation of the indicator is proportional to the rate of transfer of O_2 from the headspace into the solution which in turn is proportional to the O_2 concentration in the headspace. With the double-septum cap, a significant fraction of the O_2 that passes through the first septum is purged out with N_2 before it reaches the bottom septum so that the vial headspace O_2 concentration remains lower. For further experiments, these newly designed double-septum caps were used to minimize contamination/air permeation into the vial through the septum during an injection.

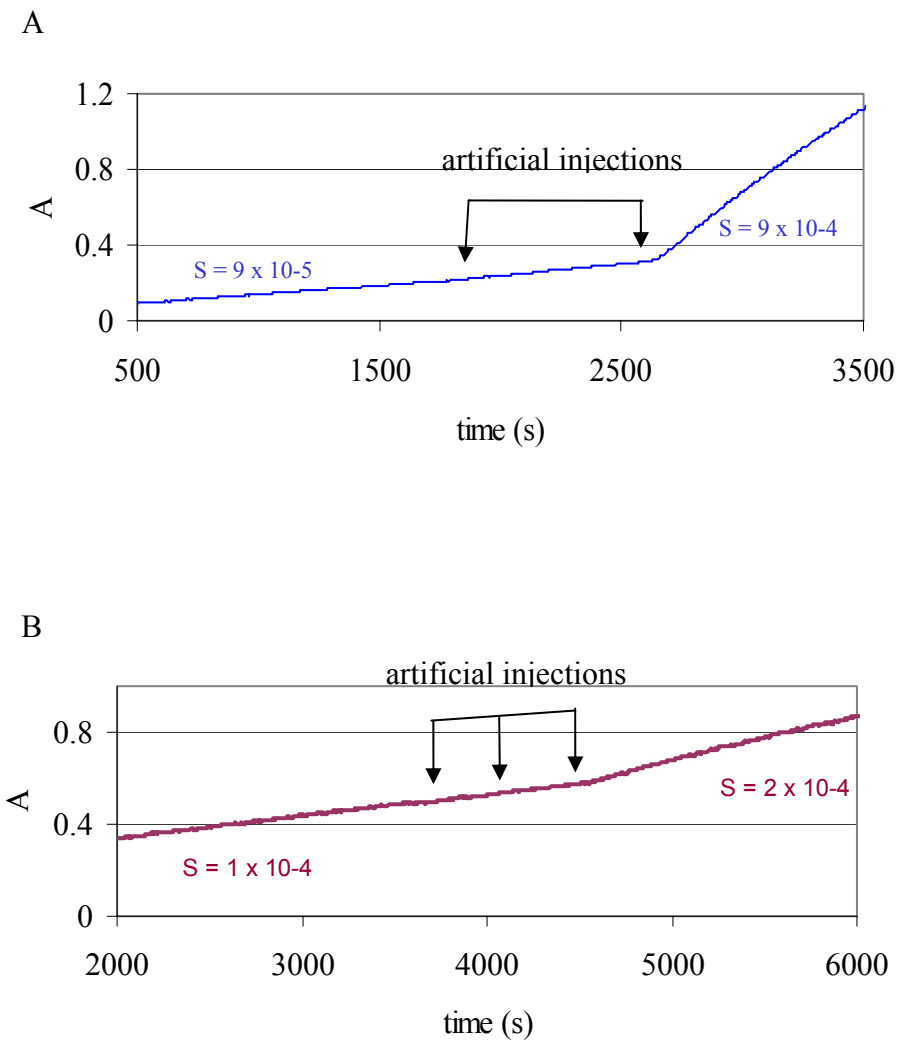

Figure 3.9 Effect of artificial injections on the baseline for the single-septum vial and the double-septum vial. The initial slope corresponds to the consumption of the oxygen at a rate of 34 nL of air/min for both: A) Single-Septum Vial B) Double-Septum Vial

3.3.1.3. Minimization of Sample Contamination during Pump Transfer

The materials of construction for all components of the system that are in contact with the test solution or reagent solution, the headspace over the test solution or the reagent solution are critical when sampling from an anoxic environment (Kjeldson, 1993). For flow systems, it is best to minimize the number of connections (e.g., 1/4-28) (See Appendix E). Although, all polymers are known to be permeable to oxygen, compared to glass and metals they are more flexible, easier to machine and sometimes less expensive. Polyetheretherketone (PEEK) connectors and tubing were preferred in this study due to PEEK's low oxygen permeability which is 6.4 x 10^{-10} cm^3 cm cm^{-2} $s^{-1}atm^{-1}$(Upchurch, 2007). Oxygen permeabilities of Tefzel (ethylene tetrafluoroethlene) and Teflon are 7 and 63 times higher, respectively, in comparison to PEEK. The septum caps for the vials and sample bottles were made of Delrin. The permeability of these caps is less relevant because they are sealed to the bottles with the septum and not in direct contact with the headspace.

The pump body, the inlet and the outlet connections are made of PEEK. Inside the pump, the material for the diaphragm and check valves is EPDM (ethylene propylene rubber). The oxygen permeability of EPDM is ~600 x 10^{-10} cm^3 cm cm^{-2} $s^{-1}atm^{-1}$ (Rutherford et al., 2005). Due to this high O_2 permeability, the micro pump is one of the main sources of contamination in the sampling system. However, submerging the pump head in a reductant solution or enclosing the pump in a N_2 purged box did not reduce the blank signal.

As discussed in the experimental section, the transfer tubing was purged for 10 min by pumping N_2 prior to sampling with the pump. Then, 1.5 mL of the sample, which is about 4 times the total internal volume of the sampling system (~0.35 mL), was pumped to further clean the lines of residual O_2. In initial studies (See Appendix F), different sample flush volumes were tested without a N_2 purge. The smallest blank absorbance (A_{bk}) or A_{ox} with a blank was 0.03 AU which was measured with a 15-mL sample flush which equals 43 times the total internal volume of the sampling system. The addition of a N_2 purge for 1 min (~3 mL) before a final blank washout (1.5-mL) reduced the blank signal by a factor of ~4 to 0.045 AU. Increasing the N_2 purge period to 10 min with the same blank rinse, lowered A_{bk} further to 0.023 AU. Further increases in the N_2 purge period were deemed not to be justified as they decreased the blank signal less than a factor of 2 and increased the analysis time by a factor of 2 or more. The removal of most of the residual O_2 from the sampling equipment with N_2 flow appears to be efficient and eliminates the need for excessive consumption of sample to purge the tubing.

Figure 3.10 shows the effect of delaying sample delivery on the blank signal and the signals for samples under methanogenic conditions. Sample injection delay time represents the time elapsed after the regular flush of the sampling-pump lines with the sample. The “blank” absorbance due to contamination of solution in the sample transfer line increased linearly with increasing delay time for both blank solutions and samples. The rate of O_2 contamination of the injected blank solution

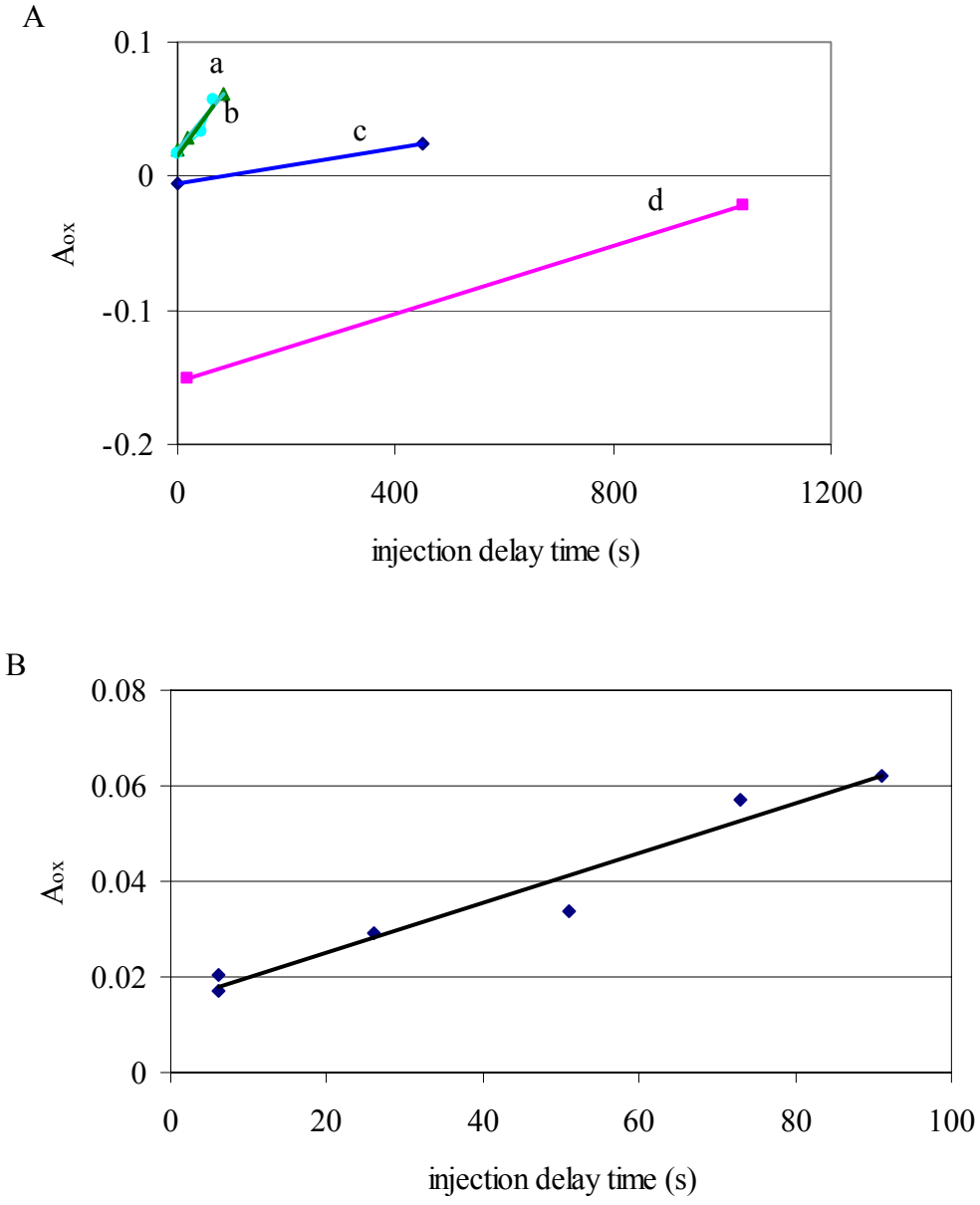

Figure 3.10 Contamination of the blanks and anoxic sample during delayed sampling with micropump. A) Two different blank solutions (a, b) and two different methanogenic samples (c, d) were sampled. Linear fits for the trend lines are as follows: a) $A_{ox} = (0.0006t + 0.015)$, b) $A_{ox} = (0.0005t + 0.019)$, c) $A_{ox} = (0.0001t - 0.005)$, d) $A_{ox} = (0.0001t - 0.15)$ B) A closer look at the contamination of blank solution during delayed sampling. $A_{ox} = (0.0005t + 0.015)$. The default delay time (t) of the injection is 6 s and the sample volume was 0.5 mL.

(0.48 mL) was 0.6 μM/min (277 pmol/min). Note that this contamination rate is about half the rate observed for the IC in the sample vial with the double-septum cap.

The O_2 contamination rate for the methanogenic samples was 0.1 μM/min (46 pmol/min)which is 6 times slower than the contamination of blank. This lower rate is an expected result because methanogenic conditions are very reductive and the sample may contain reductants that can react rapidly with O_2 (Starr M.P. et al., 1981).

The flow rate of the sampling pump was set to 48 μL/s (one stroke per second). The minimum time required to pump a 48-μL sample plug from the inlet (sample solution) to the outlet (sample cell) of the pump lines was ~7 s. Also, the practical value of the minimum sample injection time (the time for initiation of the sample or blank injection including the piercing action with the needle and adjusting the needle tip position into the reagent solution) was ~ 6 s. Hence, a sample or blanks spends a minimum time of about 13 s in the pump and pump lines before it reaches the spectrometer cell.

Figure 3.10B shows the increase in the blank signal over the first 100 s due to delayed sampling with the micropump sampler. At time zero, the extrapolated signal is positive (0.015 AU) and significantly larger than the standard deviation of the blank signal (typically, 0.004 AU). This intercept suggests that, even with no delay before initiation of the injection after the sample flush, some O_2 contamination occurred during the 7 s that the sample was being pumped through the transfer lines.

The effect of delaying sample delivery on the blank signal during sampling with the gas-tight syringe was also studied. The blank signal did not increase with longer injection delay times. Apparently the bulk of solution in the syringe is well protected by the glass barrel and most of the contamination may occur during the filling or the injection process.

One of the primary advantages of double-septum caps is that it enables purging of the sampling syringe/pump tubing with N_2 before the needle is inserted through the lower septum into the anaerobic sample medium. Thus, the sample solution encounters minimum contamination even if the first septum is somewhat compromised with holes from several injections. When the removable septum cap was attached onto the bottle during syringe sampling, A_{bk} was significantly lower (a factor of 4).

Another advantage of the removable septum cap is that it protects the contents of the sample bottle from O_2 contamination during injection. This is essential for the survival of obligate anaerobes over a long period.

3.3.2 Calibration

3.3.2.1 Calibration with Air

Calibration with air and solution standards was studied. Initially air injections were tested as gaseous standards. Headspace analysis would be very advantageous for gaseous species such as oxygen that have high air-water partitioning coefficient

(K_{aw} of 33 for O_2). The equilibrium concentration (moles per liter) of O_2 in the gas phase would be 33 times that of the dissolved oxygen concentration in the sample (Kjeldson, 1993).

The absorbance step due to air injections into the reagent solution was over a 100 times lower than expected and was not reproducible (see Figure 3.11). For example, the experimental absorbance step for a 100-μL air injection was 0.04 AU. The theoretical absorbance step, which was calculated with the ideal gas law and Beer's law, is 11 AU. A volume of air of 100 μL contains 860 nmol of O_2, and there were ~220 nmol of reduced IC in the sample cell. Because 1 mol of O_2 reacts per 2 moles of IC, all the IC should have been oxidized with ~8 fold excess O_2. The low absorbances for air standards, which will be discussed in further detail in this section, are attributed to inefficient transfer of O_2 from the bubbles into the reagent because the air bubbles spend little time in the reduced IC solution.

Air injections into the DSV headspace resulted in an increase in the slope of the baseline (see Figure 3.12) but no instantaneous step change. The 25-μL air injection increased the slope with a factor of 2 (from 2×10^{-4} AU/s to 4×10^{-4} AU/s).

The response to injected air was enhanced when the injected air bubbles were trapped in the reagent solution (within Pt wire) to prevent them rising up to the headspace of the vial for at least ~1 min. Figure 3.13 shows that the response is a broad peak rather than a step because the IC oxidized by O_2 is re-reduced by H_2. Continuous reduction was maintained by continuous purging throughout the experiment with H_2 with the Pt wire in the sample vial. The peaks until 140 min

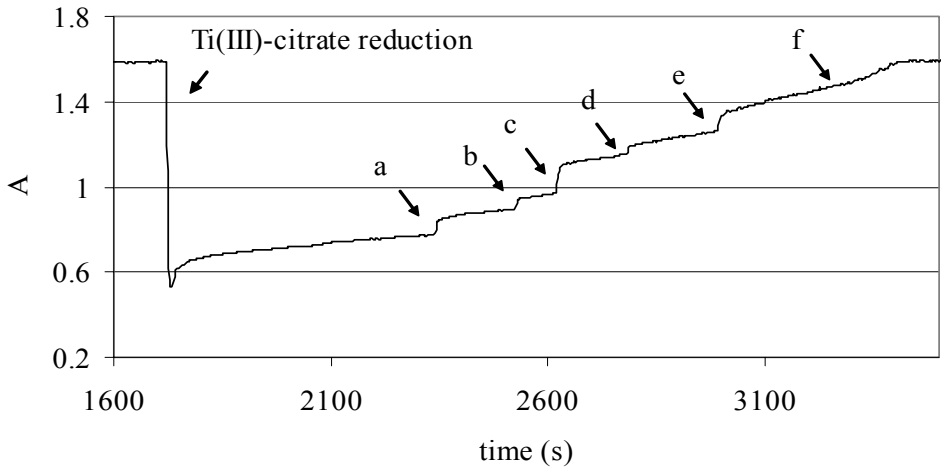

Figure 3.11 Stepwise absorbance changes due to air injections into the reagent solution after reduction with Ti(III)-citrate in a 1-cm cuvette. Volumes of air injections were as follows: a) 25 μL, b) 50 μL, c) 50 μL, d) 100 μL, e) 200 μL, f) vial opened to air.

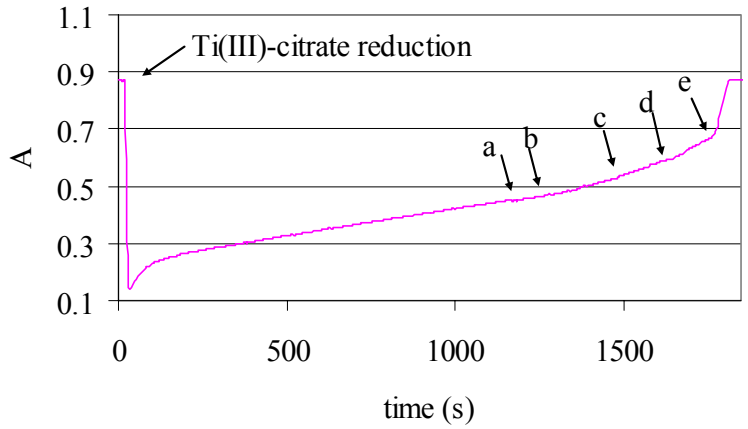

Figure 3.12 Change in baseline slope due to air injections into the headspace of a 1-cm cuvette after reduction with Ti(III)-citrate. Volumes of air injections were as follows: a) ~2 µL, b) 25 µL, c) 50 µL, d) 100 µL, e) vial opened to air.

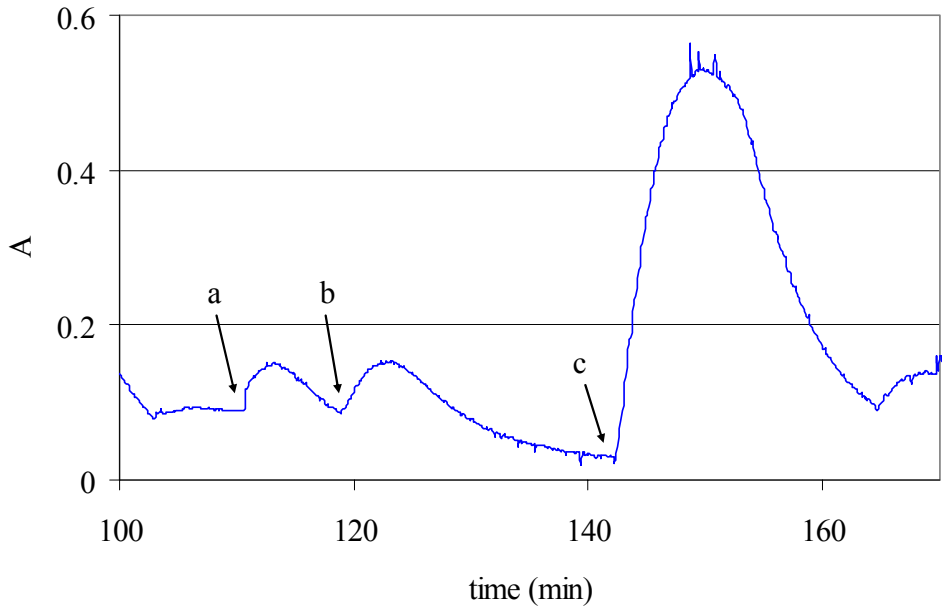

Figure 3.13 The response due to air injection into the IC reagent solution and trapping of the air bubbles with Pt wire. The IC was reduced with H_2 and continuously purged with H_2 throughout the experiment. Injected air standard volumes were a) ~2 µL b) ~2 µL c) 10 µL.

represent 2-3 μL bubbles. These bubbles were trapped for a short amount of time (~1 min) before they escaped to the surface. The largest peak was observed at ~150 min with the injection and trapping of 10-μL air bubble for ~8 min. The theoretical absorbance increase for a 10-μL air injection is 1 AU which was only 2 times larger than the experimental absorbance change (0.5 AU).

These results suggest that the transfer of the gaseous O_2 from air bubbles into the solution is slow. During a normal injection (without bubble trapping), most of the injected air reaches the headspace before the O_2 can diffuse into the reagent and react with the reduced indicator. Once the O_2 reaches the headspace, its concentration is greatly diluted which reduces its rate of diffusion back into the reagent solution. When the injected air is trapped in the solution, there is sufficient time for a large fraction of O_2 in the bubble to diffuse into the solution and react with the reduced indicator. Further experiments were not performed with gaseous trapped samples. Gas standards are not recommended because it is difficult to deliver and trap microliter scale gaseous samples reproducibly. Also the degree of contamination of gas samples during sample transfer would probably be worse than for solution samples because of the higher diffusion rate within the gas sample.

3.3.2.2. Calibration with Solution Oxygen Standards

Injection of solution O_2 standards was studied in detail. First, air-saturated water was injected because contamination during sampling is less of a concern at high DO concentrations. Figure 3.14 shows the step response over time during water

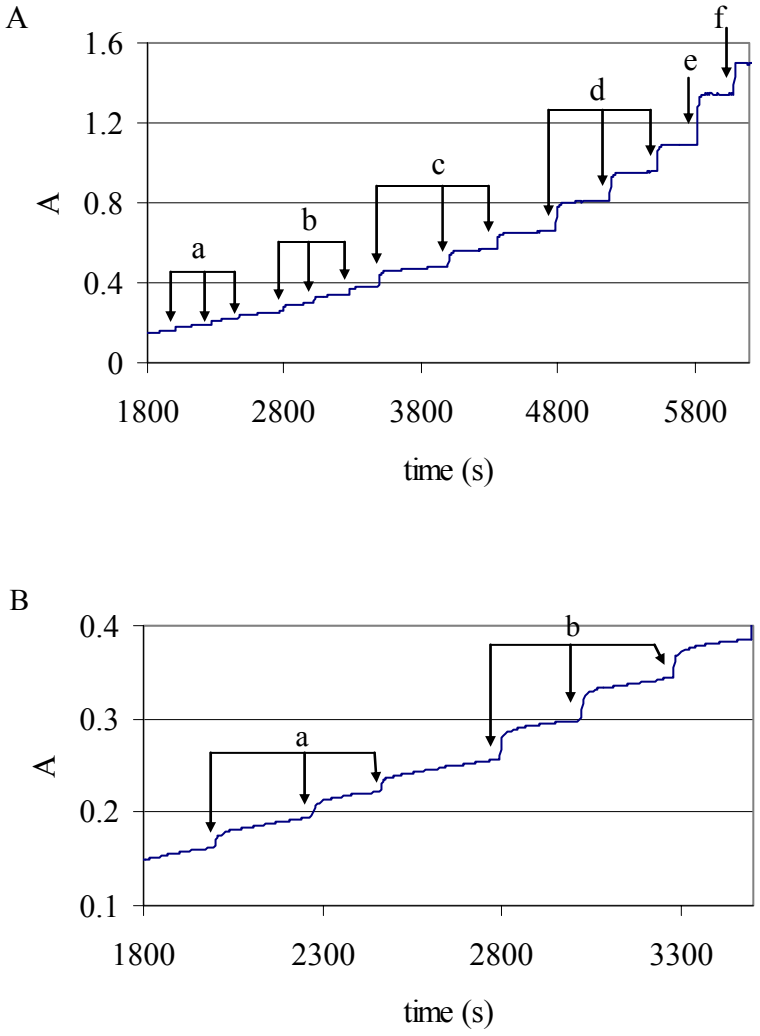

Figure 3.14 Stepwise oxidation with multiple injections of air-saturated water into the DSV containing reduced IC. The IC was reduced with H_2 in the presence of Pt wire. Volumes of injections were as follows: a) 5 µL, b) 10 µL, c) 25 µL, d) 50 µL, e) 100 µL, f) vial opened to air. Triplicates of 5- to 50-µL and one 100-µL water injections (A) were performed with 25-µL (pressure lok, Precision Sampling Corp.) and 250-µL (Hamilton #1825) gas-tight syringes, respectively. The DSV contained 4 mL of 600-µM reduced IC (pH 7). A more detailed view of the small-volume injections is given in part B. An injection of 5 µL of air-saturated water corresponds to a 0.3-µM increase in DO concentration in the 4 mL of reagent.

injections. The step increase is relatively rapid (30-50 s) and repetitive injections yield a staircase pattern. There is a continual baseline increase due to residual O_2 entering the reagent from the headspace or possibly diffusing out of the stirbar. The baseline slope decreased by a factor of 3 as the fraction of the reduced IC approached 0.3. This result is possibly due to slower reaction kinetics as the concentration of the reduced IC decreases by 70%.

The precision and the accuracy of the method are summarized in Table 3.2. The RSD was better than 5% for all standards. The measured absorbance step (A_{ox}) and theoretical (A_t) absorbance change are compared in the table and largest difference is 19% for the smallest volume injected (5 μL). The accuracy of 5-μL injections with the particular syringe (25-μL, Precision Sampling Inc.) was measured as 10%. There is a linear relationship between absorbance change and sample volume for the air-saturated water injections as demonstrated in Figure 3.15.

Low-level DO standard and blank solutions (0-1 mg/L) were measured following the analytical procedure given in section 3.2.4 of this thesis. Typical time profiles are given in Figure 3.16. The negative step of absorbance at the point of sample injection for 0.2 mg/L O_2 is clearly due to the dilution of the reagent with the blank. As the concentration of the standards increase, the major component of the signal becomes the absorbance increase due to the oxidation of reduced IC with DO (A_{ox}).

Response time is defined as the time for signal to reach a constant slope after the injection (i.e., the time for complete reaction). It was determined by

Table 3.2 The precision and accuracy of determination of dissolved oxygen in air-saturated water standards.

Volume injected (μL)	A_{ox} [a] (measured)	RSD of ΔA_{ox} (meas) (%)	A_t [b] (theoretical)	Difference [f] (%)
5 [c]	0.013	0.4	0.016	-19
10	0.028	3	0.032	-13
25 [d]	0.071	0.9	0.064	11
50	0.13	4	0.13	0
100	0.25	NA [e]	0.26	-4

[a] Average of A_{ox} for 3 consecutive injections that was corrected for baseline slope.
[b] Calculated from ideal gas law (T = 298 K, p = 1 atm) and Beer's law with b = 1.2 cm, ε_{610} = 21,647 M^{-1} cm^{-1} and the in-cell concentration of the injected standard (2 mol IC per 1 mol O_2).
[c] With an accuracy of 10 %.
[d] With an accuracy of 3 %.
[e] Not applicable because only a single injection was performed.
[f] $(A_{ox} - A_t) / A_t$

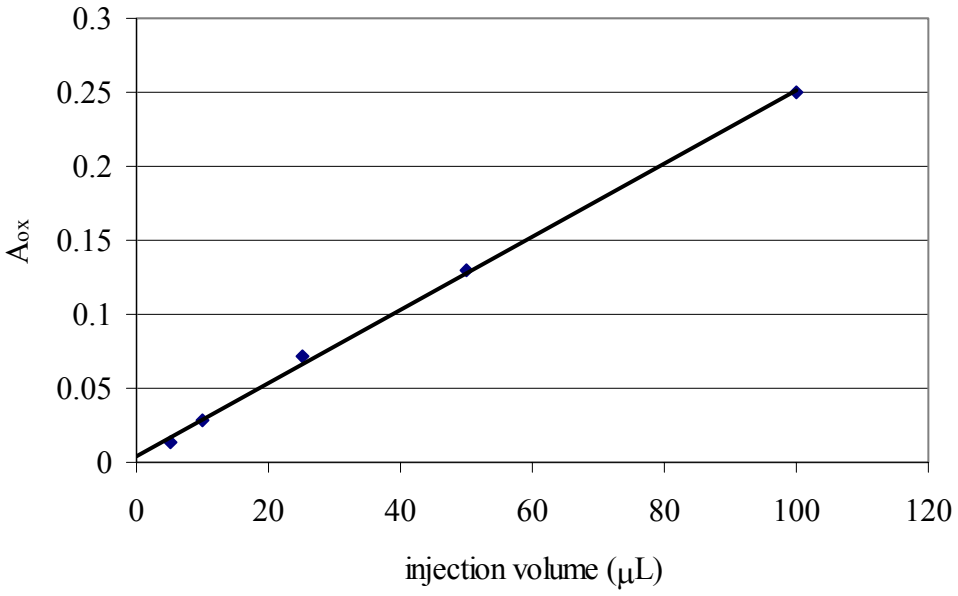

Figure 3.15 Calibration curve for injection of different volumes of air-saturated water. The linear fit is $A_{ox} = (0.0025V + 0.0045)$ where V is the injected volume standard errors: intercept = 0.0025; slope = 4.9 x 10^{-5} AU/μL.

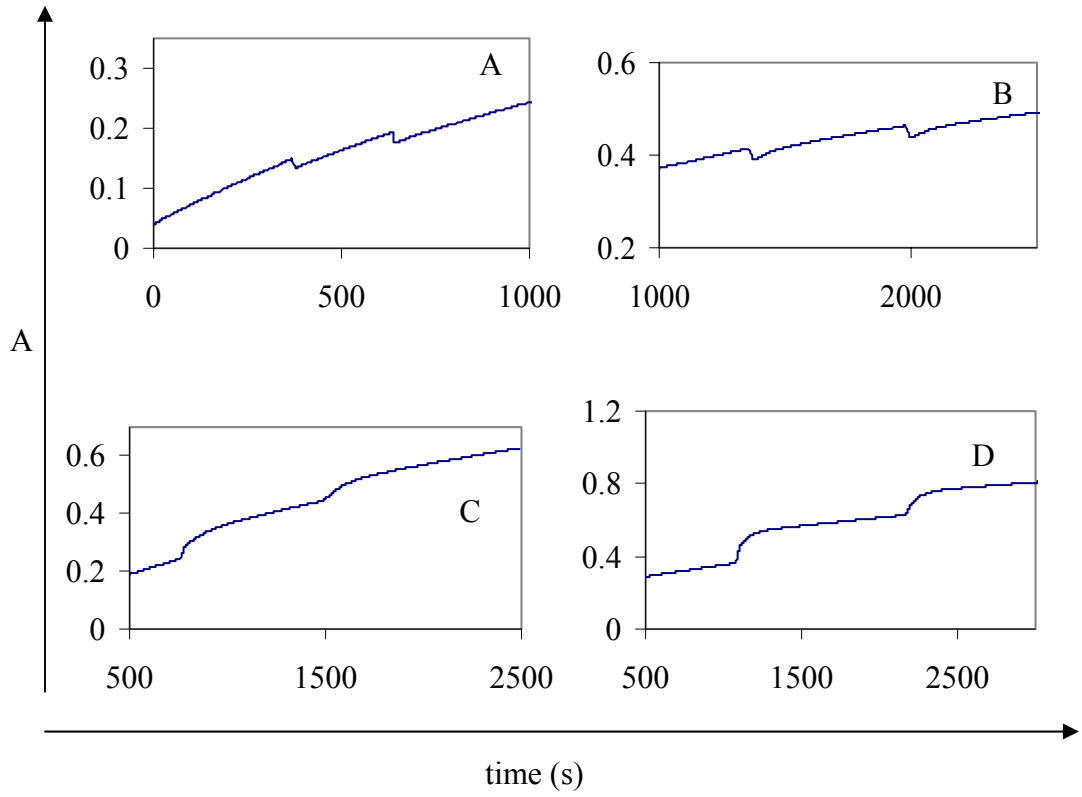

Figure 3.16 Typical time spectra for blank and standard measurements. Solutions were sampled as 0.5 mL with the micropump setup twice for each run. DO concentrations were A) Blank, B) 0.2 mg/L, C) 0.6 mg/L, D) 1.2 mg/L. In figures A and B, the dilution effect is dominant resulting in a negative step.

extrapolating the sloping baseline well after injection back toward the injection time and estimating where the experimental response is indiscernible from this extrapolated line. The response time for 0.2, 1.2 and 2.4 mg/L standards was measured as 2.6, 6.2 and 6.4 min, respectively. The IC-DSV method is intended for DO levels below 2 mg/L and thus, 6.6 min (400 s) was chosen as the default reaction period (Δt_{ox}) for all blanks, standards and samples. The times for 95% and 98% response for the 2.4 mg/L standard were estimated to be 3.7 and 4.8 min, respectively. The response time appears to be controlled by the kinetics of the oxidation reaction. The response time due to mixing (i.e., injection of a colored solution such as oxidized IC) is ~2 s.

For both sampling methods, A_{bk} typically varied over 0.008 - 0.03 AU. The average A_{bk} was 0.020 AU (n = 5) with a standard deviation of 0.004 with the portable flow sampler. Syringe sampling yielded an average A_{bk} of 0.022 AU (n = 5) with a standard deviation of 0.002.

Calibration curves (Figure 3.17) were constructed for the syringe and pump sampling methods. Ordinate values represent the blank-corrected absorbance (A_{ox}) for each standard that was measured twice in the same run. Abscissa values represent the concentration of dissolved oxygen in mg/L in the original sample. Absorbance values of the standard solutions (A_{ox}) were corrected by subtracting the average blank signals (0.020 and 0.022 AU). Relative standard deviations (RSD) were 7% and 4% for standards of 0.2 - 0.6 mg/L and 0.8 - 1.2 mg/L, respectively, when the micro-pump was used as a sampler. With the syringe sampling, RSD's were 6 - 4%

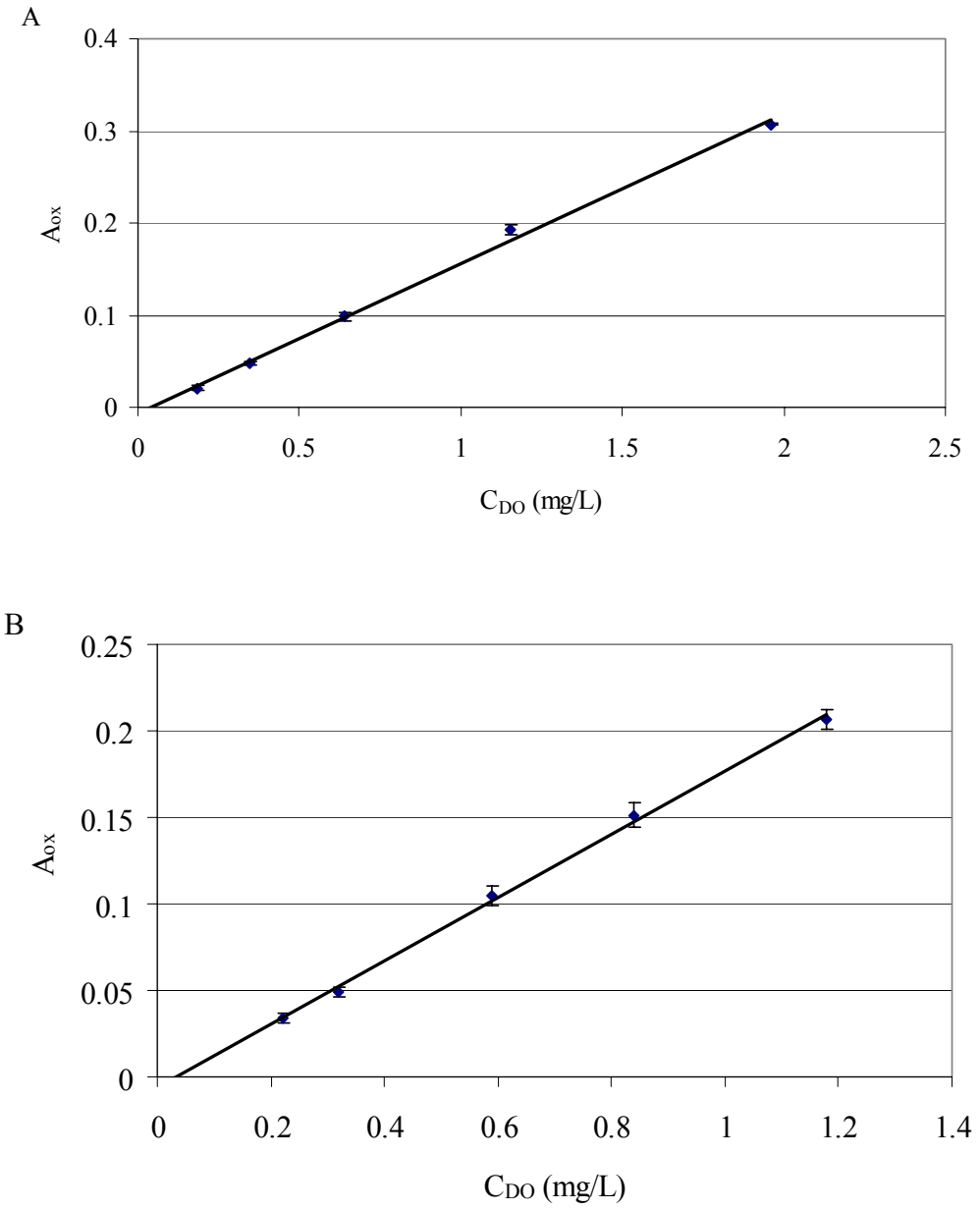

Figure 3.17 Calibration curve for low level DO standards sampled with a manual syringe (A) and a micropump (B). A_{ox} is corrected for blank signal.
A) $A_{ox} = (0.163\ C_{DO} - 0.0063)$, $R^2 = 0.9972$, standard errors of the slope and the intercept were 0.0064 for both.
B) $A_{ox} = (0.183\ C_{DO} - 0.0059)$, $R^2 = 0.9967$, standard errors of the slope and the intercept were 0.0059 and 0.0074, respectively.

for 0.2 - 0.6 mg/L and 2 - 0.3% for 0.8 - 1.2 mg/L. A standard with a DO of 0.1 mg/L was also measured with syringe injection and the SD of two measurements and RSD were 0.002 AU and 8%, respectively.

The slope of the calibration curve with syringe injection is ~11% less than the slope with micropump injection. The intercepts are within one standard deviation of the blank signal. The reasons for this difference are not known, but the standard errors in the slopes are about 4%. The injection volume with the syringe is actually 4% greater. It is possible that the calibration of one of the mass flow controllers used to prepare the standards changed. The calibration of the mass flow controllers was checked annually with a digital flowmeter.

The detection limit (DL) was calculated as the concentration that corresponds to a signal 3 times the standard deviation of the blank signal (n = 5). Detection limits of the DSV-IC method are 0.037 mg/L and 0.066 mg/L for the syringe sampling and the pump sampling, respectively.

The precision of a blank measurement appears to be limited by the variability of O_2 contamination. Details of the evaluation of the precision of the blank measurements are given in Appendix G. The standard deviation due to the random error in the volume delivered, instrumental noise, and dilution correction was determined by injecting an absorbing solution (oxidized IC). With the portable sampler, this standard deviation was 0.0008 AU (0.8% RSD) which is significantly less than the standard deviation of the real blank signal with the pump sampler (0.004 AU). The baseline slope does decrease significantly over the measurement

period and results in an acceptable error in the correction for baseline slope and the value of the blank absorbance. This error does not affect the accuracy of calibration correction for sample measurements or the precision of measurements.

The accuracy of the preparation of the blanks and standards were evaluated with "Oxygen CHEMets" which is a standard method for low level dissolved oxygen in ASTM (2005). Oxygen CHEMets colorimetric test kits (K-7540 and K-7501) contain reduced indicator Rhodazine D that is oxidized by oxygen in the aqueous sample. The sampling procedure for Rhodazine D ampoules (K-7540) was modified such that standard solutions were measured in-situ and did not include the transfer of the sample via a syringe or flow system. Excluding the sample/standard transfer step reduces the contamination of the sample during sampling. However, our modification of in-situ sampling into Rhodazine-D ampoules is not applicable for a real laboratory sample because the septum bottle is opened to air.

The DO concentrations determined with the CHEMets Rhodazine D method and IC-DSV method in this study are compared in Table 3.3 for a blank and a low concentration standard. There is no detectable O_2 in the blank with either method. For the IC-DSV method, the signal for the blank was corrected with the value for a typical blank. The average concentration in the low standard (0.2 mg/L) that was determined with the Rhodazine D method (C_{RD}) agree very well with the theoretical concentrations (C_t) and the concentration that was determined with IC-DSV method (C_{IC}).

Table 3.3 Comparison of IC-DSV method and Rhodazine-D method

C_t (mg/L) [a]	C_{RD} (mg/L) [b]	C_{IC} (mg/L) [c]
0.0	ND [d]	ND [d]
0.21 (0.002)	0.2	0.22 (0.01)

[a] Theoretical concentration for the DO standard. The SD is given in parenthesis and is estimated based on a fluctuation of 1 digit in the least significant digit of the readout.
[b] Average concentration (n = 2) determined with Rhodazine-D methods with MDL of 2.5 μg/L (K-7540) for the blank and 0.025 mg/L (K-7501) for the standard. The method provides only 1 significant figure.
[c] Average concentration (n = 2) determined with IC- DSV Method (DL = 0.04 mg/L with blank correction. The SD is given in parenthesis.
[d] Not detected (below detection limit)

The method detection limits for K-7540 test kit given by the manufacturer is 0.0025 mg/L which is 16 times lower than the DL of the IC-DSV method. The better detection limit with the Rhodazine D method is possibly due to longer pathlength (~8 cm) and the higher absorptivity of Rhodazine D relative to IC which was determined to be a factor of 3 higher than for IC (see Appendix J). These factors provide a higher calibration slope or absorbance for a given DO concentration in the sample. The improved detection limit also depends on the sampling procedure which reduces contamination due to sample transfer and possibly the blank standard deviation which was not evaluated here (ASTM, 2005).

The summary of calibration and blank data for different sample volumes is given in Table 3.4. Because the number of samples or blanks is small, a difference between two standard deviations or detection limits of a factor of 2 is not statistically significant.

The calibration slope of indigo carmine method was ~2 times higher when sample volume was increased to 1 mL from 0.5 mL. However, the detection limit did not improve because the standard deviation of the blank measurements also increased by a factor of 2.

In addition, one-point calibration slopes were calculated for indigo carmine and Rhodazine D with air-saturated water (50 μL) as a high DO standard and the blank standard deviation was evaluated with a 100 μL blank. To estimate the DL with the blank data, the slope with the 50-μL standard was doubled. As expected, the calibration slope with IC for a 50-μL volume was ~10 times smaller than the

Table 3.4 Summary of the calibration and DL data for indigo carmine (IC) and Rhodazine-D (RD)

Indicator/ injection technique	Injected volume (mL) (%RSD)	Standard solution [e]	Number of calibration points	Calibration slope (AU-L/mg)	Blank signal (AU)	Blank SD (AU)	DL [a] (mg/L)
IC/Pump	1 (0.06)	Air-N_2 purged	3	0.371 (0.212)	0.023	0.008 (n = 7)	0.065
IC/Pump	0.5 (0.05)	Air-N_2 purged	5	0.183	0.020	0.004 (n = 5)	0.066
IC/Syringe	0.5 (2)	Air-N_2 purged	5	0.163	0.022	0.002 (n = 5)	0.037
IC/Pump	0.05 (3)	Air-saturated	1 [b]	0.0161 (0.140) [c]	0.006 [f]	0.002 (n = 5) [f]	0.19
IC/Syringe	0.05 (0.4)	Air-saturated	1 [b]	0.0157 (0.139) [c]	0.005 [f]	0.002 (n = 6) [f]	0.19
RD/Syringe [d]	0.05 (0.4)	Air-saturated	1 [b]	0.0493 (0.430) [c]	0.008 [f]	0.001 (n = 5) [f]	0.031

Table 3.4 Summary of the calibration and DL data for indigo carmine (IC) and Rhodazine-D (RD)

[a] Detection limit (DL) = 3 x blank standard deviation / calibration slope. For lower volume injections, the calibration slope for the DL calculation is taken as 2 x (3.05/3.1) of the slope for the 50 μL injection.
[b] Intercept set to zero.
[c] The calibration slope in parenthesis is normalized to what the slope would be if the volume of the standard was 0.5 mL with the same DO concentration as in the original sample volume. The normalization factor for low volume standards is 10 x (3.05/3.5) where the first factor accounts for increase in moles of O_2 added and the second factor accounts for the final dilution factor.
[d] Rhodazine-D was reduced with H_2 in the presence of Pt wire and was tested as another indicator for the procedures given in section 3.3 of this thesis (see Appendix J for details).
[e] Deionized water purged with air and N_2 to yield standards with DO in the range of 0.2 to 1.2 mg/L or stirred open to air to yield a DO of 8 - 9 mg/L.
[f] The volume of the blank solution was 100 μL.

calibration slope obtained with a 0.5-mL sample volume. Because the blank standard deviation was the same with 0.5-mL and 0.1-mL sample volumes, the DL was ~5 times worse (higher) with a 50-µL sample volume.

Note that similar calibration slopes are obtained when the DO concentration in 50-µL air-saturated water is normalized to a larger sample volume (0.5 mL). The absorbance measured for a given standard or sample depends on the number of moles of oxygen added and the final solution volume as was demonstrated with the data in Table 3.2. Thus, the measurement of a smaller volume air-saturated water standard is a reliable and fast calibration methodology and is suitable for field studies or in the laboratory. It eliminates the need to prepare and store a low concentration DO standard for a short term that can become contaminated.

The one-point calibration with Rhodazine D with the double-septum vial yielded a calibration slope that is ~3 times the calibration slope with IC with the same conditions because the molar absorptivity of Rhodazine D is higher (see Appendix J). The detection limit based on a 100 µL injection volume with Rhodazine D is ~6 times better than with IC because of the higher calibration slope and the lower blank standard deviation. Note that this DL with Rhodazine D is effectively the same as obtained with 0.5 mL of IC.

As shown in Table 3.4, the blank signal is significantly lower with a smaller injection volume. Because the absolute error in the baseline slope correction is about 0.005 AU (Appendix G), there is high uncertainty in these small blank signals.

Effectively, the oxidation contamination becomes insignificant or buried in the noise with sample volumes of 100 μL or less and syringe injection.

The blank standard deviations with lower sample volumes are not significantly different from the blank standard deviation (~0.001) due to the precision of the sample and buffer volumes delivered, instrumental noise, and random error due to the corrections for dilution and baseline slope. Basically, the blank contamination signal becomes small enough that variations in the level of contamination are no longer discernible.

3.3.3. Determination of Dissolved Oxygen in Wastewater Samples

Three types of wastewater samples were evaluated for DO. With conditions favoring Fe(III)-reducing bacteria, Fe(II) concentrations reached 50 - 100 μM within a week and continued to increase suggesting high anaerobic microbial activity in sample bottles (see Figure 3.18). However, measured DO concentrations were not reproducible and approached levels as high as 1 mg/L. The large apparent DO value was caused by the interference from the large amount of Fe(III)-hydroxides in the sample that oxidize reduced IC.

Injection of a 1% (w/v) $FeCl_3$ solution to pH 7 into the DSV resulted in positive interference similar to anaerobic samples. Iron was reported as the most abundant interfering element in field measurement of dissolved oxygen in groundwater (Wilkin, 1990 and White, 1990).

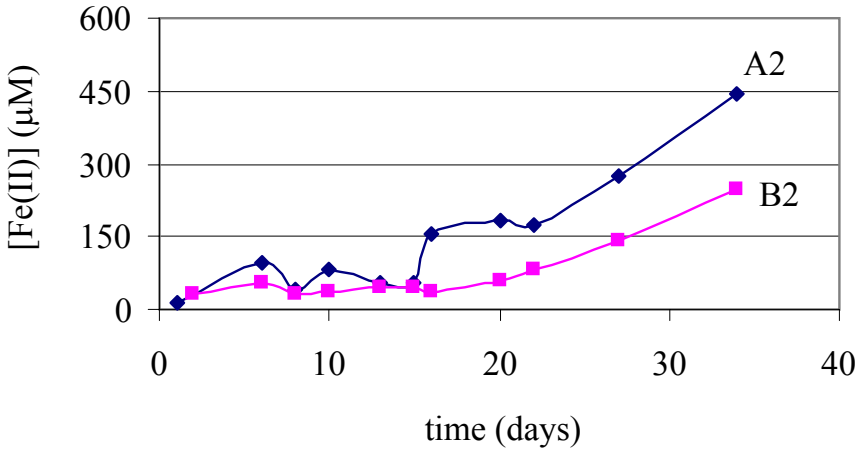

Figure 3.18 Time dependence of Fe(II) concentration in wastewater samples under iron-reducing conditions. Septum bottles A2 and B2 were sampled every other day with a gas-tight syringe.

Sulfate-reducing bacteria samples were monitored for sulfide and after 3 days of inoculation, sulfide concentrations exceeded 47 μM (1.50 mg/L) suggesting highly anaerobic conditions. Results of DO determination in 3 different samples are given in Table 3.5. All of the measurements yielded negative absorbances and DO values below the detection limit of 0.04 mg/L. When samples were measured after the 2nd or 3rd day of inoculation, the corrected absorbance step was negative. This behavior is attributed to reduction of IC by reductants in the highly reducing anaerobic sample.

Methanogens require lower reduction potentials to replenish compared to sulfate- and iron-reducing bacteria. Thus, methanogenic conditions have lower tolerance to oxygen (Starr M.P. et al., 1981). Two weeks after inoculation, biogas production was inferred from bulging of the septa. Methanogenic conditions were reached and CH_4 levels in the headspace of samples were measured as 40-50% (v/v) after a month. Results of DO determination in 6 different samples are given in Table 3.6. Most absorbance values are negative and all of the measurements yield DO values below the detection limit. After 30 to 40 days, samples started to further reduce IC. Apparently, the samples become anaerobic and produce more reducing agents over time.

The absorbance values due to scattering (A_{sc}) values were in the range of 0.00 - 0.024 AU and 0.024 - 0.040 AU for samples governed by methanogenic and sulfate reducing conditions, respectively. The absorbance values before correction for scattering were in the range of 0.018 to 0.041. Even without this background

Table 3.5 Results for wastewater samples under sulfate-reducing conditions.

Bottle ID	time after preparation (days)	A_{ox} (AU) [a]	Sampling with pump/syringe	C_{DO} (mg/L)
S1	10	-0.007	syringe	ND [b]
S1	11	0.001	syringe	ND
S3	2	-0.07	syringe	ND
S4	3	-0.06	syringe	ND
S4	6	-0.01	syringe	ND
S4	6	-0.009	syringe	ND
S3	6	0.0007	pump	ND
S3	6	-0.0004	pump	ND

[a] A_{ox} is for n = 2 and blank corrected and corrected for scattering. The average blank absorbance was 0.02 AU.
[b] ND = Not detected

Table 3.6 Results for wastewater samples under methanogenic conditions.

Bottle ID	Time after preparation (days)	A_{ox} (AU) [a]	Sampling with pump/syringe	C_{DO} (mg/L)
M3	13	0.02	syringe	ND [b]
M3	27	-0.004	syringe	ND
M1	30	-0.02	syringe	ND
M5	20	-0.01	syringe	ND
M4	20	0.0003	syringe	ND
M6	32	-0.03	pump	ND
M7	39	-0.03	pump	ND
M7	46	-0.2	pump	ND

[a] A_{ox} is for n = 2 and blank corrected and corrected for scattering. The average blank absorbance was 0.02 AU.
[b] ND = Not detected

scattering correction, the measured oxygen concentration was below the detection limits in all samples.

3.4. Conclusions

A new method has been developed and validated for determining DO concentrations as low as 0.1 mg/L in small sample volumes of 0.05 to 0.5 mL. It is based on the well known oxidation reaction of reduced indigo carmine (IC) with O_2 and includes sample transfer with a syringe or a micropump. The design and materials in the apparatus were carefully evaluated and chosen to minimize O_2 contamination. Novel critical components include the double-septum cap and the removable septum cap. The double-septum cap minimizes the atmospheric contamination of H_2-reduced IC in the reagent vial and in the spectrophotometer vial after reagent transfer and the removable septum cap for microcosm bottles minimizes contamination of the sample. The new method was evaluated with microcosm bottles under sulfate-reducing and methanogenic conditions. As expected, no O_2 was detected in these very anaerobic systems. The sample throughput is about 20 min per sample with pump sampling and 8 min per sample with a syringe.

The reported sampling methodology and instrumentation allows the transfer of a low-level DO samples from a closed anoxic system, such as a microcosm bottle or column, where the sample volume is limited. The total consumption of the sample is ~2 mL which includes the volume necessary for purging the sampling device to eliminate the previous sample and to minimize O_2 contamination occurring after the previous sampling. This volume is 100 to 1000 times less than the volume required with conventional DO methods such as the Winkler titration or CHEMets Rhodazine-D DO kits (ASTM, 2005).

The detection limit (DL) of 0.05 mg/L, obtained with the proposed methods, is a factor of 4 or 5 times better (lower) than that achieved with the Winkler titration (APHA, AWWA and WEF, 1989) and the Clark-type DO probe (Hitchman, 1978) and equivalent to that reported for the fluorescence optrodes (ASTM D888-05, 2005). Some of the commercial kits, based on the visual detection of oxidized IC or Rhodazine D, provide a DL that is a factor of 10 to 50 better than 0.05 mg/L. The CHEMets' Rhodazine-D visual method (Dissolved Oxygen ULR CHEMets for 0-20 ppb (K-7511) has the lowest reported DL (0.001 mg/L) with a sampling procedure that requires 1 to 2 L of sample prior to analysis. The lowest reported DL with IC and a CHEMetrics kit (K-7503) is 0.2 mg/L and is based on instrumental measurement of the absorbance. The best DL with IC and Hach AccuVac Ampules is based on instrumental measurement of the absorbance and is 0.006 mg/L. The methods based on ampules with pre-reduced indicator perform well because the sample transfer takes place with the ampoule immersed in the sample. Thus, O_2 contamination is minimized. The calibration slope is higher for this method because of little dilution (the ratio of sample volume to reagent is high) and a longer pathlength.

Standards or samples with DO concentration less than 10% of saturation can not be stored unless sealed in an ampoule because they become contaminated within seconds. With conventional DO methods, transferring the sample requires the consumption of the large volumes of sample (typically more than 300 mL) to washout the sample bottles, overflow sampling cells, or flow cells prior to sampling or

measurement. Ideally, in-situ measurements overcome this problem if the sensor is deployed into the anoxic sample and does not require sample transfer.

The blank standard deviation and detection limit (DL) of IC method with double-septum vial and a 0.5 mL sample appears to be limited by the variability of O_2 contamination of the blank during transfer. The level of contamination with the micropump increased as the time delay between rinsing the sample tube and the injection increased. Contamination also occurs with the gas-tight syringe, but the contamination level does not increase significantly with the time delay before injection as it does with the micropump. Hence, control of the time between filling the syringe and injection is not as critical as it is with the micropump. Thus, the use of gas-tight syringe is recommended for transfer of lower DO samples coupled to double-septum capped containers. For smaller sample volumes, such as 50 or 100 μL, the blank signal is less and blank standard deviation is due to instrumental noise.

The instrumental system could be configured into a relatively compact package for bench-top or field analysis. The ideal system would have no removable connectors and minimum moving parts and would be made of materials that have no permeability to gases such as glass and metals. In reality, such a system is difficult to build and must still involve purging with inert anoxic gases. Another approach is scavenging of atmospheric O_2 from internal components in contact with the sample with a reducing agent solution prior to analysis. However, most reducing agents consume the dissolved O_2 in the sample and interfere with the measurement so that they would have to be rinsed with purged water or the sample.

Measurements with reduced Rhodazine D and the presented instrumentation and methodology provided a detection limit of better than 0.05 mg/L with a 100-μL sample volume. The higher molar absorptivity of Rhodazine D relative to IC increased the calibration slope by a factor of 3 without an increase in the blank standard deviation.

For future studies, the use of Rhodazine D or another redox indicator with a higher molar absorptivity than IC should be explored further. A higher calibration slope results in a larger baseline slope and eventually larger blank signals and blank standard deviations for larger sample volumes such as 0.5 mL. The maximum improvement in detection limit with larger sample volumes will be ultimately limited by contamination of the blank (or a low DO sample) with O_2 during the sample transfer process.

Further improvements in DL can only be achieved by minimizing the blank standard deviation by reducing the contamination of blanks and samples. It might be possible to wash out the micropump sampling lines with a greater excess of sample with the penalty of a larger required sample volume. Micropump sampling has the potential to be automated but it appears it is easier to control O_2 contamination with syringe sampling. The positive baseline slope in the reagent absorbance before sample injection is a clear indication of O_2 contamination from the headspace or diffusion out of materials in contact with the solution. Further minimizing this baseline slope would make it easier to determine the increase in absorbance due to the sample and errors caused by the correction for the sloping baseline. It might be possible to incorporate

electrodes into the sample to implement continuous reduction of IC to maintain a more stable baseline.

Further development is needed to make the method more suitable for field analysis. The software should be refined to eliminate the need to manually transfer data into a spreadsheet and to determine which data to use to extract the absorbance value used for calibration plots. For field analysis, the IC should be pre-reduced and brought to the field in a double-septum cap vial with H_2 in the headspace and Pt wire in the vial. A one-point calibration with a small-volume standard (e.g. 50 μL) of air-saturated water is suggested to eliminate the need to bring prepared standards to the field. A small tank of nitrogen is required for purging between the septa of the double-septum cap and the headspace in the spectrophotometer vial.

For sampling of wells, the sample should be drawn from a septum-capped flow cell in line with the sampling line from the well that allows the sample to be taken before it becomes significantly contaminated. The flow cell should be placed before the inlet of any pumps on the surface. This concept was evaluated in this research with N_2-purged water pumped through a flow cell from a large container (Appendix H). The blank signal and blank standard deviation were equivalent to those obtained with N_2-purged water from a microcosm bottle.

3.5. Acknowledgements

This research was supported by a research grant from the U.S. Environmental Protection Agency sponsored Western Region Hazardous Substance Research Center under agreement R-828772. This article has not been reviewed by the agency, and no official endorsement should be inferred. We appreciate the patience, effort and skill of Ted Hinke at the Machine Shop and Joe Megner at the Electronics Shop of the Department of Chemistry at Oregon State University for construction of double-septum caps and micropump interfacing, respectively.

3.6. References

Annu. Book ASTM Stand. **2004,** *11.01,* D888-03, 59-67.

Annu. Book ASTM Stand. **2005,** *11.01,* D888-05, 60 -70.

Annu. Book ASTM Stand. **2005,** *11.02,* D5543-94, 759 -765.

Bishop, E. *Indicators*, Pergamon Press: New York; 1972.

Carignan, R.; St-Pierre, S.; Gachter, R. *Limnol. Oceanogr.,* **1994**, *39(2)*, 468-474.

Chapelle, F. H. *Ground-water Microbiology and Geochemistry*, Wiley & Sons: Canada; 2001.

CHEMetrics product specifications in www.chemetris.com, 2007.

Freeman, B.D.; Pinnau, I. *Polymer membranes for gas and vapor separation chemistry and materials science;* ACS Symposium series 733; 1999; pp 3.

Furuya, K.; Harada, K. *J. Oceanogr.*, **1995,** *51*, 375-383.

Green, F. J. *The Sigma-Aldrich Handbook of Stains, Dyes and Indicators*, Aldrich Chemical Company: Wisconsin; 1990.

Garner, S. *Ground Water Monit. Rem.,* **1988,** *8(3),* 60-66.

Harbury H. A. *J. Am. Chem. Soc.,* **1953**, *75*, 4625. In *Oxidation-Reduction Potentials of Organic Systems;* Clark, W. M.; Williams and Wilkins: Baltimore, 1960; pp 304-305.

Hungate, R. E.; Smith, W.; Clarke, R. T .J. *J. Bacteriol.,* **1966**, *91(2)*, 908-909.

Hitchman, M. L. Measurement of Dissolved Oxygen, In *Chemical Analysis, v. 49* (ed. by Elving, P. J.; Winefordner, J. D.; Kolthoff, I. M.), Wiley-Interscience: New York, 1978; pp. 130-159.

Ingle, J. D. Jr.; Crouch, S. R. *Spectrochemical Analysis*; Prentice-Hall: New Jersey; 1988.

Jones, B. D., Applications of redox indicators for evaluating redox conditions in environmental samples. Ph.D. thesis, Oregon State University, Corvallis, OR. 1999.

Kjeldson, P. *Water Res*., **1993**, *27*, 121-131.

Mah, R. A.; Smith, M. R. In *The Prokaryotes*; Starr, M. P.; Stolp, H.; Trüper, H. G.; A. Balows & H. G. Schlegel. Springer: Berlin, 1981; pp 948-977.

Muray, J. W.; Codispoti, L. A.; Friedrich, G. E. *Adv. Chem. Ser.*, **1995**, *244*, 157-76.

Park, E. J.; Reid, K. R. Tang, W.; Kennedy, R. T.; Kopelman, R., *J. Mater. Chem.*, **2005**, *15*, 2913-2919.

Rose, S.; Long, A. *Ground Water Monit. Rem.,* **1988,** *8(1),* 93-97.

Ruiz-Haas, P. R., Ph.D. thesis, Oregon State University, Corvallis, OR, 2006.

Rutherford, S.W.; Kurtz, R.E.; Smith, M.G.; Honnell, K.G.; Coons, J.E. *J. Membrane Sci.*, **2005**, *263*, 57-65.

Standard Methods for the Examination of Water and Wastewater, 17th Ed.; 4500-O Oxygen (Dissolved), APHA, AWWA and WEF, 1989.

Stumm, W.; Morgan, J. J. *Aquatic Chemistry*, 2nd ed.; Wiley-Interscience: New York; 1981; pp 780.

Seppi, T.; Stubauer, G.; Obendorf, D.; Lukas, P. *Anal. Chem*. **1997**, *69*, 4476-4481.

Sosna, M.; Denuault, G.; Pascal, R.W.; Prien, R.D.; Mowlem, M. Sens. Actuators B: Chem., **2007**, *123,* 344-351.

Standard Methods for the Examination of Water and Wastewater, 17th Ed.; 4500-O Oxygen (Dissolved), APHA, AWWA and WEF, 1989.

Upchurch Sci. web site, www.upchurch.com; 2007.

USGS, http://toxics.usgs.gov/definitions/hypoxia.html; 2006.

Wilkin, R. T.; McNeil, M. S.; Adair, C. J.; Wilson, J. T. *Ground Water Monit. Rem.,* **2001,** *21(4),* 124-132.

White, A. F.; Peterson, M. L.; Solbau, R. D. *Ground Water,* **1990**, *28*, 584-590.

Zehnder, A. J. B.; Whurmann, K. *Science* **1976**, *194*, 1165-1166.

CHAPTER 4:

Design and Characterization of a Liquid-Core-Waveguide based Spectrometer for Determination of Low Levels of Dissolved Oxygen

ABSTRACT:

A novel liquid core waveguide (LCW) based spectrophotometer for the determination of dissolved oxygen (DO) at low concentrations (below 1 mg/L DO) is presented in this study. The analytical method is based on monitoring the oxidation of reduced indigo carmine (IC) in low volume samples (1 mL or less). The LCW system includes a miniature peristaltic pump, a multi-port reactor, and a LCW cell (24-cm Teflon-AF). These three components were connected together in a flow loop and placed in a unique Plexiglas housing that was filled with ascorbic acid to minimize the contact of all flow components with atmospheric oxygen. Sample volumes as low as 0.1 mL were injected into the reactor containing IC that was continuously reduced by H_2 with Pt wire as the catalyst. The determination of DO below 1 mg/L was also successfully demonstrated in a 1.2-cm double-septum vial (as the spectrometer cell) with continuous reduction of IC. A unique double-septum cap was used with the vial cell and the reactor of the LCW system to minimize oxygen contamination during sample injection.

A detection limit for DO of 0.02 mg/L was determined with the LCW cell and the 1.2-cm vial cell. The relative standard deviations for the standards were 1% (0.7 mg/L DO) and 14% (0.5 mg/L DO) for the vial cell and the LCW re-circulating system, respectively.

4.1. Introduction

Long-path cells have been a subject of interest in analytical chemistry over 20 years. A long-path cell can be made from special capillary tubing that can propagate light through its liquid core behaving as a waveguide. Thus, it is referred as a liquid core waveguide (LCW) cell or a liquid-waveguide capillary cell (LWCC) (Song et al., 1998).

According to the Lambert-Beer's Law, the calibration slope of an absorbance measurement is proportional to the optical pathlength of a cell (Wei et al., 1983). LWCCs can have very long pathlengths (i.e., up to 5 m) depending on the application, and hence can increase the calibration slope by a factor of 100 or more. Thus, lower detection limits can be obtained if the blank standard deviation does not increase with pathlength.

During transmission of light at such a long distance, total internal reflection occurs (Figure 4.1). The angle of the incident light entering the core must have a value of θ_0 that satisfies $\eta_0 \sin \theta_0 \leq (\eta_1^2 - \eta_2^2)^{1/2}$ where η_0, η_1, η_2 are the refractive indices for the medium of the light source, liquid-core and clad, respectively (Ingle and Crouch, 1988). To achieve total internal reflection η_1 should be higher than η_2.

With a long path cell, the calibration sensitivity of the absorption measurement can be improved compared to conventional 1-cm cells. For many trace-level analytes, a preconcentration scheme is needed before detection. These schemes can be tedious, time consuming and may require large sample volumes. LWCC's have small diameters such as 100-600 μm and internal volumes less than 1 mL

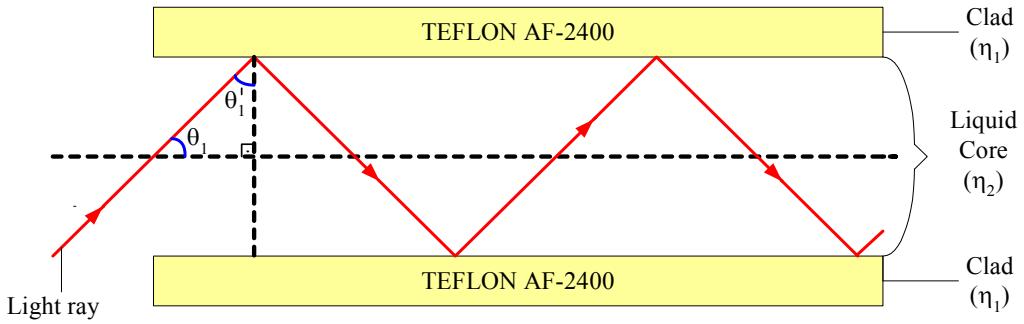

Figure 4.1 Illustration of the total internal reflection of a light ray in Teflon-AF liquid core waveguide. The refractive index of pure water (η_2) and Teflon-AF 2400 (η_1) are 1.33 and 1.29, respectively. Angles greater than $\theta_1' = 75.4°$ ($\theta_1 = 14.6°$) provide total internal reflection at the water-Teflon AF 2400 interface.

providing very low detection limits without preconcentration or the need for large sample volumes.

Some early research was focused on liquid core waveguides with high refractive index liquid core such as carbon sulfide, aromatics, concentrated sugar solutions, or halogenated compounds. With the advances in polymer synthesis, using low refractive index capillary waveguides became a more efficient approach. A LWCC, which has a lower refractive index than water, enables the analysis of aqueous solutions without addition of another high refractive index liquid (Dasgupta et al., 1998). Altkorn et al. (1997) divided waveguide capillary cells into three categories:

1. *Glass or fused silica tubes coated with refractive metals:* The light propagates through transparent core media and the glass wall of the tube. However, high attenuation of light occurs as the pathlength increases.

2. *Tubes made of, or coated internally or externally with, low refractive index polymers:* Plastic and plastic-coated tubes mostly consist of low refractive index perfluorinated polymers such as poly(tetrafluoroethylene) (PTFE). The most widely used materials are the amorphous copolymers of tetrafluoroethylene and 2,2-bistrifluoromethyl-4,5-difluoro-1,3-dioxole (Teflon AF) which have lower refractive index than water (Buck et al., 1993).

3. *Bare glass or fused silica tubes:* The numerical aperture of these waveguides depend only on the refractive indices of the core liquid and outer medium which is air. However, they are very hard to work with because the outer surface determines

the efficiency of the total internal reflection. The material is difficult to bend and must be kept optically clear at all times.

Teflon-AF 2400 tubing has been the most favored LCW in the last 10 years due to its low refractive index and physical flexibility. Recent environmental applications of LCW based spectrometers include the determination of Cu (Callahan et al., 2004), Cr(VI) (Yao et al., 1999), CO_2(g) (Wang et al., 2002), PO_4^{3-} (Zhang et al., 2002), H_2O_2(g) (Pappas et al., 2002), Fe (Zhang et al., 2001), total inorganic carbon (Bryne et al., 2002), and H_2S (Bryne et al., 2000) in aqueous samples. The pathlength was typically in the range of 10 – 200 cm for these applications.

In this study, we present a LCW based spectrophotometer for the determination of dissolved oxygen at low concentrations (below 1 mg/L DO) based on monitoring the oxidation of reduced indigo carmine (IC). This method builds upon related research based on the same reagent system, a conventional spectrometer cell (1.2-cm pathlength), and N_2 purging to minimize O_2 contamination (Cakin, 2008). Application of LCW cells for low-level DO has not been reported to the best of our knowledge. The new apparatus includes a miniature peristaltic pump, a multi-port reactor, and a LCW (24-cm Teflon-AF) which were connected together in a flow loop and placed in a unique Plexiglas housing to minimize to minimize the contact of the flow components with atmospheric oxygen. Small sample volumes (0.1 mL) were injected into the reactor containing indigo carmine that was reduced by H_2 with Pt wire as the catalyst. Determination of low DO concentrations in a more conventional vial cell with H_2-reduced indigo carmine was also evaluated.

4.2. Experimental Section

4.2.1. Chemicals and Solution Preparation

4.2.1.1. Solutions for Determination of Iron at Nanomolar Concentrations

The stock Fe(III) solution (500 mL, 2.2 mM) was prepared by dissolving 0.301 g of $FeCl_3 \cdot 6H_2O$ (Mallinckrodt) in deionized water. The solution was acidified with 5 mL of concentrated HCl (EM Science) to prevent the precipitation of Fe(III) hydroxides. Another stock solution was prepared by diluting 2.2 mM Fe(III) solution with 0.24 mM HCl to 6.6 μM.

The complexing colorimetric reagent for determining Fe was 0.1% (w/v) o-phenanthroline that was obtained as a solution from VWR. A stock solution of reducing agent hydroxylamine (9%) was prepared by dissolving 9 g of $NH_2OH \cdot HCl$ (EM Science, NJ) in 100 mL of deionized water. An acetate buffer (1 M) was used to adjust the pH 4 for the complexation reaction.

4.2.1.2. Solutions for Determination of Iron at Micromolar Concentrations

A stock solution of Fe(II) (3.01 mM, 250 mL) was prepared by dissolving 0.2729 g of $Fe(ClO_4)_2 \cdot 6H_2O$ (Mallinckrodt) in 0.01 M $HClO_4$. A stock solution of $HClO_4$ (0.1 M) was prepared by dilution of 8.5 mL of concentrated (70%) $HClO_4$ (EM Science) to 1 L with deionized water. Standard solutions (1 – 10 μM Fe(II)) were prepared in 25-mL volumetric flasks by dilution of the stock solution.

The mixed reagent solution was the combination of 0.2 mL of o-phenanthroline (0.1%) solution, 0.02 mL of ethanol and 5 mL of pH buffer in a 25-mL volumetric flask (brought to volume with deionized water). Hydroxylamine was not needed because the standard solutions were Fe(II) and no reduction was needed.

4.2.1.3. Solutions for Determination of Dissolved Oxygen

Indigo carmine (IC) was obtained from Aldrich with 92% purity. An IC stock solution (2 mM) was prepared in deionized water. An IC reagent solution (0.5 mM, 20 mL) was prepared weekly by dilution of the stock solution in 0.1 M, pH 7 buffer (TRIZMA hydrochloride, Sigma Aldrich). The solution was reduced with H_2 (100%, BOC Gases) at a flow rate of 10 mL/min in the presence of coiled Pt wire (gauge 31, length of 10-30 cm) as the catalyst for normally a minimum of 2 hr in a 20-mL vial with a double-septum cap (Cakin, 2008). As seen in the Figures 4.2 and 4.3, the vial screw cap has a female-threaded bottom and a male-threaded top (22-400 GPI size for both). The gap between two septa (20-mm butyl rubber septa from Agilent Tech.) was continuously purged with N_2 (~30 mL/min) to minimize permeation of air into the vial during piercing action. Hydrogen flow was not maintained after the reduction of the reagent. Stock solutions were stored at 4°C and in the dark to minimize photodecomposition from daylight for longer periods.

Ti(III) citrate was used as a soluble reductant for initial experiments (Jones, 1999, Zehnder and Whurmann, 1976). A stock solution of ~80 mM Ti(III) citrate was prepared by dissolving 4 g of TRIZMA·HCl and 7.4 g of sodium citrate

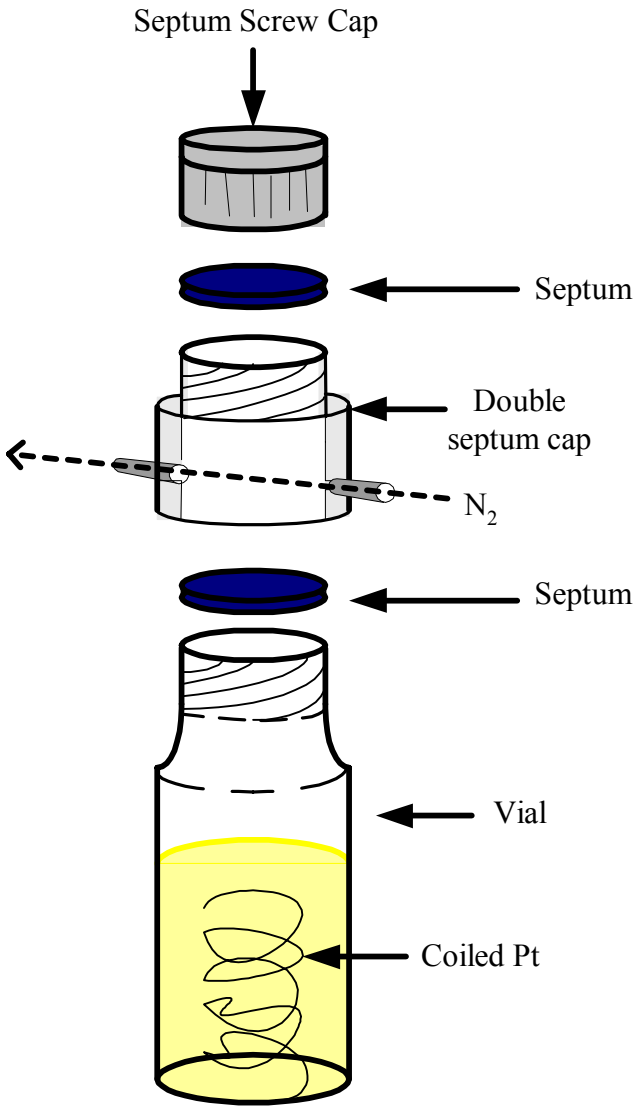

Figure 4.2 Details of the double-septum vial for preparation and storage of reduced indigo carmine. The space in between septa is purged with N_2.

Figure 4.3 Photograph of reduced indigo carmine stock in a double-septum vial. The vial screw cap has a female threaded bottom and a male threaded top (22-400 GPI size for both). The gap between two septa (20-mm butyl rubber septa from Agilent Tech.) was continuously purged with N_2.

monohydrate (Sigma Aldrich) in 20 mL of deionized water, followed by the addition of 5 mL of $TiCl_3$ (13 % w/w in 20 % v/v HCl, Fluka). While the solution was continuously purged with N_2, the pH was adjusted to 7 with concentrated NaOH and the volume was brought to 50 mL with deionized water in a volumetric flask. Then the solution was transferred into a septum vial (I-CHEM Vials) and stored at 4°C. More dilute Ti(III) citrate solutions were prepared by diluting ~80 mM stock and keeping the citrate and buffer concentrations constant. Because the concentration of Ti(III) citrate solutions decrease quickly overtime, multiple additions were required for reduction of the indicators.

DO standard solutions with concentrations of 0 – 1 ppm (mg/L) were prepared by purging deionized water in septum bottles with mixtures of N_2 and O_2/air (BOC gases) for 2 hr. Individual gas flow rates were adjusted with a Tylan RO-28 electronic flow rate controller/readout and mass flow controllers (FC-280 and FC-260) and the outlet flows were mixed within a tee. Mass flow controllers were calibrated with a solid state flowmeter (Restek Flowmeter 6000) and the accuracy of the DO standards was verified with a Clark-type DO probe (Hach, DO175 Dissolved Oxygen-meter Model 50175). Prepure N_2 was further purified with a Restek heated purifier unit (Model 21496).

The standard solutions for DO were prepared in 125-mL septum media bottles (Wheaton) and capped with butyl rubber, locking-flange septa (Wheaton). Hypodermic needles (gauge 22, Popper and Sons) were used for the gas inlet and vent. Gas inlet and vent needles were connected to PEEK tubing (Upchurch Sci.) via

¼-28 fittings and unions. The distal end of the vent tubing was submerged in a flask or a beaker that contained water to prevent back diffusion of O_2. All solutions were prepared with deionized water obtained from a Millipore Milli-Q water purifying system.

Ascorbic acid solution was used as the reductant to protect the liquid core waveguide spectrometer components from atmospheric oxygen. The solution was prepared by dissolving 4 g of ascorbic acid (Mallinckrodt) in 1 L of tap water.

4.2.2. Instrumentation

Three different versions of liquid core waveguide (LCW) spectrometers were constructed. The first version is a one-pass continuous flow spectrometer with a pump and a 1-m LCW as the flow cell in series. The reagents and standards were mixed in volumetric flasks before introduction into the LCW cell. The waveguide was in contact with air because the first version of the spectrometer was not intended for measurement of anoxic samples. The second version is a re-circulating flow system with a pump, reactor, and a 20-cm LCW cell. In this case, the waveguide is encased in a Plexiglas housing and the reagents and analyte solutions are added into and mixed in the reactor in the closed flow loop. The third version is also a re-circulating flow system and includes a miniature pump, a reactor, and a 24-cm LCW cell and all three components are contained in a Plexiglas housing. The housings of the second and the third versions were filled with a reductant solution to minimize oxygen leakage into the LCW cell and other components during the measurements.

For all the spectrometer versions, intensity spectra and the absorbance of the solutions was monitored with a spectrometer (S2000 FL, Ocean Optics) that has a 200-μm entrance slit and a grating with 600 lines/mm and blazed at 500 nm. The light source and the spectrometer were interfaced to a laptop computer with a data acquisition card (DAQ-700 Card, National Instruments). The S2000-FL provides multi-wavelength monitoring with a 2048-element charged coupled device (CCD) as the detector and with OOIBase32 (Ocean Optics) as the operating software.

4.2.2.1. Version 1 of the Liquid Core Waveguide-Based Spectrophotometer

The diagram of the first LCW spectrometer constructed is given in Figure 4.4. It is based on a one-pass continuous flow of samples through a LCW that serves as the spectrometer cell. The internal volume of the flow cell was 0.24 cm^3. The spectrometer was used for Fe determination at nanomolar concentrations.

The LCW cell and tee connectors were contained in a box made by Ocean Optics, Inc (model LPC-1 long path cell) with 1 m of Teflon AF 2400 tubing with an ID of 550 μm. The tee connectors had three ¼-28 female ports.

The peristaltic pump was made by Alitea (model C8/2-XV, Alitea Instruments, WA) and the outlet peristaltic pump tubing (silicon, 1.143 mm ID, Red/red) was connected to a barb-to-¼ -28 male adapter that screwed into one ½-28-port of the tee connector. The pump flow rate was varied from 1 to 3 mL/min.

The other two ports of each tee were connected to the LCW tubing and a fiber optic cable. Each end of the LCW tubing was flared and secured to one port of

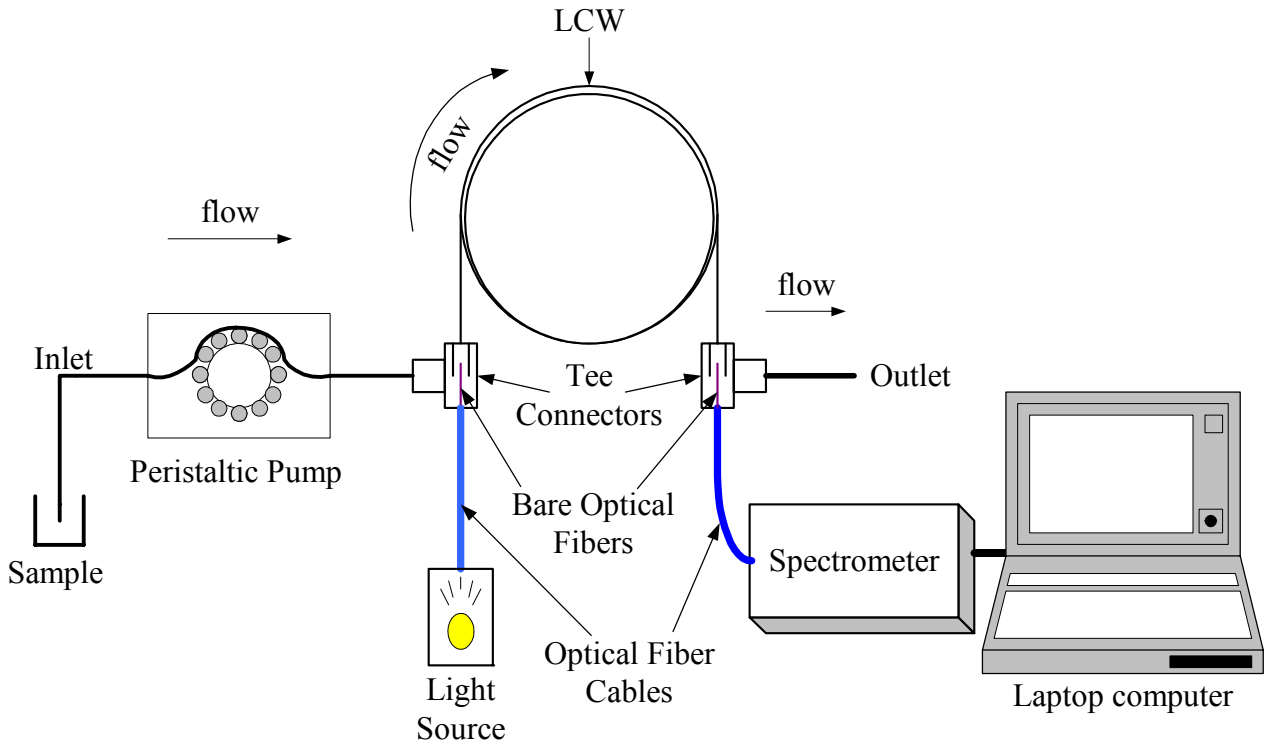

Figure 4.4 Diagram of the apparatus for the determination of nanomolar concentrations of dissolved iron. The first version 1 of the LCW spectrometer is based on continuous flow maintained with a peristaltic pump. The LCW capillary cell (LWCC) was ~1-m long with an ID of 550 μm and was made from Teflon AF 2400 tubing. The tee connectors (1/4-28 type ports) allowed connection of the LCW tubing to the pump, the outlet, the light source, and the spectrometer. Two bare optical fibers (200-μm OD) inserted into the LCW tubing provided optical coupling of the LCW cell to the tungsten light source and to the CCD spectrometer with fiber optics cables.

the tee with a male ¼-28 connector and included a ferrule and an o-ring at the bottom of the port. The commercial LCW cell box included two bare optical fibers (200-μm OD) that are terminated on one end with a male SMA 905 connector and coupled to the LCW tubing. The bare end of each optical fiber slipped into the LCW tubing typically 1 to 2 cm and was secured to at the LCW port by the O-ring in the port. The SMA end of the optical fibers was connected to a female coupler with threads on the outside of both ends. One fiber optic cable with SMA male connectors (400−μm core diameter, Ocean Optics, Inc) connected the cell inlet coupler to the SMA connector of a tungsten light source (Analytical Instrument Systems Inc., DT 1000). A second equivalent fiber optic cable (200−μm core diameter) connected the cell outlet coupler to the spectrometer SMA input port.

4.2.2.2. Version 2 of the Liquid Core Waveguide-Based Spectrophotometer

The instrumentation for the second LCW spectrometer is illustrated in Figure 4.5. This spectrometer was used for determination of micromolar concentrations of Fe. The apparatus is based on a 20-cm LCW cell in a re-circulating flow system with a pump and reactor. Teflon AF-2400 tubing (610-μm ID) was obtained from Biogeneral, Inc. and was cut to ~20-cm long providing for a very low internal cell volume (0.06 cm^3). PEEK tubing (1/16" OD, cat. no. 1533, Upchurch Sci.) with ¼-28 male fittings was used for solution re-circulation from the reactor to the LCW and back to the reactor through the pump.

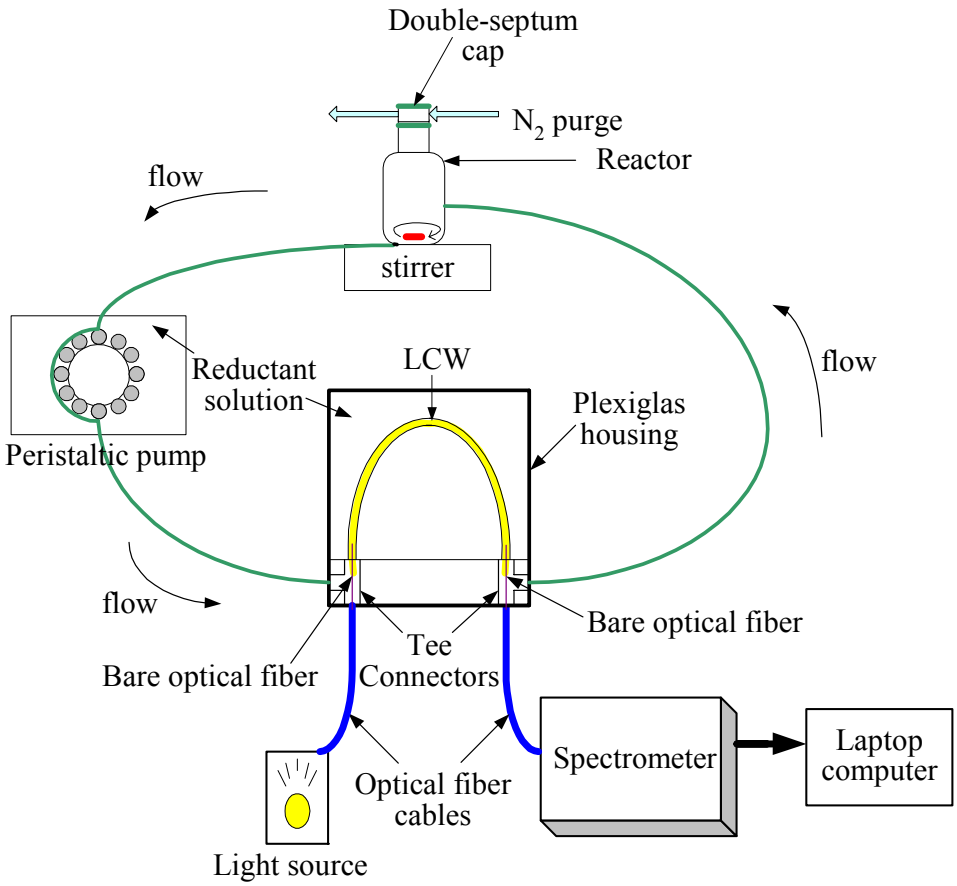

Figure 4.5 Diagram of the instrument for determination of iron at micromolar concentrations. For version 2 of the liquid-core waveguide (LCW) spectrometer, the LCW tubing was ~20-cm long with an ID of 610 μm and was made of Teflon AF 2400 tubing which was placed in a Plexiglas housing constructed in-house. The housing was filled with an ascorbic acid solution to minimize oxygen reaching and diffusing through the LCW tubing. Tee connectors (1/4-28 and SMA ports) were a part of the housing and enabled the coupling of the light and the reagent solutions into the LCW. Two bare optical fibers (200-μm OD) inserted into the LCW tubing provided optical coupling of the LCW cell to the tungsten light source and to the CCD spectrometer with fiber optics cables. The pump was a peristaltic pump with the pump head encased in an in-house made Plexiglas housing filled with ascorbic acid solution to reduce diffusion of oxygen into the pump tubing. Details of the reactor are given in Figure 4.6.

The peristaltic pump is an inexpensive SP-200 peristaltic pump (APT Instruments Litchfield, IL) that was mounted to cylindrical box as described in detail by Ruiz –Hass (2007). The pump DC motor was situated outside on top of the chamber lid along with ¼ -28 female ports to connect to the external tubing pump head inside the enclosure. The enclosure was filled with a solution of 4 g/L ascorbic acid to protect the pump tubing. The pump tubing was made of Norprene (0.8-mm ID, SP201.990 from APT Instruments Litchfield, IL). The pump was powered from a power supply (Proam Universal AC-DC adaptor, Model 900-100) and the voltage was 7.5 V. The flow rate was ~1 mL/min.

For version 2 of the spectrometer, the Plexiglas housing was filled with ascorbic acid solution to reduce diffusion of oxygen into the pump tubing. The tungsten lamp is the same as specified for the first version of the LCW spectrometer.

The reactor was made of Plexiglas and its diagram and photograph are given in Figure 4.6. The reactor has multiple ¼-28 ports that can be used for solution inlet and outlet and gas purging. Sample and reagents were added through the double-septum cap with a syringe and the solution in the reactor was purged with N_2 through input and vent needles that pierce the septa. The cylindrical shape of the reactor provided efficient mixing due to a 10-mm Teflon stir bar (VWR) driven and spin rapidly and consistently by a HANNA Instruments (HI 190M) magnetic stirrer.

The reactor screw cap has a female-threaded bottom and a male-threaded top (13-425 GPI size for both). The gap between two septa (gray butyl rubber stoppers with a 12-mm diameter, Kimble) was continuously purged with N_2 (~30 mL/min) to

A

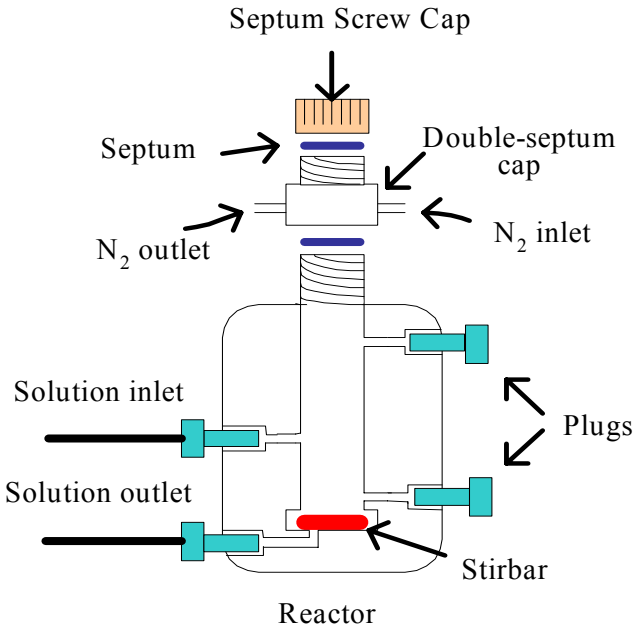

B

Figure 4.6 Diagram and photograph of the multi-port reactor. All the ports were designed for ¼-28 male fittings. Extra ports were plugged when not in use. The double-septum cap was used to minimize oxygen contamination during sample introduction. Dimensions are 38 cm OD, and 60 cm for height from the bottom to the top of the neck. The diameters for the lower and upper sections of the cavity are 1 cm and 0.8 cm, respectively. The distance from the bottom to the center of the inlet port is 0.7 cm.

minimize permeation of air into the vial when pierced by needles. The cap was kept on the reactor until a run was completed (Cakin, 2008).

Continuous stirring of the solution in the reactor was maintained throughout a run. Normally the solution inlet was at the bottom because this provides efficient mixing and the solution level in the reactor can be below the inlet port to minimize the total volume of solution needed. With the low internal volume of the cell, the tubing, and the reactor, only ~1 mL of reagent solution was required for effective flow and operation. The distance between the solution inlet port and the septum cap must be sufficiently large to prevent bubbles from reaching the cap during purging of solutions. Otherwise, the solution in the reactor vents out with the purging gas.

The LCW cell was placed in a Plexiglas housing constructed in-house that consisted of two sections that were screwed together. The larger section of the housing has the cavity for the LCW tubing and is open only at the front. The other section is attached to the open side of the first section with O-ring sealing after the LCW tubing is installed inside. This section was machined to have two internal tee connectors with two ¼-28 ports and one SMA 905 port and enabled the coupling of the light source and the solutions in and out of the LCW tubing. The housing cavity was filled with the reductant solution of ascorbic acid (4 g/L) to minimize oxygen reaching and diffusing through the LCW tubing or into the internal ports. Other species including reduced thionine were added to the reductant solution, but they did not improve oxygen scavenging and were not used for final measurements. The box has extra ¼-ports not shown to add the reductant solution.

The connections to the tees were similar to version 1 of the spectrometer. For each tee, one ¼-28 port was connected to the male fitting of PEEK tubing for solution flow. Each end of the LCW tubing was secured to another ¼ -28 port of the tee with a male ¼ -28 connector (P-668, Upchurch Sci.) and included an o-ring at the bottom of the port. The end of the LCW was pushed through the hole of the connector and the o-ring and then the connector was screwed to the tee.

Two identical fiber optic interfaces were constructed. This interface was made from a short length of bare optical fiber (200-μm OD) with a male SMA connector at each end (see Appendix K). The SMA connector at one end of the interface was screwed to a simple metal SMA coupler and the bare fiber optic protruded ~3 cm beyond the end. The optical fiber was slipped into the LCW tubing ~1 cm and the SMA coupler was screwed into the SMA port of the tee. The SMA connector at the other end of the interface was connected with a second SMA coupler to a fiber optic cable with a SMA male connector (400−μm core diameter, Ocean Optics, Inc). One fiber optic cable connected to the inlet coupler to the SMA connector of a tungsten light source. A second fiber optic cable (200−μm core diameter) connected the cell outlet coupler to the spectrometer SMA input port.

4.2.2.3. Version 3 of the Liquid Core Waveguide-Based Spectrophotometer

An illustration and photographs of the third LCW spectrometer system are given in Figures 4.7 and 4.8. This LCW based re-circulating flow system was

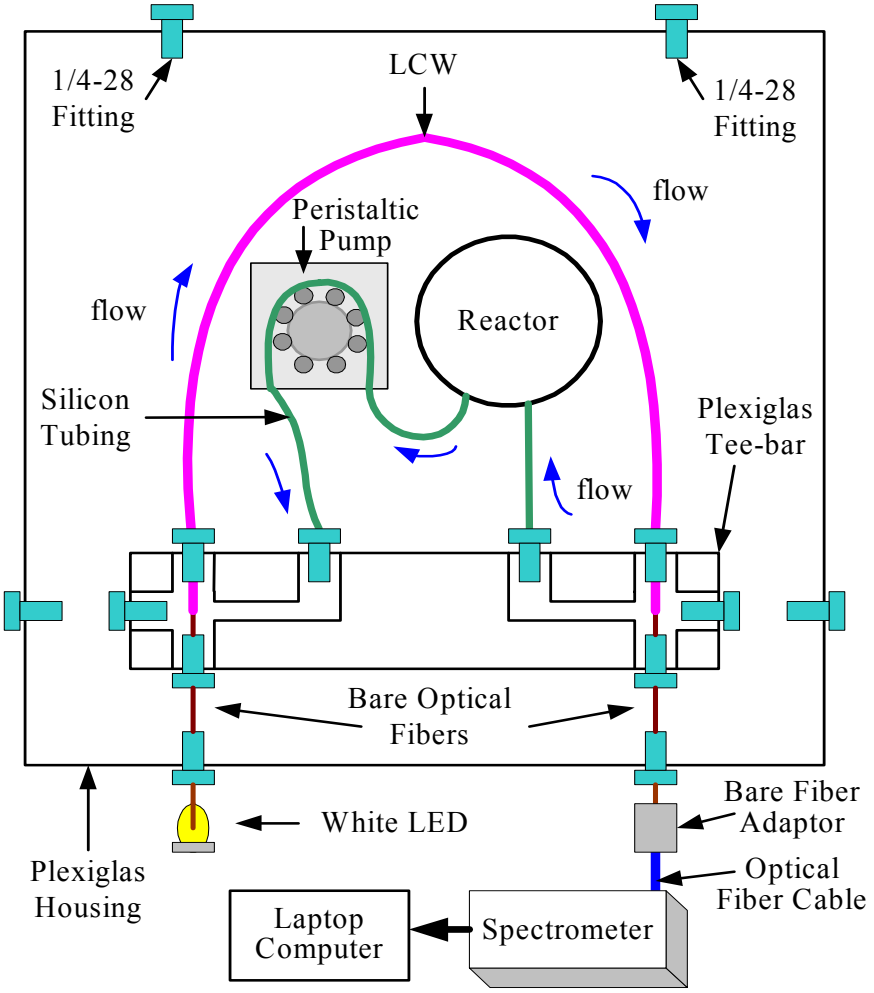

Figure 4.7 Diagram of the liquid core waveguide based re-circulating system used for determining oxygen. The LCW cell was ~24-cm long with an ID of 609 μm and was made of Teflon AF 2400 tubing. The cell tubing was placed in a Plexiglas housing constructed in-house along with the reactor, the peristaltic pump head, and the T-bar which provided tubing connections (1/4-28 ports) and enabled the coupling of the light and the reagent solutions into the LCW tubing. Details of the reactor are given in Figure 4.6. The Plexiglas housing was filled an ascorbic acid solution to minimize oxygen reaching and diffusing into flow loop through the LCW tubing, the pump tubing, or connections. Other components included the bare optical fibers (600-μm ID) with one end butted against the LCW tubing within the tees. The other end of one bare fiber was connected to a commercial fiber optic cable that directed light into the CCD spectrometer. The light source was a white light emitting diode (LED) that coupled to the other bare optical fiber.

A

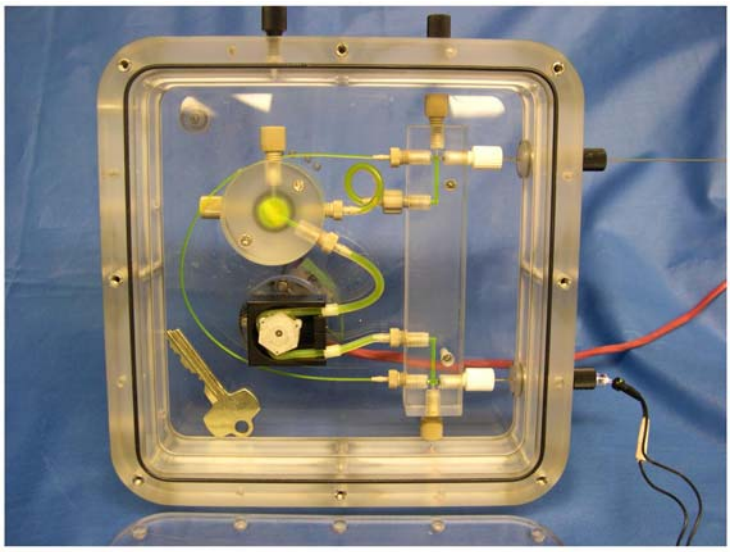

B

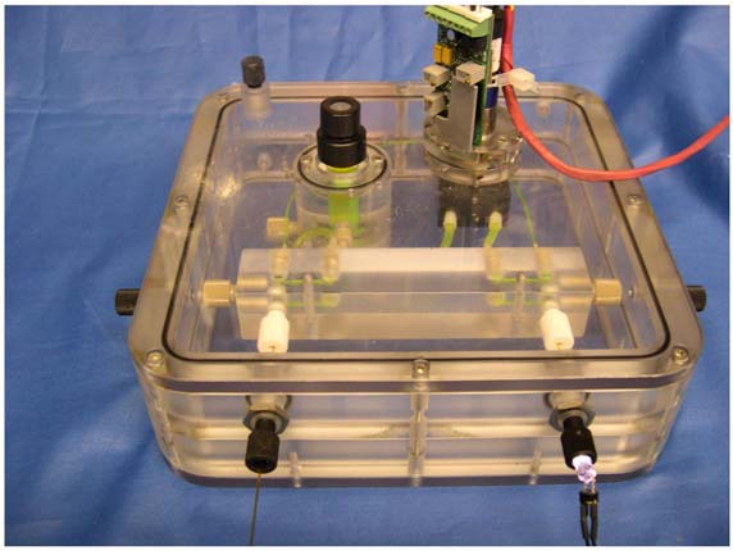

Figure 4.8 Photographs of the liquid core waveguide based re-circulating system. Fluorescein solution was injected into the system for visualization of the flow path. A) The photograph of the system from the bottom. B) The photograph of the system from the top with an angle.

developed for the determination of DO. A miniature peristaltic pump, a 24-cm LCW cell (Biogeneral), a multi-port reactor, and the flow loop tubing were placed in a unique Plexiglas housing which was filled with a reductant solution (ascorbic acid). The design of enclosing all components in the housing eliminates direct contact of the flow components and solutions with atmospheric oxygen and miniaturizes the apparatus for on-site measurements. The closed loop flow system allows purging of reagents and analysis of anoxic samples.

The Plexiglas housing has dimensions of 17.5 cm x 17.5 cm x 5.5 cm as length, width and height, respectively and has a top and bottom lid. The bottom lid provides access for connecting the components with the tubing. The pump and the reactor are mounted onto the top lid of the box such that the injection port of the reactor and the motor of the pump are outside of the box. The body of the reactor and the pump rollers and tubing are inside the box. Also, a Plexiglas tee-bar with two unique tees and ¼-28 ports is mounted to the top lid so it is inside the housing. The tee-bar enables coupling of the light and the test solutions in and out of the LCW cell at the same time. Soft pump tubing (silicone) connects the pump and the reactor to each other and the two tees forming a closed loop. The Plexiglas housing was filled with ascorbic acid solution (4 g/L) through one of the extra ¼-28 ports to minimize oxygen reaching and diffusing into flow loop through the LCW tubing, the pump tubing, or any solution or optical connections.

The miniature peristaltic pump (P625) and the tubing set (P625/TS062S, 0.157 cm ID) were purchased from Instech Laboratories, Inc. The flow rate range of

the pump was adjusted from 0.5 to 3.6 mL/min by providing +7 V for DC power input and 0 to +5 V for speed control input. A dual power supply was used (Model 1500, Spar Electronics Inc., CA). Normally, the maximum pump speed was used to prevent adhering of gas bubbles on the walls of the LCW. One section of silicone pump tubing (147 cm) feeds through the pump rollers and connects to one of the tees (left hand side) and to the outlet of the reactor. The other section of the same type of tubing (65 cm) connects the inlet of the reactor to the second tee (right hand side).

The light source was a white light emitting diode (LED) (Nichia, Inc., SPW500BS) coupled to a 600-μm bare optical fiber (P600-2-UV-VIS, Ocean Optics). The power for the LED (1.5 mA) was supplied from a commercial LED module (LS-450, Ocean Optics). The bulb of the LED was flattened and polished manually with aluminum oxide lapping film sheets (Mark V. Laboratory, Inc.) until there was a ~0.5-mm thick transparent coating over the LED die. The optical fiber (~3 cm) was cut with a diamond fiber optic scribe (Clauss DS-90-W, The Light Brigade) and both ends of the fiber were polished with aluminum oxide lapping film sheets. One end of the fiber was glued on the sweet spot of the flattened LED with optical grade epoxy (Epoxy Technology) as recommended by Dasgupta et al. (2003). The free end of the LED-fiber optic was connected to the LCW through a port on the enclosure and then through a port on the left hand side tee (see Figure 4.7) of the tee-bar.

Another optical fiber (600-μm ID, ~10-cm length) was cut and polished at both ends for collection of the light from LCW and feeds from a port on the right

hand side tee (see Figure 4.7) and through a port of the enclosure. The free end of the collection fiber was terminated with a bare fiber adaptor (catalog no. BFA-KIT chuck and BFA-SMA from Ocean Optics) that enables coupling of the out coming light with the spectrometer.

The bare optical fibers and the LCW tubing were connected to the tee-bars with ¼-28 fittings (P-201x with P-200x, Upchurch Sci.) (see Figure 4.7). O-rings were placed at the seat of the ports for the bare optical fibers and LCW to provide a liquid-tight connection and a good optical alignment. Each end of the LCW tubing was secured to another ¼ -28 port of the tee with a male ¼ -28 connector (P-668, Upchurch Sci.) and included an o-ring at the bottom of the port. The LCW was pushed through the hole of the connector and the o-ring and then the connector was screwed to the tee. These o-rings (ORV-001-10, Small Parts, Inc.) have dimensions of 1/32" ID, 3/32" OD, and 1/32" thickness. The bare optical fibers are butted as close as possible to the LCW for an efficient light throughput. The housing was covered with a black cloth to prevent stray light during measurements.

The Plexiglas reactor with multiple ¼-28 ports and magnetic stirrer were the same as described for version 2 of the spectrometer and in given in Figure 4.6. For this version, the top of the bottom section was modified with an o-ring and two tapped holes so that it could be sealed and secured to the top lid of the enclosure and the threaded neck (13-425 GPI size) fit through a hole in the top lid. In addition, a coiled Pt wire (gauge 31, length 10 cm) was placed in the reactor to serve as the

catalyst for continuous reduction of IC with a H_2 purge through a needle piercing the septa.

For comparison data, a double-septum vial was used as a 1.2-cm spectrophotometric cell with the same light source and CCD spectrometer. The double-septum vial was evaluated for DO determinations previously (Cakin, 2008). In this case, the IC in the vial was continuously reduced with 10 mL/min of H_2 (100%, BOC Gases) in the presence of coiled Pt wire (gauge 31, length 10 cm) as the catalyst.

Sample and reagent introduction into the spectrometer vial or the reactor was performed with two different devices: gas-tight syringes and a solenoid-actuated diaphragm pump (The Lee Co., LPLA 1230350L) with a preset volume of 50 μL. The instrumentation and the analytical procedure for sample introduction for DO are previously described (Cakin, 2008). The buffer solution in the reactor or the 1.2-cm cell was purged with an H_2 input through vent needles that pierce the septa for 1 hr before reduced IC was added and throughout the addition of IC and eventually the sample.

4.2.3. Analytical Procedures

To estimate the throughput of a LCW cell, the raw intensity signal observed with cell was compared to the raw intensity observed with a 1-cm cuvette in a cuvette holder (CUV-UV, Ocean Optics) connected to fiber optic cables. The cells were filled with water. Experimental conditions such as the light source, input and

output fiber optic cables, and the integration time of the spectrometer were kept constant. The sample module includes focusing lenses that were not used for the LCW cell. Because the detector was overloaded (saturated) with the 1-cm cell and experimental conditions used for the LCW cell, it was necessary to add a filter (neutral density filter with a nominal absorbance of 1.5 AU) in the light path to reduce the intensity by a known amount.

The raw intensity with the 1-cm cell with the filter and of the 1-m LCW cell (550-μm ID) without the filter was measured at 600 nm. The raw signal of the 1-cm cell was normalized to represent the intensity without the filter. The normalization factor was calculated by converting the absorbance value (A = 1.5) of the filter to transmittance value ($T = 10^{-1.5} = 0.031$) and taking the inverse (1/0.031 = 32.2). The throughput of the 1-m cell relative to the 1-cm cell was calculated as the ratio of the intensities at 600 nm of the 1-m cell to the 1-cm cell divided by 32.2.

The intensity spectra with the 1-m LCW cell and the 1-cm cell (with the neutral density filter) were recorded. To compare the two spectra on the same graph, the intensity spectrum of the 1-m LCW (at all wavelengths) was multiplied by 1.55 to normalize the spectrum so that the intensity for both cells was the same at 600 nm.

At times for all spectrometer versions, the light throughput for the LCW cell decreased significantly due to sorption of reagents and reaction products into the cell walls. When a low reference (blank) signal (counts) was observed, the LCW was cleaned with bleach (38%), hydrogen peroxide (30%) or acetone solutions to restore the transmittance to expected levels. First, the LCW cell was removed from the

system because cleaning reagents such as acetone would damage the Plexiglas components. The LCW cell was connected to a 10-mL syringe (Becton-Dickinson, NJ) via a male luer to female ¼ -28 adaptor (P-655, Upchurch Sci.) and a barbed adaptor (P-668, Upchurch Sci.). The waveguide was flushed manually with the contents of the syringe. This procedure was repeated until good light throughput (raw intensity of 3000 counts at 600 nm) was measured with a relatively small integration time such as 10 – 300 ms.

4.2.3.1. Analytical Procedure for Determination of Iron at Nanomolar Concentrations

First, 20 – 8000 μL of 6.6 μM Fe(III) stock solution was transferred to 25 mL volumetric flask with electronic digital pipettes (Rainin) to provide standard solutions of 5.3 – 2112 nM Fe(III). Next, NH_2OH solution (250 μL) was added to flasks to reduce Fe(III) to Fe(II). Reduced standards were buffered by adding 250 μL of 1 M acetate buffer (pH 4). The complexing reagent, o-phenanthroline (62 μL), was added last and the solutions were brought to volume with deionized water. After 10 min, the absorbance of the standards was measured with a flow rate of 1.6 mL /min. The absorbance values were recorded after 10 mL of the standard solution passed through the cell (6 min). The data acquisition period was 10 s and the number of data points stored was typically 10 for each standard. Diluted buffer solution (0.01 M acetate buffer) was fed in between standards and blanks until the baseline stabilized (1-5 min). Buffer was preferred over water because it minimized changes

in refractive index that cause baseline shifts. In-cell concentrations of the reagents were 13 mM, 13 μM, and 0.01 M for NH_2OH, o-phenanthroline, and acetate buffer, respectively. The blank solution included all reagents but not Fe(III). For calibration curves, the absorbance of each standard was blank corrected by subtracting the average blank signal.

4.2.3.2. Analytical Procedure for Determination of Iron at Micromolar Concentrations

The mixed reagent solution included o-phenanthroline, sodium acetate buffer (pH 4) and ethanol with in-cell concentrations of 22 μM, 0.1 M and 1 % (v/v), respectively. The reagent solution (1 mL) was injected into the reactor of 20-cm LCW recirculating system and the absorbance was monitored. The sample (1 mL) was injected directly into the reactor where it mixed with the reagent mixture. The data acquisition period was 20 s and the typical reaction time and baseline stabilization time was 100 s after the injection of the standard. The absorbance of the each standard was blank corrected by subtracting the average blank signal. The blank solution was $HClO_4$ (0.1 M) stock solution.

Determination of Fe with a 1-cm cell was performed with o-phenanthroline method according to the analytical procedures given by Jones (1999). The reagents were NH_2OH (10% w/v), o-phenanthroline (0.5%), acetate buffer (1 M), and Fe(III) standards in (0.2 - 1.2 mM). The Fe standard (1 mL) was transferred to a 10-mL flask along with 0.2 mL of NH_2OH, 0.4 mL of acetate buffer, and 0.4 mL of the complexing reagent. The in-cell concentrations for o-phenanthroline, sodium acetate

buffer (pH 4) and NH_2OH were 1 mM, 0.041 M, and 0.03 M, respectively. The cell contents were stirred with a stirring bar.

4.2.3.3. Evaluation of Oxygen Contamination of the with the Liquid Core Waveguide Based Spectrophotometer

Visual tests were performed to evaluate the weak points of the spectrometer systems (versions 2 and 3) in terms of oxygen contamination. Most of the studies were done with version 3 after initial studies with version 2 of the spectrometer revealed O_2 contamination at the connection points of the LCW tubing.

The cavity of Plexiglas housing of version 3 was continuously purged with prepure N_2 (BOC Gases) through one of the extra ¼-28 ports at 110 mL/min. After 1 hr, oxidized IC solution (1.5 mL, 0.5 mM) was injected into the reactor system and deaerated for 1 hr with N_2 (40 mL/min) through the reactor cap septa with continuous pump flow and stirring. Next, the IC was reduced by adding Ti(III) citrate (15 μL, ~80 mM) to the reactor. The pump flow was stopped after the solution was homogeneous and the blue color of oxidized IC disappeared in every part of the system. The solution purge needles were taken out of the reactor while the housing was still being purged. The oxidation of IC at certain parts of the system was visually detected by the formation of deep blue color. The timing of the oxidation was noted as an indication of the relative concentration of oxygen contamination at that certain location.

Another visual test was conducted to demonstrate relative O_2 permeabilities of the components. After de-aeration and reduction of the IC, the pump flow was

halted and the housing was opened to air. The permeability of different components was ranked according to the timing sequence of oxidation.

The overall O_2 diffusion rate into the circulating solution was estimated by measuring the slope of the positive baseline (the increase in absorbance over time, AU/s). Version 3 of the LCW recirculating system included 26-cm of Teflon-AF tubing as the cell during this experiment. The housing was filled with ascorbic acid solution (4 g/L). With the reactor cap off and an electronic digital pipette (Rainin), 1.5 mL of pH 7 buffer (0.1 M TRIZMA) were transferred into the double-septum reactor. The stirrer and the pump were turned on. The absorbance was set to zero with this solution. With an electronic digital pipette (Rainin), 2 μL of IC (~2 mM reduced stock solution) was transferred into the spectrometer reactor and then the reactor cap was secured to close the system to air. The solution was purged with N_2 for 1 hr to remove the dissolved oxygen. The IC was further reduced by injecting 5 - 15 μL of ~80 mM Ti(III) citrate into the reactor through the septum cap with a gas-tight syringe (Precision sampling Corp.). The continuous increase in the absorbance at 610 nm (baseline corrected at 700 nm) was recorded overtime.

Further evaluation of DO contamination was conducted with the same LCW spectrometer but without Ti(III) reduction. Instead, the reactor of the re-circulating system and the double-septum reagent vial (IC) were continuously purged with 10 mL/min of H_2 (100%, BOC Gases) in the presence of coiled Pt wire (gauge 31, length of 10 cm) as the catalyst to continually reduce any oxidized IC and minimize the effects of O_2 entering the solution from the headspace or polymer components.

The IC was injected after 1 hr of purging with H_2. This procedure is the one eventually used for DO determinations.

In this case, the decrease in the absorbance at 610 nm (baseline corrected at 700 nm) was recorded overtime. The slope was not constant and decreased as the absorbance from oxidized IC decreased. Negative slopes were measured for the periods that continuous reduction of IC occurred. Because the reduction of IC in the double-septum vial was relatively fast, standard solutions were injected after the absorbance decreased below 0.08 AU. Thus, slopes for the baseline drift were calculated over 10-min periods for regions where the absorbance was below 0.08 AU. However, due to the relatively slow reduction of IC and the higher absorbances in the LCW flow system, standard solutions were injected when the absorbance had decreased to the range of 0.2 - 0.6 AU. The baseline slopes were calculated in the same absorbance region over 10-min periods.

4.2.3.4 Analytical Procedure for Determination of Dissolved Oxygen

With an electronic digital pipette (Rainin), 2 mL of pH 7 buffer (0.1 M TRIZMA) was transferred into the double-septum reactor with the cap removed. The absorbance of the version 3 of the LCW-based spectrophotometer was set to zero with this solution. Then the system was closed to air by capping the reactor with the double-septum cap. The reactor was purged continuously with H_2 (100%) in the presence of Pt wire as the catalyst to remove dissolved oxygen for at least 1 hr before the addition of IC.

With a gas-tight syringe, 2 μL of H_2-reduced IC (~0.5 mM) was transferred into the reactor. First, the syringe needle was inserted so that the needle tip was in between the septa of the 25-mL vial with reduced IC. After flushing the syringe (filling and emptying) 10 times with the N_2 flowing in between the septa, the syringe needle was inserted through the lower septum into the IC solution followed by an immediate withdrawal and transfer into the reactor. The time acquisition of OOIBase32 software was initiated for monitoring the absorbance of the reagent solution at 610 nm and 700 nm before the sample was injected. The data acquisition rate was typically 1 data point every 6-10 s.

The procedure for DO measurements was similar with the 1.2-cm double-septum vial (DSV) was similar. In this case, the buffer volume was 2 mL and 1 mL of reduced IC solution (~2 mM) was injected.

Sampling procedures for adding low-level DO standards or blanks to the reactor or the 1.2-cm cell are given by Cakin (2008). For the 1.2-cm cell, a portable flow sampler based on a miniature pump was used. The pump inlet tubing was inserted into the sample bottle and used to inject 0.5 mL of a DO standard or the blank into the double-septum spectrometer vial. For the LCW spectrometer, 100 μL of a standard or blank were injected with the same pump sampler into the reactor of the LCW system (version 3).

A unique removable double-septum bottle cap was developed to minimize the O_2 contamination of blanks or standards in the bottles containing the standards or blanks (Cakin, 2008). The cap allowed purging of the space in between septa with N_2

during sampling. Also with this cap, it was possible to purge the flow sampler lines and the syringes with N_2 before the transfer of the sample.

4.2.4. Calculations for the Determination of Dissolved Oxygen

During a run, the absorbance of the solution in version 3 of the LCW-based re-circulating system or 1.2-cm double-septum spectrometer vial was monitored and the absorbance values were continuously streamed to a data file in the format of absorbance vs. time. The response to sample injection was peak shaped and the absorbance increased to a maximum value in minutes and then decreased back to the baseline within 14 to 19 min. The absorbance change for a given sample was defined as the height of the peak relative to the initial baseline. Relatively larger sample volumes (i.e., 0.5 mL) were applied for the determination of DO with the H_2-purged double-septum vial (DSV as the 1.2-cm spectrometer cell). Thus, the absorbance change was corrected for the dilution of the reagent with the sample.

The observed absorbance change between times t_1 before the injection and t_2 after the injection of the sample has two components:

a) The dilution of the reagent with the sample (A_d)

b) The reaction of reduced IC with O_2 in the sample (A_{ox})

The absorbance of the reagent solution before the sample injection is A_1 at an initial time of t_1 with an initial volume of V_1 (3 mL for the DSV cell). According to Beer's Law (6):

$$A_1 = \varepsilon b c_1 \qquad \text{or} \qquad A_1 = \varepsilon b \left(n_1 / V_1 \right) \tag{4.1}$$

where n_1 is the initial number of moles of oxidized IC, b is the pathlength and ε is the molar absorptivity of IC (ox). After sample injection, the volume of solution in the cell increases to V_2 (3.5 mL for DSV cell) resulting in dilution and a decrease of the observed reagent absorbance to A_d. To calculate only the effect of the dilution on initial absorbance, n_1 and the final volume (V_2) are considered:

$$A_d = \varepsilon b \left(n_1 / V_2 \right) \tag{4.2}$$

Substitution of equation 3.1 into equation 3.2 yields;

$$A_d = A_1 \left(V_1 / V_2 \right) \tag{4.3}$$

The absorbance change due to the reaction of reduced IC and DO in the sample (A_{ox}) is calculated by subtracting other absorbances from the final observed absorbance (A_2);

$$A_{ox} = A_2 - A_d \tag{4.4}$$

The final absorbance (A_2) was taken as the maximum of the peak which is manually selected by the operator from the previously recorded data file in the form of absorbance vs. time. During blank measurements, a negative step rather than a maximum was obtained due to the dilution of the reagent. In that case, A_2 (at t_2) was defined as the data point representing the end of the dilution period of the reagent

with the blank solution and it was selected as the bottom corner of the negative step function.

There is a continual baseline decrease due to continuous reduction of the reagent with H_2. The absorbance change due to this baseline decrease was not included in the correction of A_{ox} as is necessary for the baseline increase without H_2-reduction (Cakin, 2008). In this case, the absorbance difference is measured over ~ 1 min and absorbance change due to the baseline is small because the baseline slope is about 2 mAU/min (with 53% RSD).

In the case of sampling twice (each 0.5 mL) during the same run, the ratio of the initial and final volume of the solution (V_1/V_2) was different for each injection. Thus, A_{ox} for the second injection was multiplied by a correction factor (final volume for the 2nd injection divided by final volume of the 1st injection (4/3.5)) to enable the comparison of A_{ox} for the first and the second injections.

For the LCW based re-circulating system, smaller volumes (100 μL) of standard solutions were injected. These low-level DO standards were measured in triplicates within the same run and the absorbance changes were corrected for dilution (correction factor for 2nd injection (2.2/2.1) and for correction factor 3rd injection (2.3/2.1)).

For the measurements of blank solutions, the blank signal was denoted as $A_{bk.}$ The blank signal (A_{bk}) is the absorbance change due to the reaction of reduced IC and DO in the injected blank and is calculated with the same procedure as A_{ox}. Before calculations, streamed data files (absorbance vs. time) were smoothed by

averaging (moving boxcar) every 6 points and 3 points for measurents with the vial and the LCW, respectively.

Concentrations of the standard solutions were calculated according to American Society for Testing and Materials' (ASTM) publications (2005). Sample calculations are given in Appendix C.

4.3. Results and Discussion

4.3.1. Evaluation of the Light Throughput and Wavelength Window of the Liquid Core Waveguide Cell

The throughput of the 1-m LCW cell relative to a conventional 1-cm cuvette at 600 nm was estimated from intensity measurements for both cells to be 1%. Toda et al. (2003) report how throughput varies with cell length for the same type of Teflon-AF tubing cell used in this work. From their literature data, the throughput for a 10 cm cell is estimated to be 0.12 (or 12%). The square of this throughput is 0.014 (or 1.4%) and is an estimate of the throughput with a 1-m LCW cell. This estimated light throughput agrees reasonably well with 1% value measured in this work.

Figure 4.9 shows the intensity spectra obtained with the 1-m Teflon AF-2400 cell and the 1-cm cuvette with deionized water as the liquid core or the cell contents and the same light source and spectrometer conditions. The useful wavelength window for the spectrometer depends on the light source, photodetector, and the throughput characteristics of the cell. For this study, the useful wavelength window is defined as the wavelength range where the raw intensity is above 1000 (counts) when the maximum intensity has been set to ~3500 counts. Intensities lower than 1000 may yield standard deviations higher than 0.0001 AU in the absorbance mode and decrease precision. With the conventional 1-cm cell, the useful wavelength range is 480 to 870 nm and the throughput of the cell is effectively independent of wavelength. For the of 1-m LCW cell, the useful wavelength range is limited to 480 – 720 nm. The range is reduced primarily by a decrease in light throughput in the

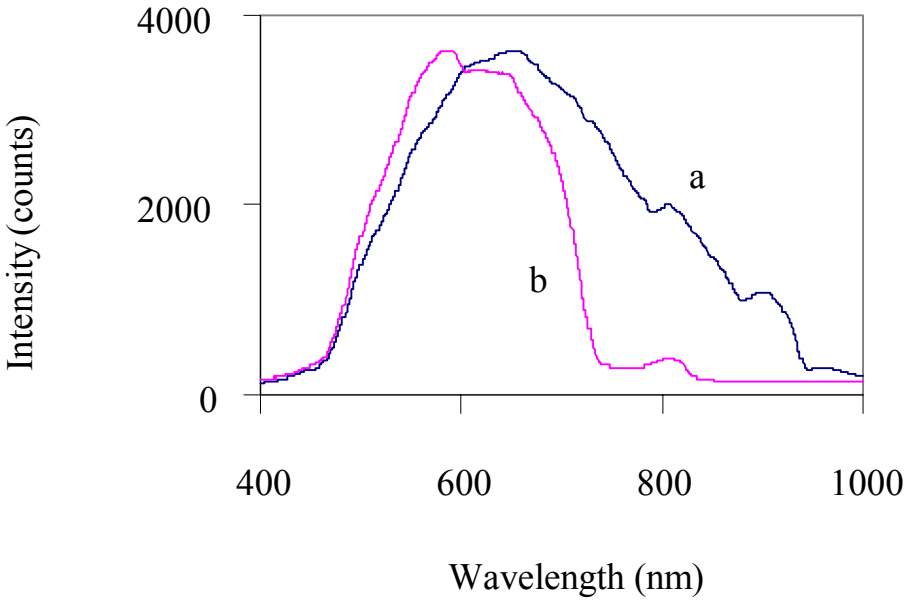

Figure 4.9 Spectra of light passing through a 1-m LCW cell with water as the liquid core and a 1-cm cell with water as the solution. The light source was a tungsten light lamp and the detection system was a CCD spectrometer. a) Spectrum for a conventional 1-cm cell with a neutral density filter (1.5 AU) in the light path. b) Spectrum for a 1-m long section of Teflon AF 2400 tubing. Spectrum b) was normalized to spectrum a) by multiplying raw intensities (at all wavelengths) by 1.55.

long wavelength region. Similar loss of throughput in the red and NIR region of Teflon-AF was also reported in the literature (Altkorn et al., 1997) and was attributed to fourth overtone of the water OH stretch at 750 nm.

Figure 4.10 demonstrates the scattering of light within the 1-m LCW with a green laser input. At the Teflon-water interface, the pores of the polymer fill with water and morphology of these pores affect the refractive index of the matrix (Toda et al., 2003). Attenuation of light depends on the surface characteristics of the inner walls of the tubing.

The light throughput of the LCW cell is affected by the reagents used in a particular analytical application. For determination of dissolved oxygen, the reagent is a redox indicator. A significant loss of the light throughput up to 95% in an hour was observed when thionine (0.2 - 1 μM) was tested as the redox indicator. It appears that thionine significantly sorbs on the inner walls of the waveguide and reduces the light throughput by absorption of some of the light as it passes through the cell with many internal reflections. Indigo carmine was eventually chosen as the redox indicator for DO determinations because sulfonated groups that reduce the tendency of dyes to stain and, in this application, reduce sorption to the Teflon AF. The loss of light throughput was up to 50% after ~10 h with 1 to 3 μM IC.

Chemical cleaning solutions such as dilute bleach solution (38%), acetone or hydrogen peroxide (30 %) were effective for cleaning and restoring light throughput for thionine, indigo carmine, and Fe reagents and essential with thionine. For DO determinations with indigo carmine or Fe determinations with o-phenanthroline, only

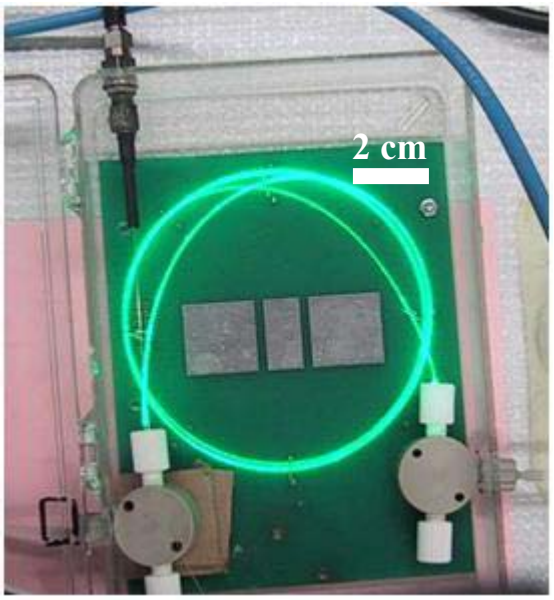

Figure 4.10 Demonstration of light scattering in a liquid core waveguide with a green laser input. See the caption of Figure 4.4 for details about the LWCC and connections.

weekly periodic cleaning (or every two weeks) was needed as indicated by a significant drop in the light throughput for the blank.

4.3.2. Evaluation of the Liquid Core Waveguide Based Spectrometer for Determination of Iron

Nanomolar and micromolar concentrations of iron were determined with versions 1 and 2 of the LCW spectrometer and with a standard 1-cm cuvette. The calibration curves for the 100-cm LCW and the 20-cm LCW systems are presented in Figures 4.11 and 4.12, respectively, and show good linearity.

Calibration curve slopes, blank standard deviations, and detection limits for the cells of different pathlength are compared in Table 4.1. The calibration slope is proportional to the pathlength as expected when all concentrations are plotted as in-cell concentrations. Also, the blank standard deviations are not significantly different and appear to be limited by detector noise. Hence, detection limits are effectively inversely proportional to the calibration slope within a factor of 2. The best detection limit of 2 nM Fe(III) was achieved with the continuous-flow based 1-m LCW system and is ~100 better than with the 1-cm cell. The dynamic range with the 1-m cell is more than 1000 with an upper limit of 2 μM (deviation from linearity of 2%).

Determination of Fe(II) at nanomolar concentrations with absorbance spectrometry and a long pathlength cell was demonstrated by Waterbury et al. (1997). They used a 4.5-m long LCW cell which was Teflon AF tubing. The described analytical method was based on the ferrozine method. Sample solutions of Fe(II) (100 mL each) were pre-mixed with the reagents (total 0.4 mL), followed by

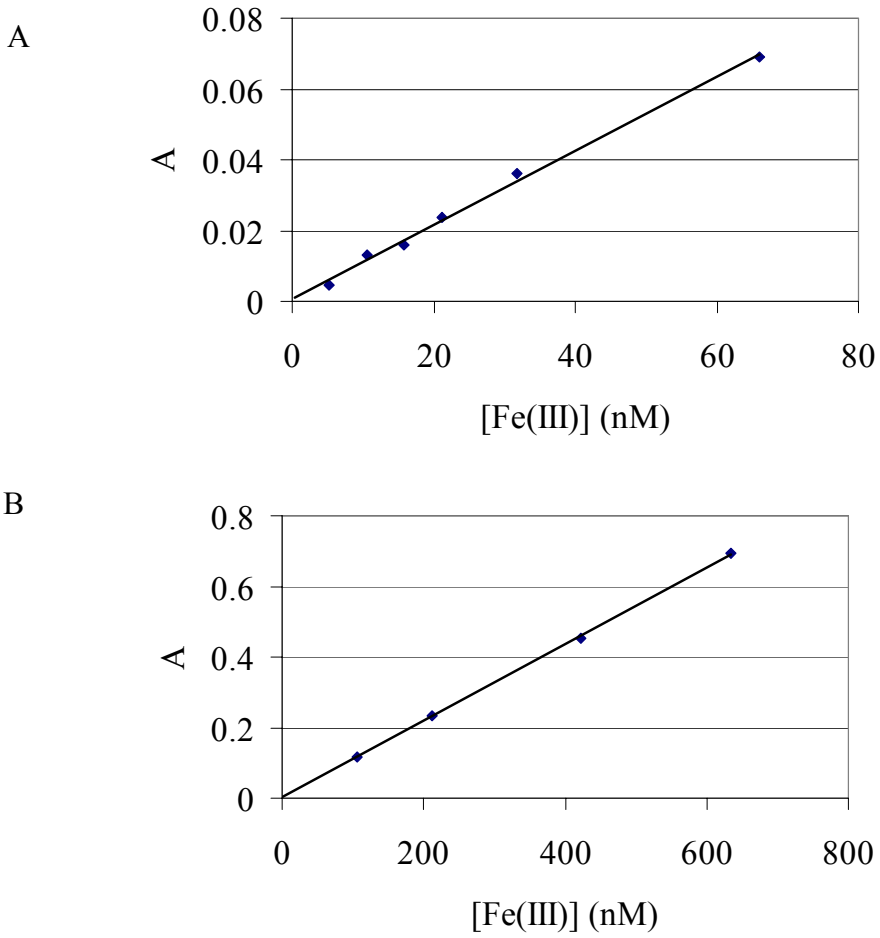

Figure 4.11 Calibration curves for the determination of dissolved iron with o-phenanthroline method. The absorbance was monitored at 510 nm and was baseline corrected at 680 nm and the reported concentrations are in-cell concentrations. The absorbance was also blank corrected. The data for figures A) and B) are from one set of data taken with version 1 of the LCW spectrometer. Two curves are shown to illustrate the dynamic range. A) Calibration curve for the determination of iron at nanomolar concentrations. $A = 0.0011 \times [Fe(III)](nM) + 8.4 \times 10^{-5}$. The standard error of the slope and intercept are 5.3×10^{-6} and 0.0013, respectively. B) Calibration curve for the determination of iron at higher nanomolar concentrations. $A = 0.0011 \times [Fe(III)](nM) + 0.002$. The standard error of the slope and intercept are 1×10^{-5} and 0.006, respectively.

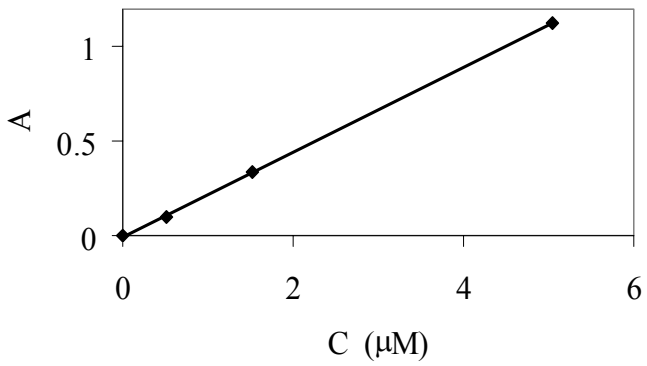

Figure 4.12 Calibration curves for the determination of dissolved iron with o-phenanthroline method at micromolar concentrations. Measurements were made with version 2 of the LCW spectrometer. The absorbance was monitored at 510 nm and was baseline corrected at 680 nm and the reported concentrations are in-cell concentrations. The absorbance was also blank corrected. A = 0.022 [Fe(II)] (μM) - 0.005. The standard error of the slope and intercept are 0.0015 and 0.0039, respectively. The in-cell concentration is one-half of the concentration in the standard before injection.

Table 4.1 Comparison of calibration slopes, blank standard deviations, and detection limits with different optical pathlengths for determination of iron. [a]

Experimental setup	Glass cuvette	LCW (version 2) recirculating system	LCW (version 1) continuous flow
Optical pathlength (cm)	1	20	100
Calibration slope (AU /μM)	0.011	0.22	1.1
Blank standard deviation (n = 5)	0.001	0.002	0.0007
Detection limit in μM (k = 3)	0.3	0.025	0.002

[a] All slopes and detection limits are based on in-cell Fe concentration.

the measurement of the absorbance of the colored complex. A detection limit of 0.2 nM was reported and is 10 times better than that achieved in this work. The better detection limit is attributed to longer pathlength and higher molar absorptivity of ferrozine complex.

4.3.3. Correcting for Changes in the Light Throughput of the Teflon-AF Waveguide for Fe Determinations

The light throughput of the waveguide is affected by the refractive index of the liquid core and the imperfections of the liquid-Teflon AF interface. Before every measurement of a reagent blank or a standard (Fe complex), the baseline (reference spectrum) was set to zero absorbance with the acetate buffer solution. The refractive index of the liquid core increased when the reagent-blank or standard (Fe complex) solution was pumped into the cell because of the increase in the concentration of dissolved species. In theory, the light throughput increases (the absorbance decreases) as the refractive index of the liquid core increases for a given LCW such as Teflon-AF. In contrast, an increase in baseline absorbance was observed with the addition of reagent blanks or standards. This increase is possibly due to complexes, bubbles or particles adhering to the liquid core interface which decrease light throughput by absorbing or scattering light.

A rapid baseline shift during the measurement period after introduction of a standard (Fe-o-phenanthroline complex) into the 100-cm LCW cell is demonstrated in Figure 4.13A. During the measurement of the standard solution, the baseline (background) absorbance at 680 nm increased ~0.03 AU and was subtracted from the

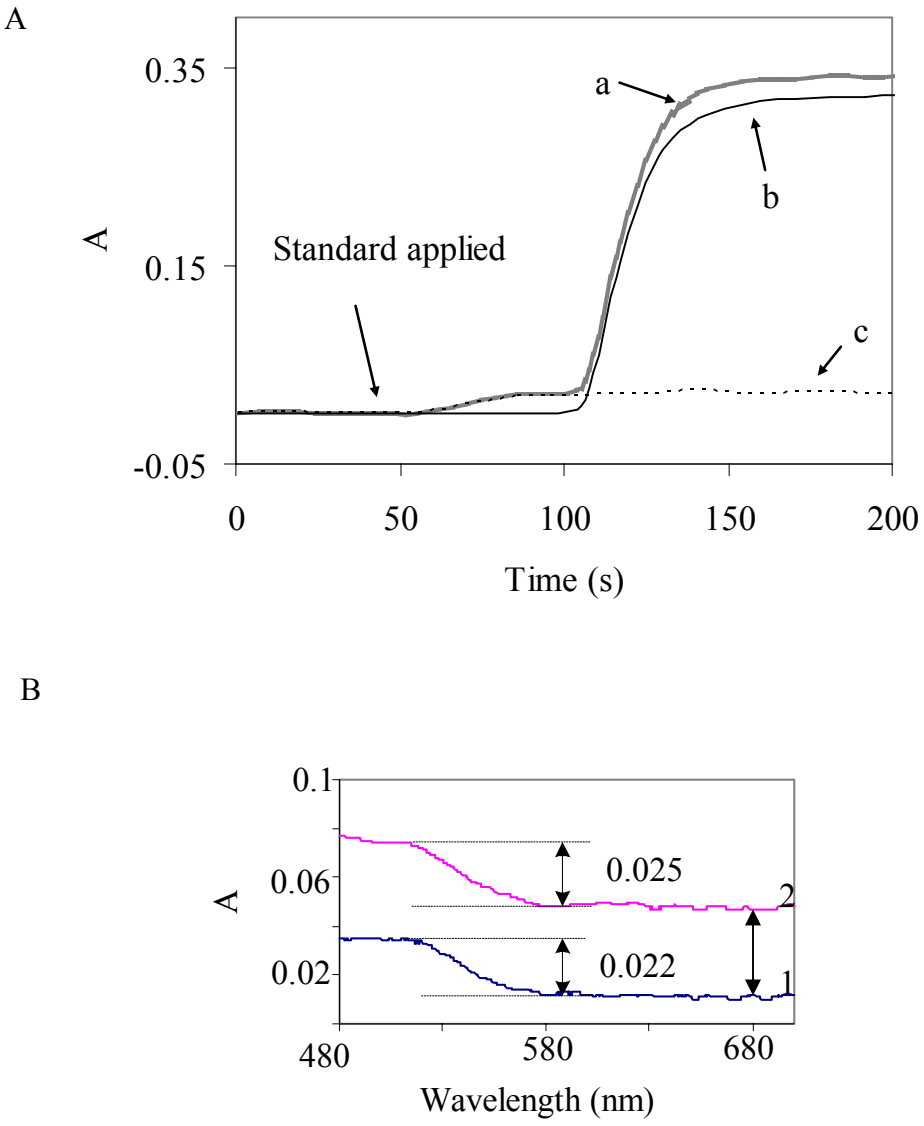

Figure 4.13 Baseline shifts and correction of the absorbance for the 100-cm LCW cell. A) Absorbance after introduction of a standard (264 nM Fe-o-phenanthroline complex) with monitoring at two wavelengths. a) A at 510 nm which is λ_m of iron o-phenanthroline complex. b) The background-corrected absorbance is the difference in absorbances at 510 nm and 680 nm ($A_{corr} = A_{510} - A_{680}$). c) A at 680 nm which is the background-correction wavelength where there is insignificant absorption by the iron o-phenanthroline complex. B) Blank spectrum measured before (1) after (2) measuring Fe standard and blank solutions for ~30 min. There was ~0.04 AU increase in the baseline at 680 nm. The corrected absorbance before and after are shown and A_{corr} increased 0.003 AU between these blank measurements.

absorbance at 510 nm at the wavelength maximum of the Fe-complex to correct for the baseline shift

Figure 4.13B shows two reagent blank spectra. One spectrum was taken before measuring several Fe standards over a period of ~30 min for a calibration curve, and the second blank spectrum was acquired after this period. After 30 min, the baseline increased ~0.04 AU. The background-corrected blank absorbance before and after measuring standards changed only 0.003 AU which is 12% of the total shift for this particular experiment. Background correction is necessary to compensate for the short and long term changes in light throughput, improves the accuracy of the absorbance measurement, and reduces the standard deviation of the blank absorbance. Drifts and shifts of the baseline during LCW measurements have been reported by other researchers. According to Li et al. (2003), refractive index changes, Schlieren effects and the adherence of gas bubbles to the Teflon AF surface are the reasons for baseline shift, drift and noise. They use background correction at a wavelength not absorbed by the analyte for compensation of these effects.

For nanomolar iron measurements, reagent concentrations were adjusted to minimum values that still provided an excess of reagent to analyte and good linearity. Decreasing the in-cell concentration of o-phenanthroline from 208 to 13 mM reduced sorption of the reagent to the Teflon AF tubing, and hence baseline shifts, and yielded a better linearity for the calibration curve.

The transmission of light is also affected by trapped bubbles which momentarily block the transmission and cause noise. Bubbles are minimized by

using continuous flow because stopping and starting the flow enhances the bubble problems.

Figure 4.14 is a summary of transmission problems faced in this study. Both baseline correction and periodic cleaning of the LCW cell are needed for reliable operation. Minimizing reagent concentrations to decrease the amount of absorbed species can also be critical. Also it is best to clean the cell between measurements of analyte solutions with a solution (e.g., buffer) that has about the same bulk concentration or refractive index as the standard/reagent solution to minimize refractive index differences.

4.3.4. Determination of Dissolved Oxygen with the Liquid Core Waveguide Based Recirculating System

4.3.4.1. Minimization of Oxygen Contamination with Double Containment and Nitrogen Purging

Oxygen leakage into the Plexiglas housing was evaluated with visual tests. For the version 2 of the instrument (Figure 4.5), oxidation of IC was observed after reduction and stopping the flow within 15 min at the tee where the LCW and peak tubing were connected to each other with ¼-28 fittings. After 2-5 hr, the excess reductant in the solution was consumed and all of the solution was oxidized.

These initial observations led to design and construction of the 3rd version of the LCW spectrophotometer (see Figures 4.7 and 4.8). The Plexiglas housing was designed to accommodate all the flow components to avoid direct contact of the components and atmospheric oxygen and to minimize the O_2 diffusion from

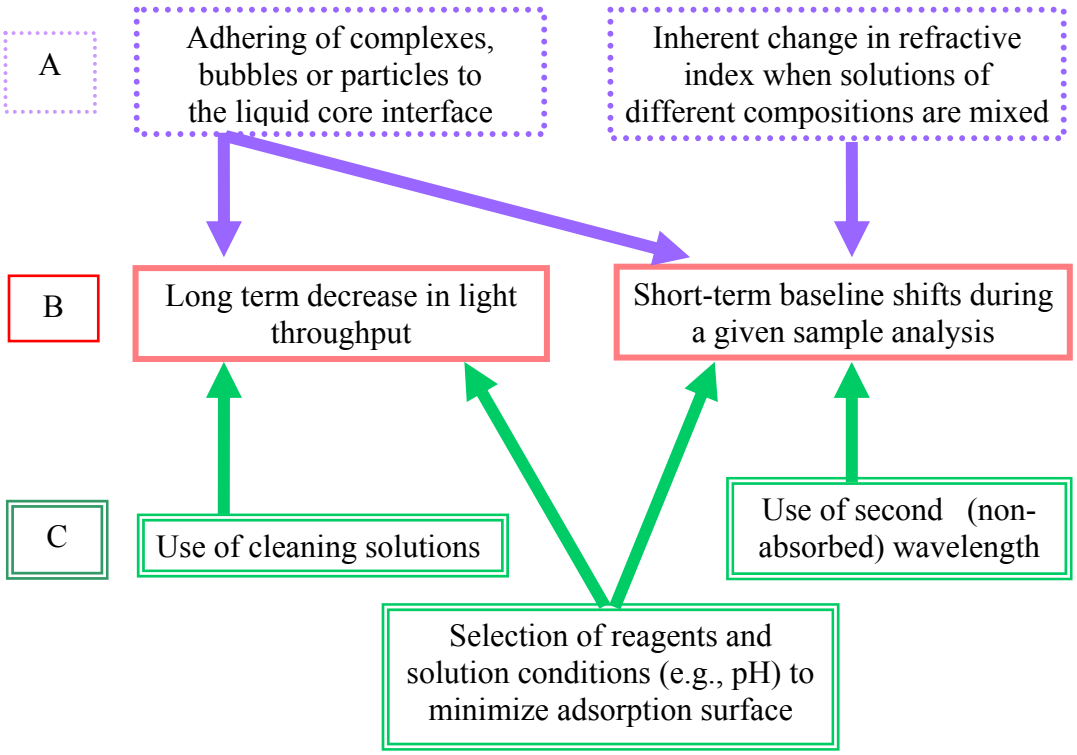

Figure 4.14 Summary of problems related to change in transmission of the liquid core waveguides. Causes (A), problems (B), and practical solutions (C) are given.

connectors. Visual oxygen leakage tests were performed to evaluate the weak points of the system. During these tests, the space in the housing was purged with prepure N_2 continuously. Oxidation of IC solution was first observed inside the ¼-28 fittings which were made of Tefzel® (ETFE, ethylene-tetrafluoroethylene). Within 30 min, the solution inside the silicone tubing became partially oxidized. The solution in the Teflon-AF LCW stayed reduced over 3 hr. These results suggest that the double containment of the LCW reduced the diffusion into waveguide but double containment of the fittings or the silicone tubing did not significantly reduce oxygen diffusion.

Another visual test was conducted to demonstrate the O_2 permeability of these components. The housing was opened to air, right after reduction of IC and halting the flow. First, the indicator inside the LCW became oxidized (in 10 s). The indicator inside the silicone tubing and the Tefzel fittings were oxidized within 5 min. This result is expected because Teflon-AF 2400 has very high permeability to oxygen (75240×10^{-10} cc cm cm^{-2} $s^{-1}atm^{-1}$) which is ~1000 times higher than Polyetheretherketone (PEEK™) and 168 times higher than Tefzel®.

As long as the housing was purged with N_2 and it was closed to air, the indicator solution in the LCW stayed reduced over 2 h. However, the solution inside the Tefzel fittings did not stay reduced even with double containment. It appears that O_2 is released from polymers over time and oxidizes the reagent. Thus, PEEK™ connectors and plugs were preferred in this study due to its relatively lower oxygen permeability which is 6.4×10^{-10} cm^3 cm cm^{-2} $s^{-1}atm^{-1}$ (Upchurch Scientific).

After the reduced IC is added to the cell or reactor and mixing is complete, there is a constant increase in absorbance due to oxidation of IC from O_2 entering the reagent solution. A constant slope suggests that there is a balance between O_2 entering the solution and reacting with the indicator yielding a steady-state DO concentration.

The rates of O_2 contamination of reduced indicator solution in the cell of the LCW spectrometer (version 3) and in the double-septum spectrometer vial are shown in Table 4.2. The headspace of vial or the reactor was constantly purged with N_2 during the measurements. The rate of contamination is calculated from the rate of oxidation of the indicator or the slope of the monitored absorbance. The baseline slope (mAU/s) due to O_2 diffusion into indicator circulating in the LCW system is 38 times higher than the slope observed with the double-septum vial.

The other slopes reported in Table 4.2 are normalized values. When the baseline slope with the LCW system is normalized to 1.2-cm pathlength (mAU/s-cm), the slopes for both cells are within a factor of 1.5. Likewise, the slopes in terms of picomole or nanomolar units are quite similar for both cells. However, due to the larger calibration sensitivity provided by longer pathlength of the LCW, the absorbance signal reaches its maximum limit (off-scale or $A > 2$) in ~7 min. Hence, time to make measurements before the redox indicator must be reduced again is very restricted with the LCW cell and is not long enough to allow the practical determination of dissolved oxygen.

Table 4.2 Comparison of the baseline slope between a 1.2-cm vial cell and a 26-cm LCW cell with nitrogen purging of the headspace of indicator solution.

Cell type	**Initial baseline slope** [b]			
	mAU/s (%RSD)	**μAU/s per 1.2 cm**	**pmol O_2/min**	**nM O_2/min**
1.2-cm double-septum vial [a]	0.13 (46)	130	450	150
26-cm LCW cell & double-septum reactor [c]	4.9 (72)	228 [d]	392	261

[a] The indicator was reduced with H_2 with Pt as the catalyst and then transferred to the double-septum spectrometer vial (Cakin, 2008). The in-cell IC concentration (oxidized and reduced) was 0.16 mM.

[b] The baseline slope in terms of pmol/min was calculated from the following formula S (pmol of O_2/min) = [S (AU/s) x 10^{12} x 60 s/min x volume (L)] / [2 x 21647 AU/ M-cm) x pathlength (cm)]. The solution volume was 3 mL for the vial and 1.5 mL for the flow system. It is assumed that 1 mol of oxygen reacts with 2 mol of IC. The baseline slope in terms of nM/min is calculated from S (nM of O_2/min) = [S (AU/s) x 10^9 x 60 s/min] / [2 x 21647 AU/ M-cm) x pathlength (cm)].
The means and RSD are based on three measurements for the vial and six for the LCW.

[c] Version 3 of the LCW spectrometer with the LCW cell in the Plexiglas house and all flow components protected with an ascorbic acid solution. The soluble reductant was Ti(III) citrate solution. The in-cell IC concentration (oxidized and reduced) was 3 μM.

[d] The absorbance value was normalized to a 1.2-cm pathlength by dividing the value by 26/1.2.

The similarity of the O_2 contamination rates is somewhat surprising. With the more conventional spectrometer vial, O_2 contamination can only originate from O_2 transfer from the purged headspace in reagent solution in the cell or possibly O_2 diffusion from the stirbar. For the LCW system, O_2 contamination can occur from the purged headspace but also through the LCW cell walls, through any of the other tubing in the recirculating system, and from diffusion out of fittings. Also the surface to volume ratio for the solution is much greater with the LCW system, but the total solution volumes are within a factor of 2. These observations support the concept that the contamination is primarily from the headspace. However, it is also possible that that rate of O_2 contamination is higher with the LCW cell, but the rate of oxidation (nM of IC/min) is less because it is proportional to the concentration of IC which is much lower in the LWC cell (3.0 μM versus 0.16 mM IC).

It is important to note that the rate of O_2 contamination for the LCW recirculating system is greatly reduced with N_2 purging of the reactor headspace, use of the double-septum cap, and double containment of the flow components in a box with ascorbic acid solution. Without these precautions, the reduced indicator solution would be completely oxidized in seconds. As with the simple spectrometer vial, there appears to be a limit to minimizing O_2 contamination of the reduced indicator.

4.3.4.2. Continuous Reduction of Indigo Carmine with Hydrogen

The overall oxidation of reduced indigo carmine added to either type of cell was stopped by continuous reduction by H_2 purging in the presence of Pt as catalyst

and effects of O_2 contamination were negated. Hence, the absorbance decreased overtime as shown in Figure 4.15, and the baseline slope was negative and decreased in time.

The baseline slopes are complied in Table 4.3 in terms of mAU/min and as normalized values. The reported values are typical values with low initial absorbance where most of the indicator was reduced (between 0.01 and 0.08 AU for the 1.2-cm cell or less than 0.6 AU for the 26-cm LCW cell). As indicated in the table footnotes, the slope with the double-septum vial was about 15 times higher (- 0.45 mAU/s) when the initial absorbance was in the range of 0.2 – 0.6 AU. The reduction rate of oxidized indicator would be expected to be correlated or proportional to the concentration of oxidized indicator. It is likely that both oxidation and reduction of IC are continually occurring during H_2 purging and the decay in absorbance indicates that the reduction of IC is dominant.

The baseline slopes in Table 4.3 in terms of measured absorbance are comparable for the two cells. When the baseline slope is normalized to a 1.2-cm pathlength or concentration units, the absolute baseline slopes with the LCW cell are ~20 times less than those with the 1.2-cm cell. This lower normalized slope may be due to the lower concentration of IC in the recirculating LCW system. The in-cell concentration of IC (1.0 μM) in the LCW was ~160 times less than the in-cell concentration of IC (0.16 mM) in the double-septum vial. Also, the H_2 concentration may be less in the LCW system because H_2 can permeate through Teflon-AF 2400

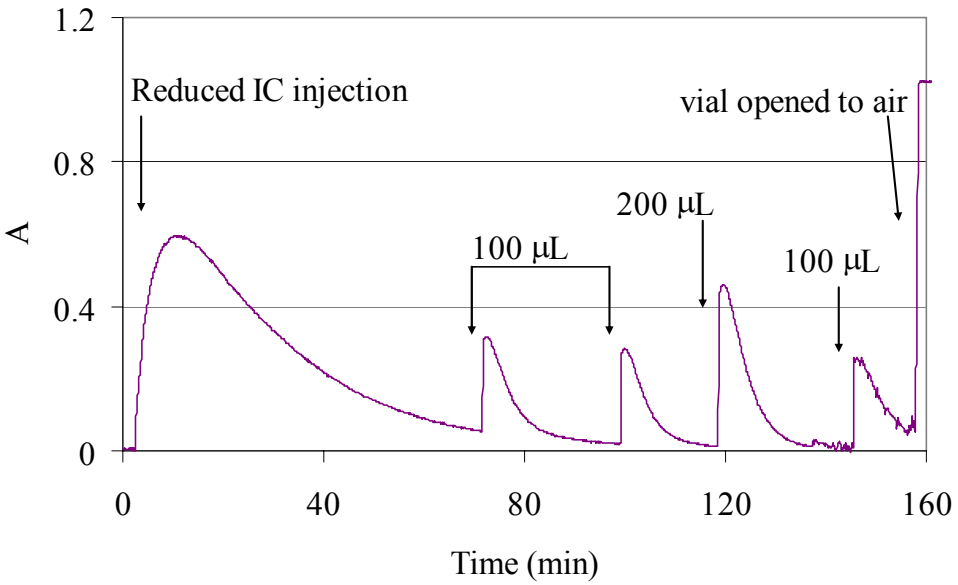

Figure 4.15 Oxidation of continuously reduced IC with air-saturated water in double-septum vial. The double-septum vial (1.2-cm pathlength) was purged with 100 % H_2 with at a 10 mL/min flow rate, in presence of Pt wire. The in-cell concentration of indigo carmine was 300 µM. Air-saturated water (100 and 200 µL) was injected as the standard solution.

Table 4.3 Comparison of baseline slopes between a 1.2-cm vial cell and a 26-cm LCW cell in a recirculating system with hydrogen purging of the indicator solution.

Experimental setup [a]	**Baseline slope** [b]			
	mAU/s (%RSD)	**μAU/s per 1.2 cm**	**pmol O_2/min**	**nM O_2/min**
1.2-cm double-septum vial	- 0.029 [c] (38)	- 29	-100	- 33
26-cm LCW flow cell & double-septum reactor	- 0.036 [e] (53)	- 1.7 [d]	- 3.8	- 1.9

[a] The indicator was reduced with H_2 initially (with Pt as the catalyst) and then transferred to H_2-purged, double-septum vial or double-septum reactor of LCW recirculating system. The in-cell IC concentration (oxidized and reduced) was 0.16 mM and 1.0 μM for the vial and LCW cell, respectively.

[b] The baseline slope in terms of pmol/min is calculated from the following formula S (pmol of O_2/min) = [S (AU/s) x 10^{12} x 60 s/min x volume (L)] / [2 x 21647 AU/ M-cm) x pathlength(cm)]. The solution volume was 3 mL for the vial and 2 mL for the flow system. It is assumed that 1 mol of oxygen reacts with 2 mol of IC. The baseline slope in terms of nM/min is calculated from S (nM of O_2/min) = [S (AU/s) x 10^9 x 60 s/min] / [2 x 21647 AU/-M cm x pathlength (cm)]. The means and RSD are based on two measurements.

[c] This baseline slope was measured for A < 0.08. For the absorbance range of 0.6 – 0.2, the baseline slope was - 0.45 mAU/s.

[d] The absorbance value was normalized to a 1.2-cm pathlength by dividing the value by 26/1.2.

[e] This baseline slope with version 3 of the LCW spectrometer was measured for A < 0.6 (A < 0.027 when normalized to a 1.2-cm pathlength).

tubing which has higher permeability for all gases (1.7×10^{-5} cm^3 cm cm^{-2} s^{-1} atm^{-1} for H_2, from Biogeneral, Inc.)

4.3.4.3. Calibration for Determination of Dissolved Oxygen

Typical responses observed with a 1.2-cm vial in the spectrometer with H_2 purging during injection of IC into the buffer and subsequent injection of air-saturated water as a high concentration standard are shown in Figure 4.15. Some of the reduced IC is oxidized due to contamination during the transfer process. The initial rise in absorbance may be due to mixing of the IC and buffer. The long tail represents the slow reduction of the oxidized IC. The oxidation peaks from injection of standards exhibit a long tail. The absorbance increased rapidly (1 min) to a maximum and then decreased more slowly back to the baseline (14 – 17 min for injection of 100 μL and 200 μL of water).

Figure 4.16 shows the oxidation peaks from injection of air-saturated water and a 0.2 mg/L (6.3 μM) standard into continuously reduced IC in the 24-cm LCW recirculating system. The time to reach the maximum absorbance was 0.5 – 1 min, after which the absorbance slowly decreased (18 – 19 min). The relationship between absorbance change and sample volume injected is linear for the air-saturated water injections as demonstrated in Figure 4.17.

Two low-level DO standards and a blank solution (0 – 0.7 mg/L) were sampled and injected with the micropump with the vial cell and the LCW cell recirculating systems. The calibration curves (Figure 4.18) show good linearity. The

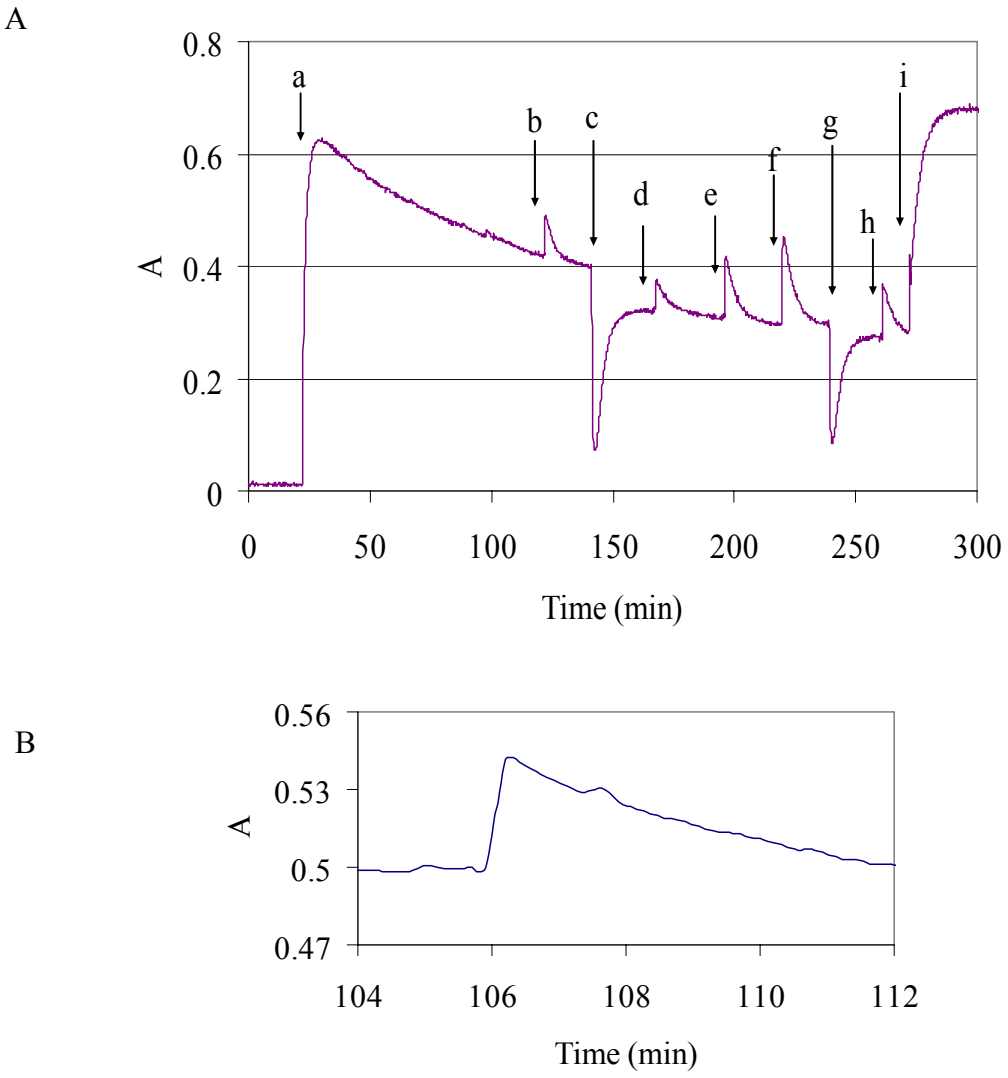

Figure 4.16 The oxidation and reduction of reduced IC with air-saturated water (A) and a low-level DO standard (B) in version 3 of the LCW spectrometer. The reactor was purged continuously with 100 % H_2 at a 10 mL/min flow rate, in the presence of Pt wire. The in-cell concentration of IC was 1 µM and the pathlength of the liquid core waveguide was 24 cm. A) Injections into the reactor were, a) reduced IC, b) 2 µL of air-saturated water, c) ~0.5 µL of Ti(III) citrate (~10 mM), d) 2 µL of air-saturated water, e) 4 µL of air-saturated water, f) 6 µL of air-saturated water, g) ~0.5 µL of Ti(III) citrate (~10 mM), h) 4 µL of air-saturated water. The H_2 purge was stopped at i. B) The peak response is due to the injection of 100 µL of 0.2 mg/L (6.3 µM) into the reactor.

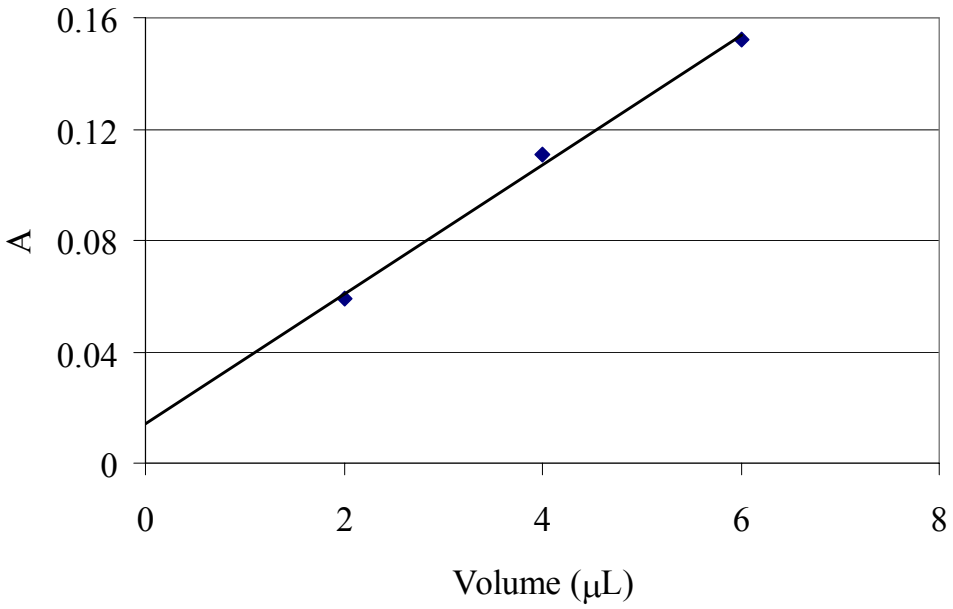

Figure 4.17 Dependence of the absorbance of the oxidation peak on the volume of air-saturated water injected into the reactor of version 3 of the LCW spectrometer. The in-cell concentration of IC was 1 μM and the pathlength of the liquid core waveguide was 24 cm. The in-cell DO concentration from injection of 2 μL was ~8 μg/L

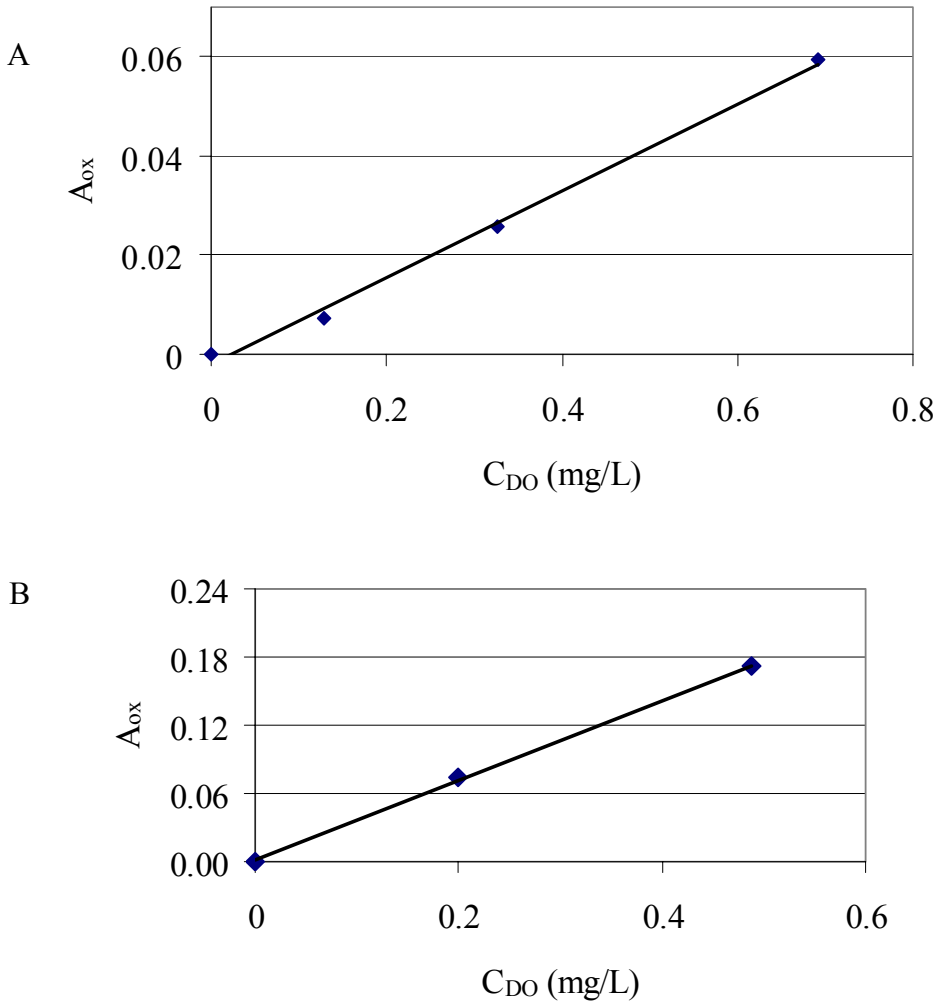

Figure 4.18 Calibration curve for low-level DO standards sampled and injected with a micropump into the hydrogen-purged, double-septum vial (A) and the hydrogen-purged reactor of the 24-cm LCW spectrometer (version 3) (B). A_{ox} values shown were corrected for blank signal and are the average of two injections for A and 3 injections for B. The DO concentration is that in the original sample. A) $A_{ox} = (0.088C_{DO} - 0.002)$ and the standard error of the slope and the intercept are 0.002 and 0.004, respectively. B) $A_{ox} = (0.35C_{DO} + 0.002)$ and the standard errors of the slope and the intercept are 0.007 and 0.002, respectively.

intercepts are within one standard deviation of the blank signal. The relative standard deviations (RSD) for the standards were 1.3% (~0.7 mg/L DO) and 14% (~0.5 mg/L DO) for the vial cell and the LCW cell, respectively.

Calibration and blank data are summarized in Table 4.4. The calibration slope is ~4 times greater with the LCW cell. The calibration slope with the LCW cell would be expected to be a factor of ~4 (20/5) greater because of the greater pathlength but smaller injected sample volume. The detection limits are not significantly different because the blank standard deviation is a factor of ~2 greater with the longer pathlength cell. If the blank standard deviation scaled with the pathlength, it would be 20 times larger or about 0.02 AU. The blank signal with the longer pathlength cell is not significantly different from zero. The blank signal for the LCW cell might be expected to be higher than the blank signal for the vial cell by the same factor (~5) as the relative increase in the calibration slope. This prediction is based on the assumption that the magnitude of the blank signal is determined by O_2 contamination before the injection.

Cakin (2008) in previous work has characterized a DO determination method based on oxidation of IC and use of the same optical spectrometer and double-septum vial cell used for this study. The primary difference was the use of N_2 as the purge gas. Without continual reduction of IC, the baseline had a positive slope due to continual oxidation of IC by O_2 diffusing into the reagent solution.

The summary of figures of merit in Table 4.5 shows that the calibration slope with H_2 purging is about half that with N_2 purging. Apparently, about half the

Table 4.4 Summary of the calibration and DL data for the vial and the LCW recirculating system with continuous hydrogen purging of the indicator solution.[d]

Experimental setup	Injected volume (mL) (%RSD)	Calibration slope (AU-L/mg)	Blank signal (AU)	Blank SD (AU)	DL [a] (mg/L)
1.2-cm double-septum vial	0.5 (0.05) [b]	0.088	0.008 (n = 5)	0.001	0.03
24-cm LCW and double-septum reactor	0.1 (0.4) [b]	0.35 [c]	0.0003 (n = 3)	0.002	0.02

[a] Detection limit (DL) = 3 x blank standard deviation (SD)/calibration slope.
[b] The number of measurements to determine the RSD was 5.
[c] When normalized to a 1.2-cm pathlength, the slope is 0.017 AU-L/mg-cm for the 0.1 mL sample.
[d] The in-cell IC concentration (oxidized and reduced) was 0.16 mM and 1.0 μM for the vial and LCW cells, respectively.

Table 4.5 Comparison of calibration slopes and detection limits for H_2- and N_2-purged 1.2-cm double-septum vials. [a]

Purge gas	Injected volume (mL)	Calibration slope (AU-L/mg)	Blank SD (AU)	DL [b] (mg/L)
N_2	0.5	0.18	0.004	0.07
H_2	0.5	0.088	0.001	0.03

[a] The data with N_2 as the purge gas is from Cakin (2008). The headspace of the vial was continuously purged with N_2 and the samples were injected with the micro pump sampler. The data with H_2 as the purge gas is from Table 4.4. The solution in the vial was continuously purged with H_2 and the samples were injected with the micro pump sampler.
[b] Detection limit (DL) = 3 x blank standard deviation (SD)/ calibration slope.

oxidized IC from the injection is reduced by H_2 by the time the peak is reached. The rate of oxidation and reduction are matched as the maximum. The primary advantage of H_2 purging with the vial cell is elimination of a significant positive baseline slope and a simple peak-shaped signal. It is simpler to extract the analytical information from this type of signal response and correction for the baseline slope is not required. The detection limit with H_2 purging is actually about a factor of 2 better due to a smaller blank SD although difference in DL is not significant.

4.4. Conclusions

A novel spectrophotometric method has been demonstrated for determining DO concentrations as low as 0.02 mg/L in small sample volumes of 0.1 to 0.5 mL with a 24-cm, liquid core waveguide (LCW) cell and a 1.2-cm sample vial. The measurement is based on the oxidation of reduced indigo carmine (IC) with O_2 in the sample. Continual reduction of IC, oxidized by the sample or by contamination due to diffusion of external O_2 into the reagent solution, maintains a lower baseline absorbance and is essential for use of the LCW cell. The final version of the LCW instrument has a re-circulating flow loop that includes a miniature peristaltic pump, a reactor, and a LCW cell. All three components are contained in a housing that was filled with a reductant solution to minimize diffusion of oxygen into the LCW cell and other components during the measurements..

The design and materials in the apparatus were carefully evaluated and chosen to minimize O_2 contamination. Novel critical components include the double-septum cap of the reactor or vial and the micropump flow sampler (Cakin, 2008). Previously, the double-septum cap, vial cell was used to minimize oxygen contamination by purging the headspace with N_2 during analysis, but continuous reduction of IC with H_2 was not employed .

Different prototypes of LCW based spectrometers were constructed and earlier versions were evaluated for Fe determination at micromolar and nanomolar concentrations with the o-phenanthroline method. Initial prototypes were also useful in evaluation of the oxygen contamination in a flow system. During all LCW

measurements, the performance and sample throughput was limited by the stabilization of signals and the baseline. The baseline shifts associated with refractive index changes were minimized by background correction at a second wavelength where the analyte did not have significant absorption. Reduction of reagent concentrations also minimizes baseline shifts and improved the linearity of the calibration curves.

The detection limit (DL) of 0.03 mg/L for DO obtained with the proposed methods is a factor of 6 to 8 times better than that achieved with the Winkler titration and the Clark-type DO probe and equivalent to that reported for the fluorescence optrodes (ASTM D888-05, 2005). Some of the commercial kits based on the visual detection of oxidized IC (CHEMetrics kit (K-7503) and Hach AccuVac Ampules) or Rhodazine D (Dissolved Oxygen ULR CHEMets for 0-20 ppb (K-7511)) provide a DL a factor of 6 to 30 better (1 -6 μg/L DO) (CHEMetrics, 2007). The methods based on ampules with pre-reduced indicator perform well because the sample transfer takes place with the ampule immersed in the sample. Thus, O_2 contamination is minimized. The calibration slope is higher due to little dilution (the ratio of sample volume to reagent is high) and a longer pathlength.

With conventional DO methods, transferring the sample requires the consumption of large volumes of sample (typically more than 300 mL) to washout the sample bottles, overflow sampling cells, or flow cells prior to sampling or measurement. For the same reason, the commercial kits (sealed ampoules) that provide the lowest DL, are not applicable for enclosed systems with of limited

volume (0.1 -1 L) such as microcosm bottles or columns. The total sample consumption for the DO methods described in this study is ~2 mL which is 100 to 1000 times less than the volume required with conventional DO methods. Overall, the new proposed DO method provides a lower detection limit for sample volumes of 2 mL than provided by any other DO method except the related methodology developed by Cakin (2008) which is based on N_2 purging.

The primary advantage of continuous H_2 purging in the presence of Pt is that the positive sloping baseline due to oxygen contamination is eliminated, and in fact, the baseline absorbance decays to a low absorbance with sufficient time. This provides a longer total analysis period with a given reagent solution which must be changed when the absorbance due to oxidized IC goes off scale. In addition, the calculations to obtain the analytical signal are simplified because there is no need to correct the observed signal for the baseline slope as is necessary with the N_2-purged 1.2-cm vial cell.

For the H_2-purged, 1.2-cm vial, once the reagent solution and the Pt wire is saturated with H_2 (within an hour), the reducing capacity is maintained for more than 3 hr even when the purging is stopped. This allows the injection of multiple samples until the vial reaches its volume limit (~4.5 mL) for efficient stirring. On the contrary, IC solution in the 24-cm LCW re-circulating system did not stay reduced when the H_2 purge was stopped. The absorbance signal increases due to oxygen contamination to its maximum limit (off-scale or $A > 2$) in ~7 min. Hence, H_2 purging is necessary to use the LCW cell in the laboratory or the field, but it provides

advantage for the use of the sample vial for field measurements. The IC solution in the vial cell could be reduced in the laboratory and then taken to the field without the need for a H_2 tank. However, a small tank of nitrogen is required for purging between the septa of the double-septum cap and the headspace in the spectrophotometer vial.

For bench-top measurements that require the lowest sample volume (e.g., 0.1 mL), the LCW based spectrometer with H_2 purging is more advantageous because the detection limit (0.02 mg/L) is ~5 times better (lower) than that with a N_2–purged, 1.2-cm vial cell with the same sample volume and IC (Cakin, 2008). The proportional increase of calibration slope of LCW system by injecting larger volumes such as 0.5 mL should be explored. The maximum improvement in detection limit with larger sample volume is ultimately limited by contamination of the blank (or a low DO sample) with O_2 during the sample transfer process. The variability of the O_2 contamination eventually limits the blank standard deviation. Syringe sampling, rather the pump sampling, may be advantageous for lower DO values because it is easier to control the contamination and less sample is required to purge the sampling system (Cakin, 2008).

Further improvements in the detection limit may be possible by using suitable redox indicators such as Rhodazine-D in place of IC that provide a larger calibration slope due to a larger molar absorptivity than IC. In previous work (Cakin, 2008), Rhodazine-D provided a detection limit that was a factor of ~6 better than that with IC with a 0.1-mL sample volume. This DO detection limit of 0.03mg/L with

Rhodazine-D is equivalent to the detection limit with the LCW cell in this work. Hence, it might be possible to improve the detection limit with Rhodazine-D in the LCW cell to10 ng/mL or below. Use of a syringe rather than the pump sampler may also improve detection limits by reducing the blank standard deviation if blank contamination is limiting.

Further development of the calculation procedure is necessary. The software should be refined to eliminate the need to manually transfer data into a spreadsheet and to determine which data to use to extract the absorbance value used for calibration plots. A better understanding of the factors affecting the precision of measurements, which is worse with the LCW cell relative to the vial cell, and baselines shifts would guide modifications that could improve precision and reduce the noise and the standard deviation of blank measurements.

4.5. Acknowledgements

This research was supported by a research grant from the U.S. Environmental Protection Agency sponsored Western Region Hazardous Substance Research Center under agreement R-828772. This article has not been reviewed by the agency, and no official endorsement should be inferred. We appreciate the patience, effort and skill of Ted Hinke at the Machine Shop of the Department of Chemistry at Oregon State University for construction of double-septum caps and Plexiglas housings for liquid core waveguides.

4.6. References

Altkorn, R.; Koev, I.; Gottlieb, A. *Appl. Spectrosc*., **1997**, *51(10)*, 1554-1558.

Altkorn, R.; Koev, I.; Van Duyne, R. P.; Litorja, M. *Appl. Optics,* **1997**, 36 (34), 8992-8998.

Annu. Book ASTM Stand. **2005,** *11.01,* D888-05, 60 -70.

Annu. Book ASTM Stand. **2005,** *11.02,* D5543-94, 759 -765.

Bryne, R. H.; Liu, X.; Kaltenbacher, E. A.; Sell, K. *Anal. Chim. Acta*, **2002**, 451, 221-229.

Bryne, R. H.; Yao, W.; Kaltenbacher, E. ; Waterbury, R. D. *Talanta*, **2000**, *50*, 1307-1312.

Buck, W. H.; Resnick, P.R. Du Pont Product Bulletin H-52454.

Cakin, D., Chapter 3 of Ph.D. thesis, Oregon State University, Corvallis, OR, 2008.

Callahan, M. R.; Kaltenbacher, E. A.; Bryne, R. H. *Environ. Sci. Technol.* **2004**, *38*, 587-593.

CHEMetrics product specifications in www.chemetris.com, 2007.

Dasgupta, P. K.; Zhang, G.; Poruthoor, S. K.; Caldwell, S.; Dong, S.; Liu, S. Y. *Anal. Chem.,* **1998,** *70(22)*, 4661-4669.

Dasgupta, P. K.; Eom, I.-Y.; Morris, K. J.; Li, J. *Anal. Chim. Acta,* **2003**, *500(1-2)*, 337-364.

Ingle, J. D. Jr.; Crouch, S. R. *Spectrochemical Analysis*; Prentice-Hall: New Jersey; 1988.

Jones, B. D., Ph.D. thesis, Oregon State University, Corvallis, OR, 1999.

Li, Q.; Morris, K. J.; Dasgupta, P. K.; Raimundo, I. M. Jr.; Temkin, H. *Anal. Chim. Acta,* **2003**, *479*, 151-165.

Pappas, A. C.; Stalikas, C. D.; Fiamegos, Y. C.; Karayannis, M. I. *Anal. Chim. Acta,* **2002**, *455*, 305-313.

Ruiz-Haas, P. R., Ingle, J. D. Jr. Geomicrobiol. J., **2007**, *24*, 465-378.

Song, L.; Liu, S.; Zhelyaskov, V.; El-Sayed, M.A. *Appl. Spectrosc.,* **1998**, *52,* 1364-1367.

Toda, K.; Yoshioka, K.-I.; Ohira, S.-I.; Li, J.; Dasgupta, P. K. *Anal. Chem,* **2003**, *75(16)*, 4050-4056.

Tsunoda, K. I.; Nomura, A.; Yamada, J.; Nishi, S. *Appl. Spectrosc*., **1989**, *43(1),* 49-55.

Upchurch Sci. web site, www.upchurch.com; 2007.

Wang, Z; Wang, Y.; Cai, W.-J.; Liu, S.- Y. Talanta, **2002**, 57, 69-80.

Wei, L.; Fujiwara, K.; Fuwa, K. *Anal. Chem.,* 1983, *55(6)*, 951-955.

Yao, W.; Bryne, R. H. *Talanta*, **1999**, *48*, 277-282.

Zhang, J.-Z.; Chi, J. *Environ. Sci. Technol.,* **2002**, *36*, 1048-1053.

Zhang, J.-Z.; Kelble, C.; Millero, F. J., *Anal. Chim. Acta,* **2001**, 438, 49-57.

CHAPTER 5:

Conclusions and Further Studies

The primary challenge in the determination of dissolved oxygen (DO) at low levels is the contamination of reagents, standards, blanks, and samples with atmospheric oxygen and the oxygen released from the materials in contact with solutions. This is the same challenge for quantification of many reduced species that react with oxygen (Ruiz-Haas, 2007). In this thesis research, new analytical methods were developed that are useful for determining DO concentrations below 1 mg/L for low volumes of aqueous environmental samples. It is much more difficult to protect samples of low volume from contamination because surface to volume ratio is higher.

The analytical methods developed in this research are based on monitoring the absorbance increase from the oxidation of reduced indigo carmine (IC) by the oxygen in the sample. This concept with indigo carmine or other redox indicators has been the basis of accepted methods to determine DO for some time. However, the techniques and instrumentation described here are more sophisticated than conventional methods. Much lower detection limits have been achieved with lower sample volumes. These characteristics should be particularly attractive for researchers doing anoxic laboratory studies with limited sample volumes. These same attributes are also beneficial for field studies because it is relatively simple to transfer small samples with a syringe from a septum capped flow cell that is in line with a pump system to sample a well.

Different spectrometer configurations were developed in this research. In the first configuration, a vial with a pathlength of 1.2 cm (near the conventional

pathlength of 1 cm) was used as the spectrometer cell where the sample and reagent were mixed. For the second configuration, liquid core waveguides (LCW) based on Teflon AF tubing served as the flow cells with long path (24 cm) to increase the calibration slope while maintaining low total solution volume. The LCW cell was in a flow loop with a small pump and a reactor to inject and mix and sample with the reagent.

Oxygen contamination was minimized with several unique innovations. First double-septum caps were used with the spectrometer vial cell, the reactor of LCW flow system and the sample bottles. For introducing reagents or samples into the sample cell or reactor of the spectrometer or withdrawing samples from the source (sample container, column, etc), the septum is the interface between the sub-oxic medium and air. Anytime a single septum is pierced, air leaks into the solution enclosed or "protected" by the septum. In contrast, a double-septum cap enables N_2 purging of the space between septa and better protects the contents of the closed sub-oxic system from atmospheric contamination introduced through the first septum.

The second innovation of double containment was necessary for the LCW spectrometer because it is a recirculating flow system with both pump tubing and LCW tubing (Teflon AF) that are permeable to O_2. The flow components in contact with the reagent solution of the LCW spectrometer (peristaltic pump head and tubing, a reactor, and 24-cm of LCW tubing) were enclosed in a Plexiglas housing. The housing was filled with ascorbic acid solution to reduce the O_2 that diffuses into the enclosure and minimize oxygen reaching the solution in the flow loop. This

technique of protecting flow components from oxygen has been used previously only to protect peristaltic pump tubing (Haas, 2006).

The third innovation was the development of a micropump sample and methodology for transferring samples from the sample container to the cell or reactor. The purging of the sampling device including all tubing is critical for obtaining low blank signals and blank standard deviations. Even with all of these precautions, some contamination occurs during the sample transfer and the blank signal is detectable. In some regards, a gas-tight syringe with careful rinsing may be more useful in some application because of it simplicity and ease of purging. The primary disadvantage is that the syringe, unlike the pump, cannot be easily automated.

Oxygen contamination of the N_2-purged, 1.2-cm vial cell or the re-circulating LCW system was minimized but could not be stopped. The slow diffusion of oxygen into the reagent solution causes a positive sloping baseline for the absorbance signal. For both systems, the headspace (of the reactor or the vial) is considered as one of the major interfaces across which O_2 can diffuse into a stirred solution. The total amount of oxygen in the nitrogen that flows through the headspace in 1 min is estimated to be ~2 nmol. This value was calculated for 50 mL/min flow rate and the purity of the N_2 (99.9999%). This oxygen transfer rate is ~4 times larger than the O_2 permeation rate of ~0.5 nmol/min that was measured with the 1.2-cm vial cell (headspace N_2 purged). However, it is expected that only a small fraction of the O_2 that passes through the headspace during the purge would diffuse into the solution.

When air standards were injected into the headspace, less than 1% of the O_2 transferred into the solution. Hence, it is likely that additional O_2 contamination of the reagents arises from external O_2 that diffuses through the septum into the headspace and eventually into the reagent solution.

Without a continual headspace purge after the initial N_2 purge, the permeation rates were not significantly different. If the O_2 already in the headspace gas were only from the initial purge, there would not be enough O_2 to cause the observed degree of oxidation in the vial. Also, there was no visual observation of the release of O_2 from the stirbar.

During the previous research in this laboratory at OSU, Ruiz-Haas (2006) measured O_2 permeation rates into a microcosm bottle (250 mL) in a flow loop that included a sample flow cell and a pump with thionine as the redox indicator and continuous flow. The reported O_2 permeation rate of ~1 nmol/min is not significantly different from the rate observed with N_2 the purged and continuously mixed systems in this study.

The components of the Plexiglas housing for the LCW system were modified numerous times to minimize the contamination. Due to the long pathlength of the LCW, the positive baseline slope is magnified and the same absolute contamination rate has a larger effect with the LCW system. The slope normalized to pathlength is not significantly different with the LCW cell.

Another strategy to stop O_2 contamination was the consumption of the excess oxygen. This was easily achieved in the 1.2-cm vial and the LCW system by

continuous reduction of IC with H_2 purging in the presence of Pt wire as the catalyst. The primary advantage is that the baseline absorbance decays to a low absorbance with sufficient time. This provides a longer total analysis period with a given reagent solution which must be changed when the absorbance due to oxidized indigo carmine goes off scale. Also, the calculations to obtain the analytical signal are simplified because there is no need to correct the observed signal for the baseline changes as is necessary with the N_2-purged, 1.2-cm vial cell.

The removal of oxygen contamination with H_2 purging in the presence of Pt could be optimized in future studies. It might be possible to adjust the concentration and the flow rate of H_2 or the amount of Pt in the solution to achieve a flat baseline before the injection. Also, electrochemical reduction of the indicator in-cell or generation of reductants such as hydrogen to compensate for the contamination should be explored. Electrochemical techniques can be very useful where extreme miniaturization is required.

Sampling methodology involves purging of the flow sampler lines or the syringes with nitrogen passing between the septa of the double-septum caps. This process helps minimize contamination of reagents and samples. With any DO method, keeping the analytical device (the parts that are in contact with the sample), the reagents for some of the methods, and the sample free of contamination from atmospheric oxygen are the keys to a reliable detection, particularly when measuring trace levels of O_2. Transfer of a low volume sample into the analytical device is

extremely difficult because oxygen contamination has higher concentrations in smaller volumes.

Many of the standard methods for low-level DO environments (i.e., boilers and ground water) rely on continuous flow (before and during sampling) of the sample through the sampling cell or chamber to purge out the residual oxygen before the measurement is made and sometimes to minimize O_2 contamination while the DO measurement is being made. Often more than 300 mL of the sample is required to purge the sampling cell or chamber. Hence, methods that require this purging approach are not applicable for closed systems with a limited volume of sample.

Further improvement of the analytical performance of the methods presented here is possible with significant reduction in the contamination rate of the samples, application of different redox indicators with a higher molar absorptivity, and elimination of possible errors associated with calculation procedures. Fluorescence monitoring of redox indicators upon oxidation with DO is another promising approach. The redox indicators Rhodazine-D and safranine-o have similar reaction kinetics with O_2 when reduced and are fluorescent.

The sampling methodology and spectrometric instrumentation developed here for DO measurements could also be particularly useful for analytes that are in highly reduced states and which react rapidly with oxygen at low concentrations. Oxygen contamination even at low levels can result in errors in determination of micromolar levels of reduced species such as Fe(II) and S(-II).

The ultimate application for ground water studies is a submergible sensor for monitoring of low-level DO. The instrumentation could be modified for in-situ sampling. Ideally, oxygen contamination would not be a problem because the instrument would not be in direct contact with air and the sample provides the double containment. It may take some time for O_2 to diffuse out of polymer components.

References

Ruiz-Haas, P. R., Ingle, J. D. Jr. Geomicrobiol. J., **2007**, *24*, 465-378.

Ruiz-Haas, P. R., Ph.D. thesis, Oregon State University, Corvallis, OR, 2006.

APPENDICES

Appendix A: Hardware and Software for Controlling Micropump

A.1. Introduction

The micropump was controlled via a home-made circuit (hardware) with a microcontroller module interfaced to the laptop computer. The number of the strokes is determined by the number of pulses sent to the pump (up to 2 per second). The BS1USB module (Parallax, Inc.) consists of a BASIC Stamp®-1 microcontroller, an on-board USB interface and a USB-A connector. A short basic stamp-1 program (software) was created with "the BASIC Stamp Editor for Windows version 2.2" for different commands such as start pumping, pump until stopped, deliver a set volume of sample and stop pumping.

In the circuit described in section A.1.2, pins (0-7) of the BS1USB module are wired to the circuit board. The status of the each pin is selected as high or low via a switch for the desired operation (i.e., stroke or pause for 0.5 s) by the user. The BS1USB module regularly checks the status of the input pins and sets the status of the output pins such that commanded operation takes place with the coded timing and sequence.

A.1.1. Hardware Details

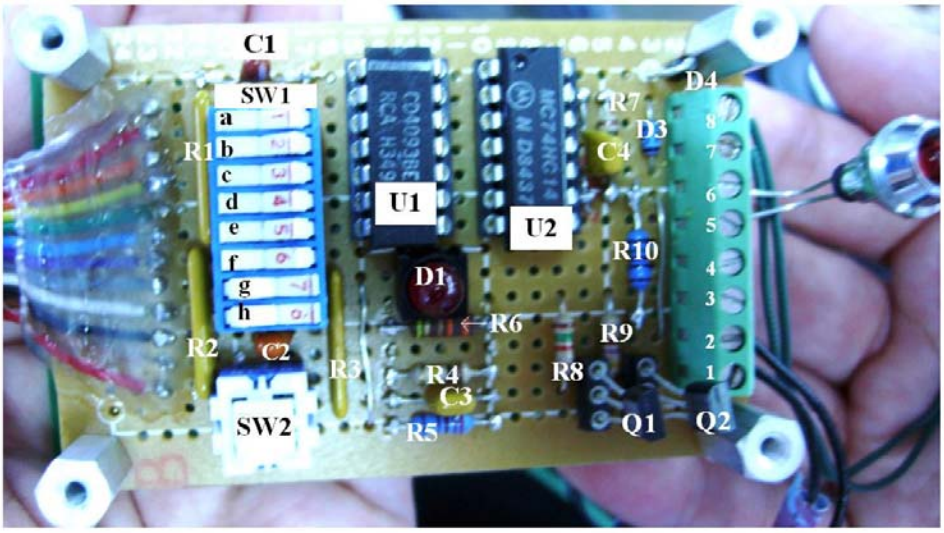

Figure A.1 Photograph of the home made circuit for controlling micropump.

R1-R10 = Resistors
SW1 = Dip switches 1 to 8
SW2 = Push button
U1 = CD4093BE CMOS Quad 2-Input NAND Schmitt Triggers
U2 = MC74HC14 N Hex Schmitt-Trigger Inverter
Q1 and Q2 = ZTX855 high current transistors
D3 = IN759 Zener diode
D4 = IN4001 diode
C1-C4 = Capacitors
P0-P7 = Input/output pins of the BS1USB module

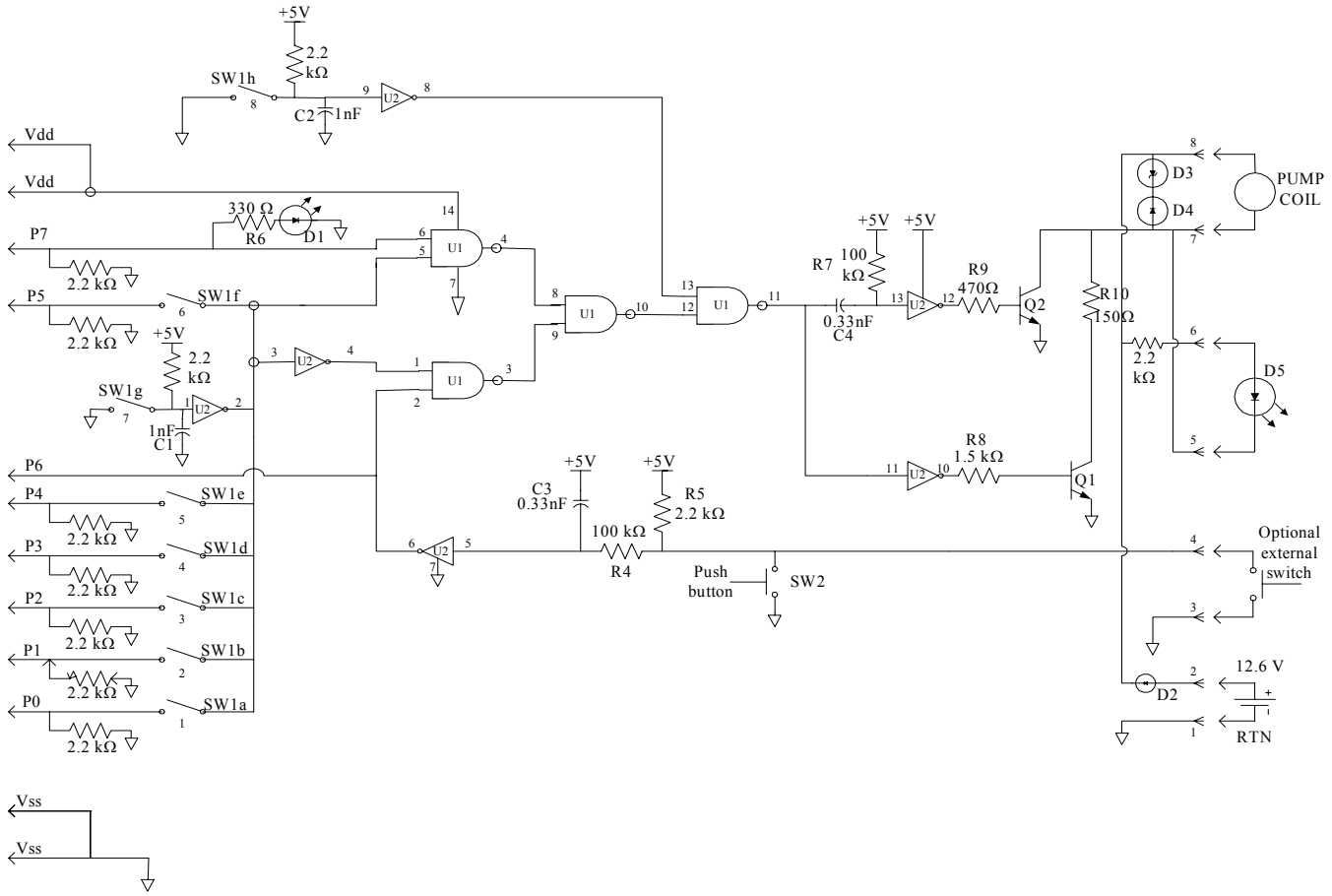

Figure A.2 Wiring diagram of the home made circuit for controlling micropump.

A.1.2. Pump Control Code

```
' {$PBASIC 1.0}


 SYMBOL counter1 = B0              'First variable for pulse/stroke counting
 SYMBOL V = B1                     'First variable for number of pulses
 SYMBOL counter2 = B2              'Second variable for pulse/stroke counting
 SYMBOL F = B3                     'Second variable for number of pulses
 V = 10                           'Set number of pulses to a constant value
 F = 30

 Main:
  DIRS = %00000000                 'Set all the pins as inputs
  IF PIN1 = 1 THEN Nonstop         'Check P1 if continuous pumping is desired
  IF PIN0 = 1 THEN Start           'Check P0 if pumping a certain volume is
desired
  IF PIN2 = 1 THEN Flush           'Check P2 if continuous flushing is desired
  DEBUG "Paused", CR
  IF PIN6 = 0 THEN Stop
  GOTO Main



Nonstop:
   DEBUG "Continuous pumping", CR
   DIR7 = 1                                  'Set P7 into output mode and low
   PAUSE 500                                 'Wait for 500 ms
   DIR7 = 0                                  'Set P7 into input mode
   PIN7 = 1                                  'Set P7 high
   PAUSE 500
   GOTO Main

Start:
   DEBUG "Pumping known volume", CR
   FOR counter1 = 0 TO V                      'Loop in “Start” 10 times
   DIR7 = 1
   PAUSE 500
   DIR7 = 0
   PIN7 = 1
   PAUSE 500
   IF counter1 = V THEN Wait
```

```
    IF PIN0 = 0 THEN Main              'Check P0 if “star loop” is stopped
    NEXT
Flush:
    DEBUG "Flushing", CR
    FOR counter2 = 0 TO F
    DIR7 = 1
    PAUSE 500
    DIR7 = 0
    PIN7 = 1
    PAUSE 500
    IF PIN2 = 0 THEN Main
    NEXT
Wait:
    PAUSE 5000
Stop:
  DEBUG "Stopped", CR
  PIN7 =0
  GOTO Main
```

Appendix B: Evaluation of the Pump Working Range for the Portable Flow Sampler

The accuracy and the working range of the pump were evaluated for different sample headspace pressures. The head pressure of the pump was controlled rather than using simple purging because the precision and the accuracy of the dispensed volume is highly dependent on the pressure difference between the inlet and outlet of the pump. In addition, the portable flow sampler requires higher pressures at the inlet because the sample bottle and the reaction vial are both closed to air and slightly pressurized with N_2.

A microcosm bottle was filled with deionized water, capped with a septum cap, and it was purged with purified N_2 (~100 mL/min) to provide the positive pressure. The vent line consisted of syringe needle and PEEK tubing and the distal end of the peak tubing is inserted through the stopper of a small Erlenmeyer half-filled with water so that it was below the surface to prevent backflow of air. The flask also has it own vent to air. The nitrogen line from the mass flow controller is connected to a PEEK tee. One line of tubing is inserted through the stopper of a small Erlenmeyer half-filled with water so that it was below the surface to prevent backflow of air. The other line passed through a needle valve (Upchurch Scientific), an analog pressure gauge (0 - 10 psi, Matheson Co. Rutherford, N.J.), and then through the microcosm bottle septum cap via a hypodermic needle. The magnitude of the gas pressure was varied with the needle valve until the pressure gauge showed the desired pressure.

Water from the microcosm bottle was dispensed into a 5-mL beaker with the diaphragm pump set for 10 strokes and the beaker was weighed before and after each increment (10 strokes). The approximate dispensed volume for every increment was calculated from the weight difference measured.

Figure B.1 shows the effect of headspace pressure on the sample volume. When the microcosm bottle was open to the atmosphere, the pressures at the inlet and at the outlet of the pump tubing were equal. The volume dispensed per 10 strokes without the headspace pressure and without the stainless steel frit (20-μm pore size) is defined as the nominal sample volume which was 0.52 mL. The percent error in volume for higher headspace gauge pressures (with or without the frit) was estimated relative to the nominal sample volume.

When the frit was not placed at the inlet of the pump, the error for sampling 0.5-mL water (10 strokes) was less than 8% for the 0 - 0.5 psi range. The error in volume was from -4 to 7% for 0 - 1.5 psi range when the frit was used. The working range was larger when the frit was used, and even with headspace pressures as high as 2 psi, a 13% error was measured. Without the frit and with a headspace pressure of 2 psi, the error was ~90%.

For further experiments, 1 psi was chosen as the optimum headspace gauge pressure for the microcosm bottles during sampling and the SS frit was used at all times. The relative standard deviation of the volume dispensed for 0.5-mL sample was 0.7% with the completed sampler apparatus (see Figure 3.3 in Chapter 3).

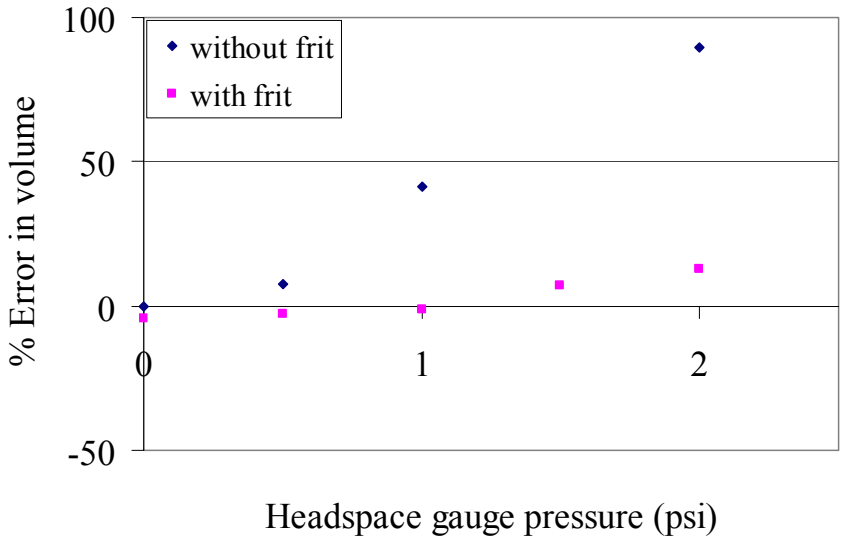

Figure B.1 The effect of headspace pressures on the sample volume.

Appendix C: Sample Calculations for the DO Concentrations of the Calibration Standards

C.1. Introduction

The concentrations of the standard solutions were calculated according to American Society for Testing and Materials' (ASTM) publications (2004). With the known fraction of O_2 in the gas mixture, barometric pressure and temperature, the concentration of dissolved oxygen in water can be calculated. Sample calculations for a 0.2-mg/L standard will be introduced step by step in this section.

C.2. Fraction of O_2

The fraction of the O_2 in the gas mixture (pressurized air and N_2) was set by adjusting the calibrated mass flow controllers to a known flow rate. The calibration equation for FC-260 (N_2 flow controller) was [$y = 5.4017\ x + 4.6616$] from 1.5 to 45 x values. The ordinate (y) represents the flow rate of N_2 (mL/min) that was measured with Restek Flowmeter 6000 and the abscissa (x) represents percent flow rate that displayed on Tylan RO-28 electronic flow rate controller/readout.

The calibration equation for FC-280 (air flow controller) was [$y = 1.275\ x - 1.1124$]. The ordinate represents percent flow rate of air that displayed on Tylan RO-28 electronic flow rate controller/readout as the abscissa represents the flow rate of air (mL/min) that was measured with Restek Flowmeter 6000.

C.2.1. Sample calculation

When N_2 and air flow controllers display 17.3% and 2.02%, respectively, the correct flow rates are calculated as 98 mL/min of N_2 and 2.46 mL/min of air with the calibration equations above. The oxygen content of the air flow is 20.9% which corresponds to 0.513 mL/min O_2. The fraction of O_2 flow in total gas mixture (N_2 + air) is 0.0052.

C.3. Dissolved Oxygen Concentration of the Standard Solution

Benson and Krause (1980) presented detailed equations and tables for the concentration of DO in equilibrium with the atmosphere from 0 - 40ºC and 0.5 - 1.1 atm. Their equations are based on Henry's Law and include corrections for the molecular interaction in the vapor phase. The following equations are from ASTM (1999) derived by Hale from Benson and Krause's study.

$$c(\mu g / L) = X(P - P_w)\exp\{16.9775 - [(5268.95 - (1004170 / T)) / T]\} \quad \text{(C.1)}$$

$$P_W = \exp\{11.857 - (3840.7 + 216961 / T) / T\} \quad \text{(C.2)}$$

The concentration of the dissolved oxygen is c (μg/L). The total gas pressure (P) and water vapor pressure (P_W) are in bar. The fraction of O_2 in the gas phase that is in equilibrium with water phase is X, which was calculated in section C.2, and T is the temperature in K.

The total gas pressure, P is the ambient air pressure if there is no positive pressure in the headspace of the microcosm bottle (open to air). The optimum headspace pressure was set to 1 psi (0.0689 bar) for accurate operation of the

sampling pump (see Appendix B for details). Thus, P becomes the addition of ambient air pressure and the positive gas pressure in the headspace. The headspace pressure was adjusted to 1 psi (above the ambient air pressure) and was monitored with the analog pressure gauge (Matheson Co. Rutherford, N.J.), which was connected to the headspace via a hypodermic needle. The barometric pressure was determined from the updated recordings of the local weather stations (KA8ZGM and CW5707) in Corvallis, OR.

C.3.1. Sample calculation (continuing from C.2.1.)

For the example demonstrated here, the fraction of O_2 is 0.0052 (X) in the gas phase in equilibrium with the water phase (deionized water) at an ambient temperature of 298 K. With an ambient air pressure of 1.015 bar and the additional positive headspace pressure as 0.0689 bar, the total gas pressure (P) in the headspace of the microcosm bottle (septum bottle) becomes 1.08 bar. From equation C.2 at 298 K, P_W is found to be 0.0309 bar. Finally, solving equation C.1 with all of the parameters yields an O_2 concentration (c) of 0.22 mg/L for the prepared standard solution. Without the pressure correction, c is 0.21 mg/L at 298 K and 0.23 mg/L at 293 K.

C.4. References

Annu. Book ASTM Stand. **2004,** *11.01,* D5543-94

Benson, B. B.; Krause, D. Jr.; *Limnol. Oceanogr*. **1980,** 25(4), 662-671.

Appendix D: Disadvantages of Pt-coated Alumina Pellets as the Catalyst for H_2 Reduction of IC

The disadvantages of using Pt-coated alumina pellets (Aldrich, 0.5 wt. % Pt) as a catalyst were sorption of the indicator onto the pellets and disintegration of the pellets over time. The sorption of the indicator onto the pellets was visually observable as the pellets became stained with an intense blue color overtime.

Figure D.1 shows the absorbance increases observed in a reduced IC solution (contained in a double-septum, 1-cm cuvette) due to injections of air-saturated water. The IC stock (~0.2 mM, 2.5 mL) was reduced in a double-septum vial via purging with 100% H_2 (10 mL/min) in the presence of 4 Pt-alumina pellets. From this stock solution, 0.5-mL reduced IC was injected into double-septum 1-cm cuvette that contained 1.5-mL deaerated buffer (pH 7, 0.1 M).

The response (increase in the absorbance due to the oxidation of reduced IC) for injection b, c, and e was 50-74% of the theoretical absorbance change calculated for air-saturated water injections. In addition, re-reduction of the indicator occurred (seen clearly for injection e) after every oxidation which caused the shape of the absorbance change to appear as a peak instead of step increase. When Pt wire was used to reduce the IC in the vial (stock solution), the increase in absorbance from injection of air-saturated water was within 98% of theoretical and the response was a step with a slight positive slope after the step.

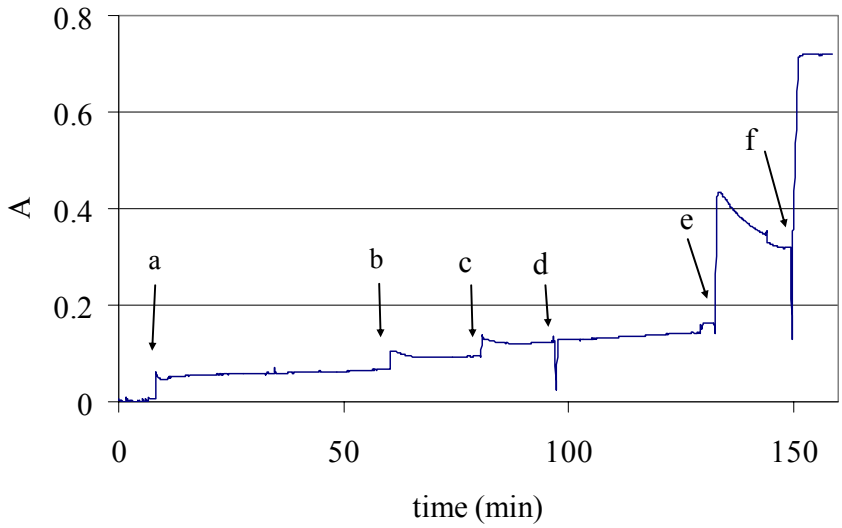

Figure D.1 Air-saturated water injections into an IC solution that was previously reduced with H_2 in the presence of Pt-pellets. Injections were a) 0.5 mL of 0.2-mM reduced IC, b) and c) 0.025 mL of air-saturated water, e) 0.1 mL of air-saturated water. d) The cuvette was removed momentarily for a manual shake. f) The cuvette was opened to air by removing the double-septum cap.

The re-reduction and non-quantitative oxidation of IC are suspected to be due to the disintegration of the Pt-pellets in reduced IC stock vial overtime. Upon disintegration, Pt powder could be transferred during the injection of reduced IC into the cell causing further reduction of the indicator during a sample run due to the H_2 injected with the reduced IC.

Appendix E: Evaluation of the O_2 Permeation of Flow Sampler Components

To evaluate the contribution of different components to O_2 contamination, reduced IC solution was pumped through a 1-cm pathlength flow cell which was placed at the outlet of the sampling system (see Figure E.1 for details of two versions of experimental apparatus). The pump was a solenoid-actuated diaphragm pump (LPLA, Lee Company Inc.) with a pre-set volume of 50 μL. The inlet and outlet connections were ¼-28 flat bottom boss. The low-volume, fiber-optic, SMA, zigzag flow-cell (Alitea Instruments LLC, Medina, WA) was used to monitor the absorbance changes of the reduced IC over time.

Figure E.2 shows typical results obtained when the pump was stopped and restarted 20 s later while continually acquiring absorbance data by the spectrophotometer at a faster than normal rate (1 point per second). This procedure revealed a fingerprint like pattern that indicated in what parts or sections of the flow system IC became more oxidized. From the resulting absorbance "peaks and dips," the calculated void volumes of individual system components (See Table E.1), and the flow rate (45 μL/s), the sources of greatest O_2 contamination were identified. A relatively small peak ("b" in Figure E.2), was observed with both setups within ~2 s of starting the pump, which corresponded to the zone in the flow-cell and its ¼-28 inlet fitting. With either setup, the first lower absorbance point (dip labeled as "c") represents solution that was approximately at the middle of first section of PEEK tubing between the flow cell and pump. Shoulders or peaks were observed for

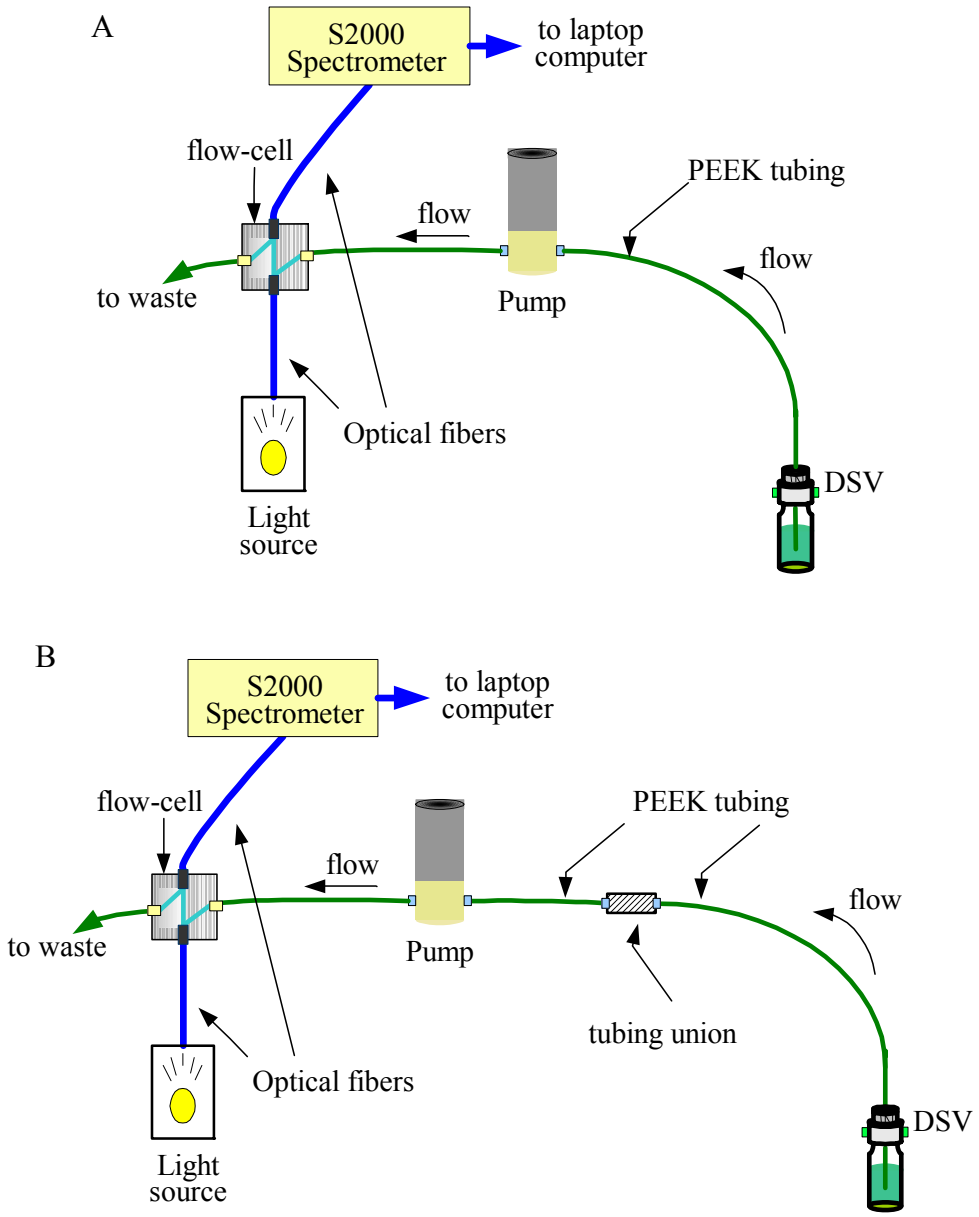

Figure E.1 Experimental apparatus for evaluation of the contribution of components to O_2 contamination. A) Components of the experimental setup starting from the outlet and ending with the inlet were the zigzag flow-cell, 1/16" OD PEEK tubing (11 cm), micro-pump, 1/16" OD PEEK tubing (25 cm) and reduced IC stock in 20-mL double-septum vial. B) Components of the experimental setup starting from the outlet and ending with the inlet were the zigzag flow-cell, 1/8" OD PEEK tubing (5 cm), micro-pump, 1/8"OD PEEK tubing (15 cm), female Tefzel® union, 1/16"OD PEEK tubing (25 cm) and reduced IC stock in 20-mL double-septum vial.

Table E.1 Void volumes of individual system components in the experimental apparatus for evaluation of O_2 permeation pattern.

Component	**ID (mm) x length (cm)**	**Internal volume (μL)**
segment of the flow cell that is in contact with ¼-28 fitting	1.6 x 1.2	24
1/8” PEEK tubing (short segment)	2 x 5.0	162
1/8” PEEK tubing (long segment)	2 x 15.5	502
1/16” PEEK tubing (short segment)	0.75 x 11.3	220
1/16” PEEK tubing(long segment)	0.75 x 25.3	493
Micro pump (Lee)	NA	100

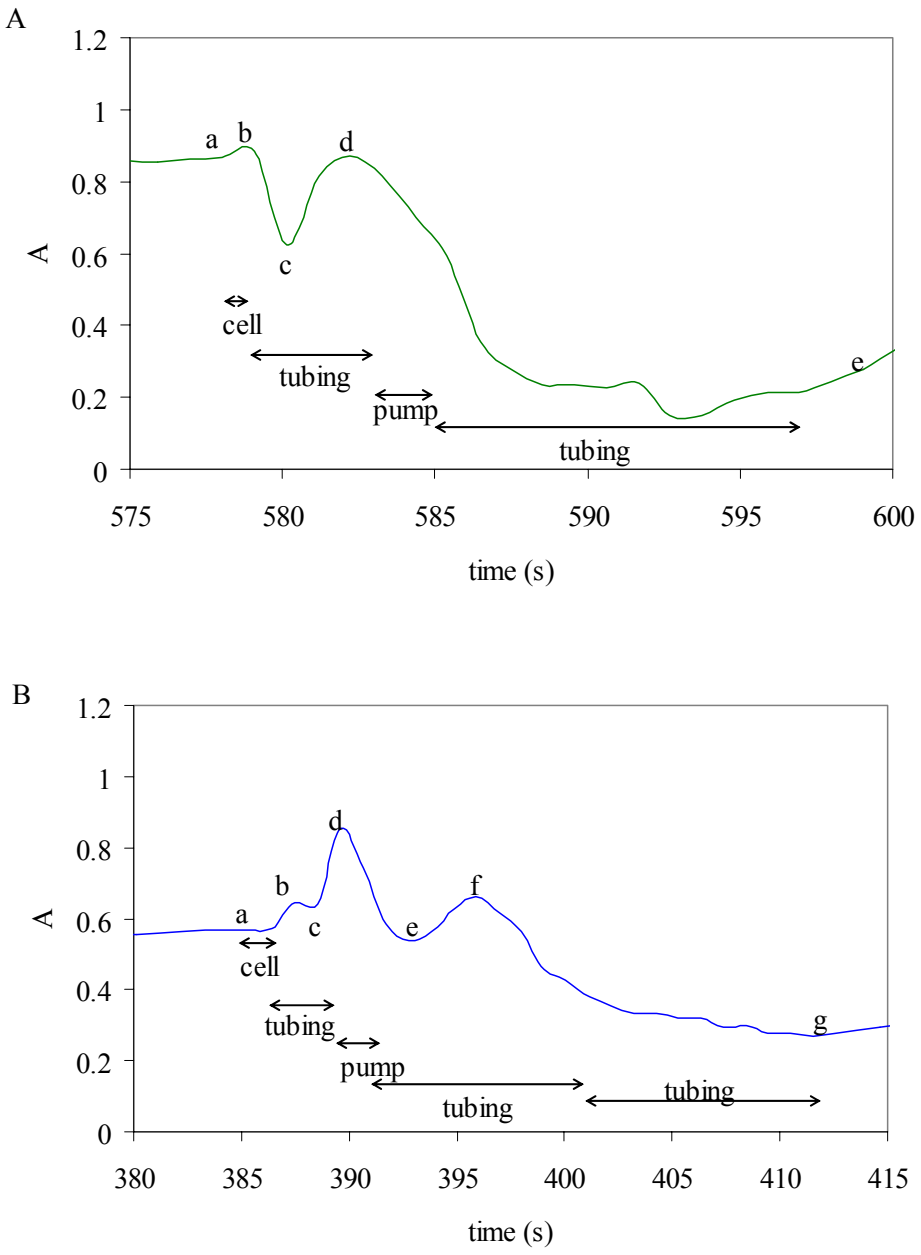

Figure E.2 O_2 permeation pattern during continuous flow after stopping the pump for 20 s. A) The experimental apparatus is depicted in Figure E.1-A. The pump was started at "a" and stopped at "e". Peaks at "b" and "d" represent the O_2 permeation into solution near the zigzag flow-cell and the pump, respectively, when the flow was stopped. B) The experimental apparatus is given in Figure E.1-B. The pump was started at "a" and stopped at "g". Peaks at "b" and "d" represent the O_2 permeation due to the zigzag flow-cell and the pump, respectively. The peak at "f" represents the contamination during the stop period that occurred at the union which was added to the system as an extra component.

solution that was stopped inside the pump and near the ¼-28 fittings of the pump as one large peak (labeled as "d" in both graphs). The plug of partially oxidized IC inside the pump (45 - 100 μL) dispersed to ~400 μL when it reached the flow cell after the pump stop (20 s) and pumping periods.

The number of dips and peaks increased if an additional component was added to the system. When an extra union was added in between two PEEK pieces, an additional peak (labeled as "f" in Figure E.2-B) was observed due to contamination of solution at both ends of the coupler.

Luer type connectors were avoided (especially when connecting needles) because they resulted in relatively higher peaks (more contamination) during pump stop-start experiments. Other tested ideas and components were using stainless steel tubing instead of PEEK tubing or double containment of the pump in N_2 atmosphere. These variations in the setup did not significantly improve (reduce) the average absorbance signal for blank solutions (N_2 purged deionized water).

Potential sources of contamination are O_2 diffusing out of the components and air permeating in through fittings and unions. As a result, it is best to minimize the number of connections (i.e., ¼-28) for low level O_2 applications.

For semi-quantitative pump start-stop experiments described above, the lowest absorbance (minimum contamination) was maintained during continuous flow through the cell after the washout of the lines. Even under these conditions the time for solution to be transferred from the DSV to the flow cell was 20-27 s.

Appendix F: Optimization of Washout Procedure of the Portable Flow Sampler

The pump and sampling lines (total ~0.35 mL) were washed out by pumping the sample or the standard or the blank solution prior to sampling to minimize the oxygen contamination. The details of the experimental apparatus are given in Figure 3.3. The micropump was a solenoid-actuated diaphragm pump (Bio-chem Valve Inc.) with an internal volume of 105 μL and the flow rate was adjusted to 48 μL/s (1 stroke per second).

Different sample washout volumes were tested with and without a N_2 purge. Figure F.1 shows the reduction in the blank signal (A_{bk}) with increased washout volumes without N_2 purging. The pump and sampling tubing were emptied and refilled with air by pumping air (~30 min) before each measurement. After the system was flushed with 15 mL of blank solution (43 times the total internal volume), A_{bk} was 0.03 AU. The blank signal did not significantly improve (decrease) with larger flush volumes such as 30 mL (86 times the total internal volume).

Further reduction of A_{bk} was achieved by first purging the pump and sampling tubing with N_2 and then washing out pump and sampling lines with the blank solution. The pump was on during both steps.

Figure F.2 shows the dependence of A_{bk} on N_2 purge time with a fixed, liquid washout volume (1.5 mL) for all measurements. A N_2 purge of 1 min (~3 mL) provided an A_{bk} (0.045) that was 4 times smaller than A_{bk} (0.18) without a N_2 purge.

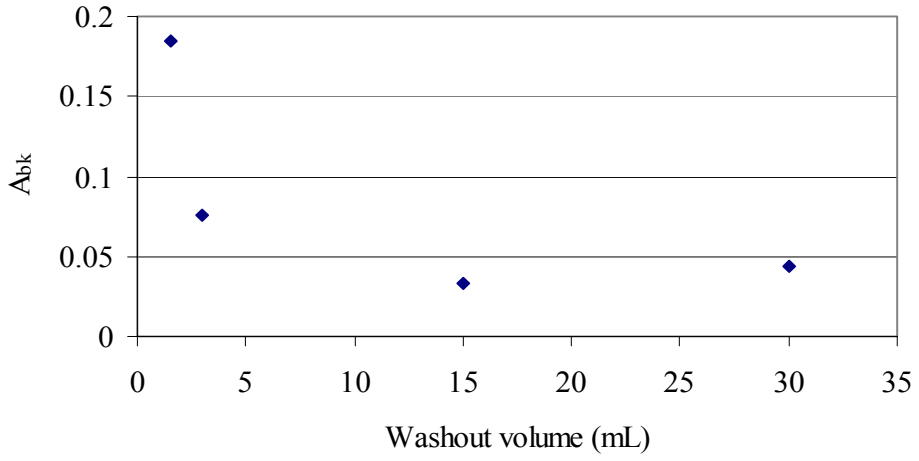

Figure F.1 The effect of increasing washout volumes on the blank signal. The pump and sampling lines (internal volume of ~0.35 mL) were washed out with the blank solution (N_2 purged deionized water) before sampling and the measurement of the blank. Each data point represents a single measurement.

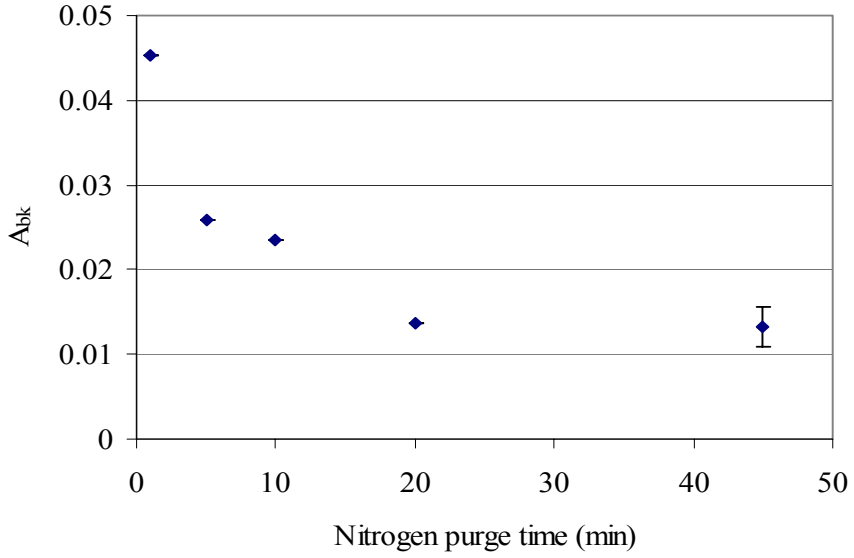

Figure F.2 The effect of longer nitrogen purge periods on the blank signal. The pump and sampling lines (internal volume of ~0.35 mL) were purged with nitrogen and then washed out with ~1.5 mL of blank solution (N_2 purged deionized water) before sampling and the measurement of the blank.

Increasing the N_2 purge period from 1 to 10 min decreased A_{bk} (0.023) by about a factor of 2. A further increase in purge time to 20 min reduced A_{bk} (0.014) about another factor of two. The blank signal did not significantly decrease with longer N_2 flush times.

In a separate study with repetitive measurements, the average A_{bk} with a 10-min N_2 purge (0.020, n = 5) was ~2 times greater than A_{bk} (0.012, n = 6) with 20-min N_2 purge. The standard deviation of the blank was 0.004 for both purge periods. The difference is significant at the 99% confidence level based a t-test for two means.

It appears that the removal of residual O_2 from the sampling equipment with N_2 flow is efficient, eliminates the excessive consumption of the sample, and results in lower blank signals then achieved with only solution rinsing. As mentioned in the experimental section, the N_2 purge period was chosen as 10 min followed by washout with 1.5 mL of the sample as a compromise between the lowest blank signal and time necessary to make a measurement. After the pump and tubing are purged with nitrogen once, low blank signals are obtained for successive blank measurements using only a rinse of the blank or sample solution as long as the sampling lines are kept filled with solution.

Appendix G: Evaluation of the Precision and the Accuracy of Blank Measurements

G.1. Introduction

The standard deviation of a blank measurement is a combination of the standard deviations due to variability in O_2 contamination from run to run, variability in the sample transfer volume and the reagent volume from run to run, instrumental noise due to the noise in the spectrometric signal from the CCD, and random error in software correction process used to determine the absorbance change (A_{bk}). Standard deviations of these processes were estimated to ascertain the limiting factors affecting the precision of the blank measurements. The typical blank standard deviation and blank signal are 0.004 AU and 0.02 AU, respectively.

G.2. Precision of Sample Transfer without O_2 Contamination

The precision of the volume delivered using portable sampler was evaluated with two different methods. The first method was weighing the injected blank solution. Regular blank solution was prepared and transferred to the spectrometer cell (vial) with the analytical procedure given in section 3.2 of this thesis. The relative standard deviation (RSD) was 0.2 % for 5 consecutive blank injections with an average volume of 0.4895 mL. Clearly the imprecision in sample delivery is not limiting.

The second approach involved measuring the precision of injections of oxidized indigo carmine (IC) solution into the spectrometer cell (vial). IC solution (125 mL, 0.02 mM) was purged and transferred under the same conditions given for

a blank solution except that the spectrometer vial contained pH 7 buffer (3 mL, 0.1 M TRIS). The absorbance was monitored during injections in 3 separate runs with 2 samples per run (2 injections per vial). The response is a step function and ΔA values are 0.098 AU and 0.074 AU for the first and second injections, respectively, which corresponds to about 5 times a typical blank absorbance.

The absorbance change due to addition of IC was calculated with the procedure given in section 3.2 and the mean was 0.098 AU (corresponds to 0.46 mg/L DO). The SD and RSD in absorbance signal (A_{ox}) were 0.0008 AU and 0.8 %, respectively. As there was no oxidation reaction, no possible contamination from O_2, or no baseline drift, the precision of the absorbance change depended on the precision of the sample and buffer volumes delivered and the instrumental noise and random error due to the corrections for dilution and baseline drift. The standard deviation due to these factors is significantly less than the standard deviation of the real blank (0.004 AU).

G.3. Error and Noise due to Correction of Absorbance

An artificial baseline drift was generated using an Excel spreadsheet. The generated data represented an increasing baseline with a constant slope of 0.0001 AU/s that is similar to a typical baseline drift with reduced IC. The data were processed with the equations specified in section 3.2 and corrected absorbance signals (A_{bk}) was calculated.

The volume of the injection was entered as 0 mL because the generated data did not include any sample/standard additions. A_{bk} was calculated as -7×10^{-16} AU. This result demonstrates that the baseline correction procedure does not cause a systematic error (i.e., a non-zero value of A_{bk}) when the assumption of constant baseline slope is true.

Figure G.1 shows how the baseline slope changes overtime for a typical blank run. The ordinate represents the magnitude of the baseline slope (AU/s) calculated over consecutive ~100-s periods; the abscissa represents the sequence order or number. For example, if sequence 3 is the period from 204 to 300 s, the slope is taken as the difference in the absorbance at these two times divided by 96 s.

The slope of baseline drift calculated from real blank measurements decreases with time within the same run. This decrease in slope is consistently observed with other blank runs or with standard injections. For a typical blank run, the initial absorbance at the time of the first injection is in the range of 0.05 to 0.09 AU and slope is in the range of 1 to 2×10^{-4} AU/s.

For the particular data shown in Figure G.1, the slopes in the first and fifth 100-s periods were 1.52×10^{-4} and 1.39×10^{-4} AU/s, respectively, and the slope used to calculate the baseline correction value (fifth 100-s period) is 8.6% lower than the estimate of initial slope at the time of injection (first period). The slope decreased 3×10^{-6} AU/s over every 100 s. After the 400-s period (default reaction period), the slope decreased ~1.2×10^{-5} AU/s. Thus, correction of the absorbance for the baseline drift (A_b from equation 3.5) is 0.0556 AU with the decreased slope (400

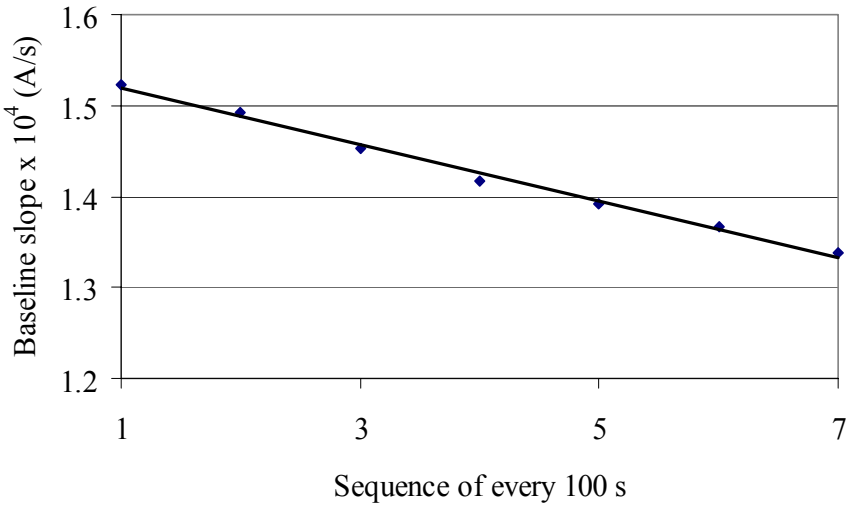

Figure G.1 Decrease in the slope of the baseline over time. The data source for these calculations is a typical blank run before a blank injection. The slopes were calculated over consecutive 100-s periods of the baseline drift before any injection. The absorbance at the beginning of the run was 0.076 AU. The first period starts at ~222 s into the run.

s after the injection) but is 0.0608 AU with the initial slope. The low estimate of the baseline slope results in an absolute error of 0.005AU (calculated as the difference of two A_b values) and a relative error of ~8%. Note that A_b is ~3 times greater than a typical blank signal of 0.02 AU and the error in this slope correction is ~25% of a typical blank signal.

Errors caused by the continual decrease of the baseline drift can be minimized by calculating an average of the slopes over a 100-s period before and after the injection/reaction period (400 s). The same blank data were treated with this alternative baseline calculation method and the normal correction method and the results are compared in Table G.1 with both pump and syringe injection.

With both pump and syringe injection, use of the average slope reduces the blank absorbance by up to a factor of 2 as it provides a better correction. There are not enough data points to conclude that the standard deviation changed significantly with the type of baseline correction. It appears that the variability of the blank signal is not limited by random error in the baseline correction process.

The more complex baseline correction scheme is not warranted. Although it provides a better estimate of the blank absorbance and hence contamination level, it does not cause a systematic error for the determination of the DO level because the same correction method is used for the standards or samples. The systematic error will be eliminated when the blank absorbance is subtracted form the standard or sample absorbance.

Table G.1 Comparison of different baseline corrections for blank measurements.

	Pump [a]		Syringe [b]	
	Normal baseline correction	Average baseline correction	Normal baseline correction	Average baseline correction
A_{bk} (AU)	0.012	0.0066	0.023	0.016
SD [c] in A_{bk}	0.0037	0.0032	0.002	0.0014

[a] n = 6 for micropump injections with 20 min N_2 washout period after 2 runs
[b] n = 5 for syringe injections
[c] SD, standard deviation

G.4. Conclusions

The decrease in the baseline slope causes a significant but acceptable systematic error in the correction for baseline drift and the value of the blank absorbance. This error does not affect the accuracy of calibration correction for sample measurements.

The precision of a blank measurement appears to be limited by the variability of O_2 contamination. The blank SD with injections of oxidized indicator without the possibility of contamination, but with dilution and baseline correction is, considerably less than the SD of a real blank.

There are differences in the two sampling procedures, the geometry, and the materials of the sampling devices. The inlet and the outlet of the micropump sampler do not directly contact atmospheric oxygen during sample transfer. On the contrary, the syringe's needle is open to air momentarily before the sample injection. The micropump is composed of polymeric materials, especially the diaphragm that has an oxygen storage capacity. The gas-tight syringe has a glass body, but it also has a moving plunger tip made of Teflon.

The DL of the method with the micropump sampler or the syringe appears limited by the inherent variability due to O_2 contamination of the blank during transfer. With the micropump, the pooled standard deviation of signal from two blank injections within the same run is 0.001 AU (calculated for the three separate runs in Table G1). It appears that this good precision is achieved because the contamination rate of the blank is similar within the same run. However the standard

deviation of the blank signals from run to run is 0.003 AU (three separate runs, total 6 injections). Between runs the micropump and tubing is emptied and flushed with N_2 and a new IC solution is added.

The contamination level with the micropump depends on the control of the timing of injection. The level of contamination increases as the time delay between rinsing the sample tube and the injection increases. From the slope of the contamination level with time (section 3.3.1.3), a 2-s difference in the delay time can change the blank signal by 5% or ~0.001 AU.

With the syringe injection, the pooled standard deviation of two blank injections within the same run is 0.0007 AU (calculated from two separate runs); whereas, the run-to-run blank standard deviation is 0.02. There are not enough data to determine if this difference is significant.

Contamination occurs with the gas-tight syringe, but the contamination level does not increase significantly with the time delay before injection as it does with the micropump. Hence, control of the time between filling the syringe and injection is not as critical as it is with the micropump.

It is possible that the run-to-run standard deviation of the blank signal is affected by the variability in the blank correction. For each run the baseline slope is slightly different. The absolute error in A_{bk} due to the imperfect baseline correction is proportional to the baseline slope. Hence, there is a random error component in A_b due to the slight variation in the error of the baseline correction from run to run because the baseline slope is different each time new reagent is used.

Appendix H: Testing of Flow-cell Sampling from a Large Volume Source

H.1. Introduction

Sampling of low-level dissolved oxygen (DO) solution from a large volume (2 L) source was tested to simulate a ground water application. Samples were drawn from a sampling flow-cell with a gas-tight syringe and analyzed with the analytical procedure in section 3.2.4 of this thesis.

H.2. Experimental Setup

The sampling system consisted of a sample solution bottle, a sampling flow cell, and a pump. PEEK tubing (1.57-mm (1/16-in) OD) and ¼-28 flangeless fittings (Upchurch Scientific) were used for connecting these components and also for purging the sample with N_2.

A low-level dissolved oxygen (DO) sample was prepared in the same manner as a blank solution. The sample source was a 2-L glass bottle (KIMAX, No 14395) and it was capped with a gas-tight, three-hole cap (Kontes, Ultra-ware 953930-series) that has three female ports for ¼-28 fittings. The glass bottle contained 1.8 L of deionized water that was purged for 5 hr with 150 mL/min of N_2 before sampling and was continuously purged during sampling. The sample was stirred with a magnetic stir-bar. A solvent filter (UHMWPE Bottom-of-the-Bottle solvent filter, A-446) was placed at the end of the PEEK N_2 purge line to produce fine bubbles.

The sampling flow-cell was placed in between the sample source and the peristaltic pump (SP 200 APT Instruments, Litchfield, IL) so that the pump pulled the sample through the flow cell to avoid any possible oxygen contamination coming from the pump. The PEEK tubing was connected at all times. The total internal volume of the sampling tubing and the flow-cell was ~2 mL and the internal volume of the flow cell is 1.7 mL. The sampling flow cell is a Plexiglas cylinder with a circular cavity, a cap, and ¼-28 ports in the inlet and outlet. The flow cell was capped with a double-septum cap. More details of the flow-cell (reactor) are given in section 4.2.2. of this thesis.

H.3. Optimization of the Sampling Flow-cell Washout Period

The low-level DO sample was pumped out of the bottle through the sampling flow-cell continuously with a flow rate of 3.23 mL/min. Samples (each 0.5 mL) were drawn every 5-10 min with a gas-tight syringe followed by determination of DO with DSV-IC method. As seen in Figure H.1, the DO for 92 % of the samples was below the detection limit (0.074 mg/L) after 10 min (32.3 mL) of washout. This washout volume is ~15 times the total volume of sampling tubing and the flow-cell.

The data confirm that the continuous flow-cell sampling from a low-level DO source for the determination of DO is feasible for DSV-IC method. The blank signal is not significantly different from that obtained from sampling a purged septum bottle.

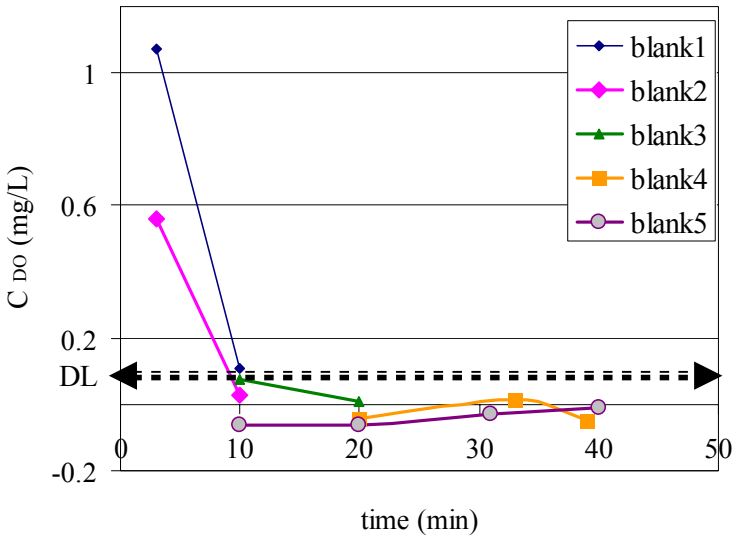

Figure H.1 Optimization of the washout period for the flow-cell sampling of a 2-L sample source. The DL, which represents the detection limit for the DSV-IC method with syringe sampling, is 0.074 mg/L.

For ground water applications, the basic methodology would be to pump the ground water from the well and through the sampling flow cell while monitoring the DO concentration, preferably with the pump after the flow cell if the pump is at the surface. For high flow rates, the flow may have to be split so that only a portion flows through the sampling flow cell. The internal volume of field equipment such as pumps with larger bore tubing and the well casing should be taken into consideration. Depending on the well, this washout procedure can be as long as several hours (Puls et al., 1995). The DO concentration should be recorded until the level becomes constant.

H.4. References

Puls, R. W.; Paul, C. J. *Ground Water Monit. Rem.,* **1995,** 15*(1),* 116-123.

Appendix I: Evaluation of the Rapid Re-oxidation of Indigo Carmine after its Reduction with Ti(III) Citrate

I.1. Introduction

After the injection of Ti(III) citrate, there is a significant re-oxidation of IC injection in the first couple hundred seconds. The rate of re-oxidation slows and eventually a constant positive slope is observed. Re-oxidation may be due to residual dissolved O_2 introduced during the injection, or some other oxidant. A deaerated Ti(IV) citrate (oxidized) solution was tested as a sample to evaluate if unwanted oxidants are formed.

I.2. Experimental Details

The preparation of Ti(III) citrate solution is given in section 3.2.1 of this thesis. Ti(III) citrate solution (4 mL, ~10 mM, pH 7) was oxidized to Ti(IV) citrate by stirring overnight in a beaker while opened to air. Upon oxidation, the brown color of Ti(III) citrate disappeared completely.

Next, Ti(IV) citrate solution was transferred into a double-septum vial and purged with N_2 for 2.5 hr. The deaerated Ti(IV) solution was injected onto a solution of H_2-reduced indigo carmine (IC) and buffer in a double-septum vial with the analytical procedure in section 3.2.4 of this thesis. The only difference was that the sample volume was in the range of 5 – 20 μL and was not 0.5 mL. Injections were performed with a glass gas-tight syringe (25 μL, Precision Sampling Corp., Louisiana).

I.3. Oxidation of H_2 Reduced Indigo Carmine upon Addition of Ti(IV) Citrate

Injection of deaerated Ti(IV) solution resulted in significant oxidation of reduced IC. As seen in Figure I.1, A increased a factor of ~2 when the sample volume was increased with a factor of 4. The equivalent, in-cell oxygen concentration of the oxidant was calculated as ~5 mg/L (156 μM). Because the oxidized Ti(IV) citrate solution (4 mL) was deaerated over 2 hr in a double-septum vial, this high level of oxidant could not be due to contamination during sample preparation or injection.

The results suggest that unknown oxidants are formed when Ti(IV) is oxidized. It appears the re-oxidation of IC after Ti(IV) reduction is due to oxidants formed during or following the reduction reaction.

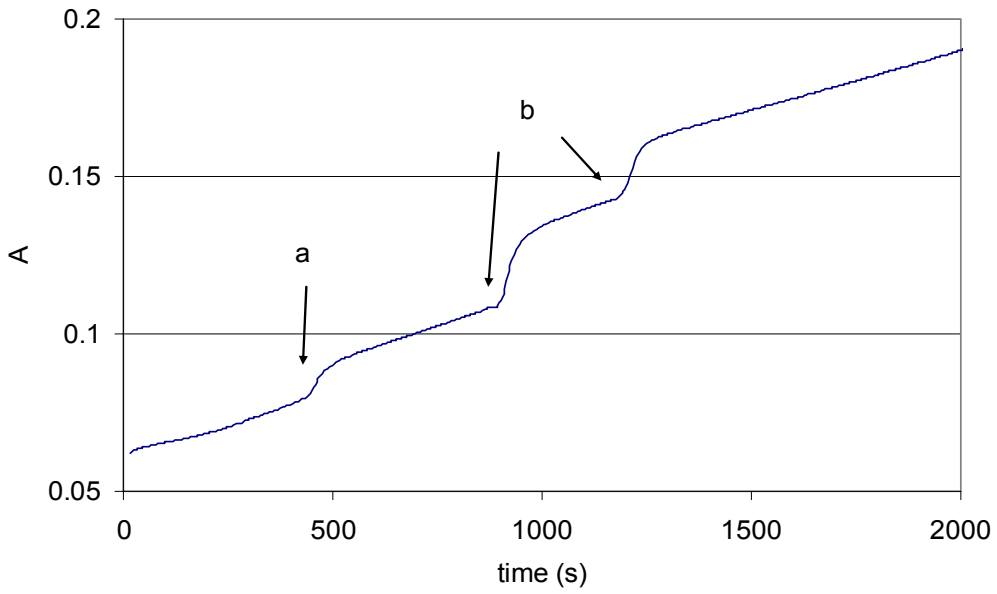

Figure I.1 Oxidation of H_2-reduced indigo carmine upon addition of Ti(IV) citrate. The injection volume was a) 5 μL or b) 20 μL.

Appendix J: Oxidation of H_2-Reduced Rhodazine-D with Air-saturated Water

J.1. Introduction

Rhodazine D was tested as the redox indicator with a double-septum vial for the determination of oxygen. Air-saturated water was injected as a standard solution and used to determine a calibration slope for the comparison of molar absorptivities of indigo carmine and Rhodazine D.

J.2. Experimental Details

Rhodazine D was obtained as a part of Oxygen CHEMets (Calverton, VA) colorimetric test kit (K-7501). Eight Vacuvials were snapped manually and contents (~ 4.5 mL total) were transferred into a double-septum vial (see section 3.2.3.1 of this thesis for a detailed description). Rhodazine D was reduced in this vial with 10 mL/min H_2 (100%, BOC Gases) in the presence of coiled Pt wire (gauge 31, length 10-30 cm) as the catalyst.

A spectrometer vial (another double-septum vial) that contained 2 mL of deionized water was purged for 30 min with N_2. The reduced Rhodazine D (1 mL) was transferred into spectrometer vial. The procedure of reagent and sample delivery was the same as specified in section 3.2.4 of this thesis with the exception of using Rhodazine D instead of indigo carmine.

Injections of air-saturated water (10-20 μL) were performed with a gas-tight syringe (total volume of 25 μL, HP 9301-0633). The absorbance was monitored at

550 nm with a baseline correction at 700 nm. Reported values of are not blank corrected.

J.3. Results and Discussion

Figure J.1 shows the step absorbance increases that occurred with injections air-saturated water into reduced Rhodazine D. A baseline slope (S) of 3 x 10^{-4} ($\pm$1 x 10^{-4}) AU/s was observed. The baseline slope with indigo carmine is typically 1.3 x 10^{-4} ($\pm$0.6 x 10^{-4}) AU/s. The mean A_{ox} values for 10-μL and 20-μL injections (n = 2 each) were 0.10 and 0.21 AU, respectively. From another run (data not shown here), the standard deviation of A_{ox} values for 5 consecutive injections of 10 μL of water was 0.002 AU with an RSD of 2%. The mean A_{ox} value for 10-μL injections with indigo carmine was 0.028 (Table 3.2).

A one-point calibration curve slope was determined based on the injection of 50 μL of water as a standard and an assumed blank absorbance of 0.0 AU. The resulting A_{ox} value of 0.45 (AU) was divided by the concentration of dissolved oxygen (mg/L) to yield a slope of 0.0493 AU/mg/L.

Next, the concentration of dissolved oxygen (DO) was normalized to a larger sample volume (0.5 mL) so that it represents the DO in a 0.5-mL sample that would yield the same number of moles in 50 μL of air-saturated water. This normalized DO value is 0.92 mg/L (29 μM) and the normalized calibration slope for Rhodazine D is 0.493 (AU/mg/L). This slope is 3 times the slope that was obtained with indigo carmine (0.161 AU/mg/L) with the same pathlength (from Table3.4). Thus, the

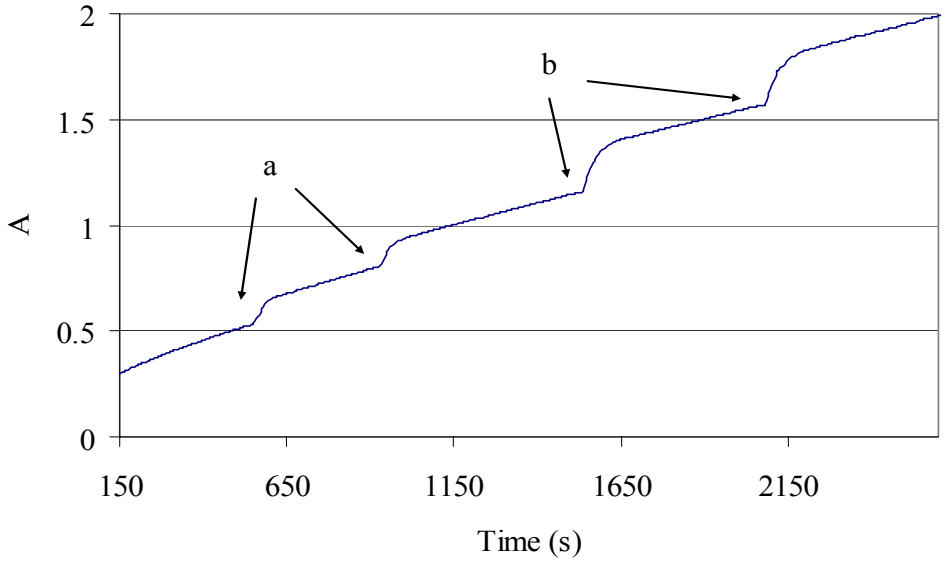

Figure J.1 Oxidation of H_2 -reduced Rhodazine-D with air-saturated water injections. The injection volume was a) 10 μL or b) 20 μL.

molar absorptivity of Rhodazine D is estimated to be ~3 times higher (~7.1 x 10^4 AU cm/M at 550 nm).

Appendix K: Details of the Coupling of Optical Fibers and the Liquid Core Waveguide

K.1. Coupling Tee for Version 1 of the LCW Spectrometer

The LCW cell and tee connectors were contained in a box made by Ocean Optics, Inc (model LPC-1 long path cell) with 1 m of Teflon AF 2400 tubing with an ID of 550 μm. The tee connectors have three ¼-28 female ports. There are two of these identical tees on each end of the LCW tubing. The details of the tee are given in Figure K.1. The LCW is flared at the end where it does contact the ferrule of the ¼-28 fitting.

The 200-μm OD bare fiber optic was pushed inside the LCW and is held in place with an o-ring that is at the bottom of the ferrule. The free end of the fiber optic was terminated with a SMA connector.

K.2. Coupling Tee for Version 2 of the LCW Spectrometer

For version 2 of the spectrometer, the LCW cell was placed in a Plexiglas housing constructed in-house that consisted of two sections that were screwed together. The larger section of the housing has the cavity for the LCW tubing and is open only at the front. The other section is attached to the open side of the first section with O-ring sealing after the LWC is installed inside. This section was machined to have two internal tee connectors with two ¼-28 ports and one SMA 905 port and enabled the coupling of the light source and the solutions in and out of the LCW tubing.

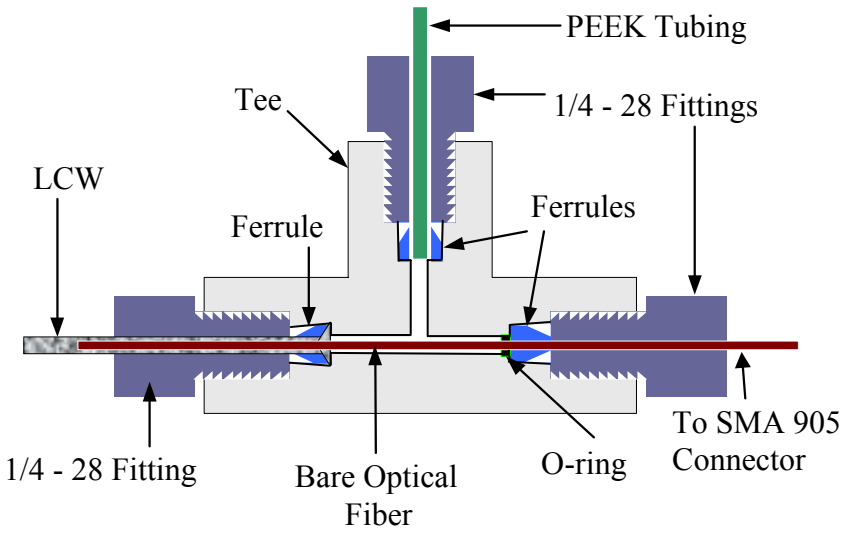

Figure K.1 Coupling tee for version 1 of the LCW spectrometer.

The detail of the internal tees is given Figure K.2. The ends of the LCW is not flared and held in place with an o-ring that is at the bottom of the ferrule. The 200-μm OD bare optical fiber was pushed inside the LCW and is permanently fixed to two SMA connectors that have a male SMA coupler. First the bare fiber was pushed through both of the SMA connectors. Then 60-s epoxy system (Versa Chem) was mixed and voids of the SMA connectors were filled with epoxy glue. The fiber was moved back and forth to spread the glue evenly inside the connectors. After the epoxy was cured completely (typically more than an hour), both ends of the optical fiber was cut and polished with aluminum oxide lapping film sheets (Mark V. Laboratory, Inc.). As seen in Figure K.2, one of the ends of the fiber was cut and polished such that it was terminated with the SMA connector. The other end of the fiber was extended 3.5 cm past the end of the SMA connector and into the LCW.

K.3. Coupling Tee for Version 3 of the LCW Spectrometer

The bare optical fibers (600-μm OD) connected to the tee-bars with ¼-28 fittings (P-201x with P-200x, Upchurch Sci.) in version 3 of the spectrometer. Figure K.3 shows the detail of one side of the tee-bar. O-rings were placed at the seat of the ports for the bare optical fibers and LCW to provide a liquid-tight connection and a good optical alignment. Each end of the LCW tubing was secured to another ¼ -28 port of the tee with a male ¼ -28 connector (P-668, Upchurch Sci.) and included an o-ring at the bottom of the port. The LCW was pushed through the hole of the connector and the o-ring and then the connector was screwed to the tee. These

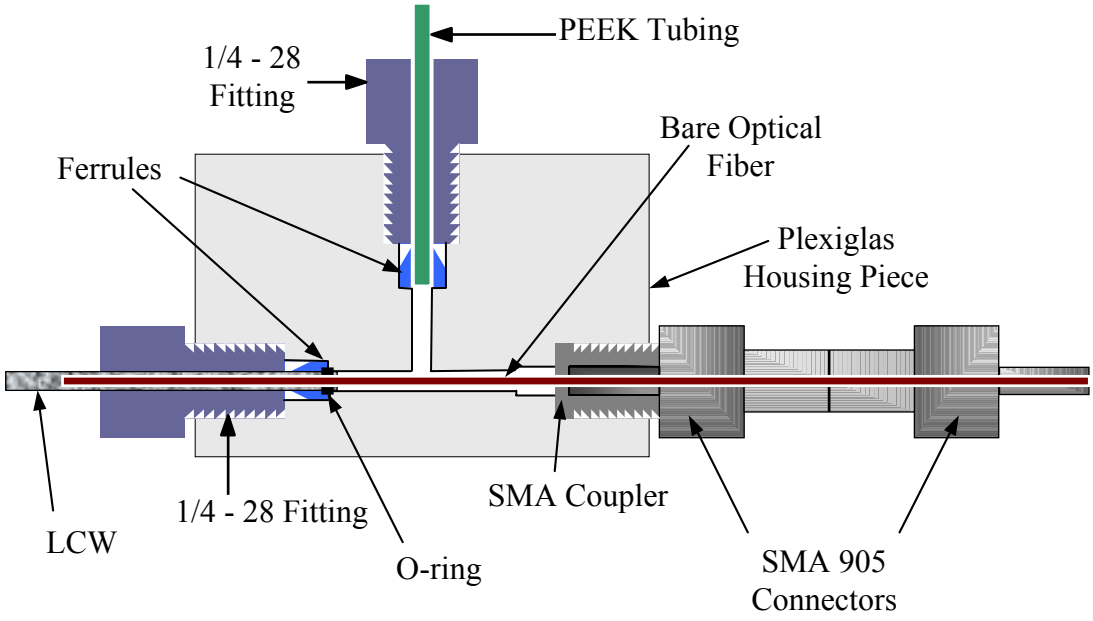

Figure K.2 Coupling tee for version 2 of the LCW spectrometer.

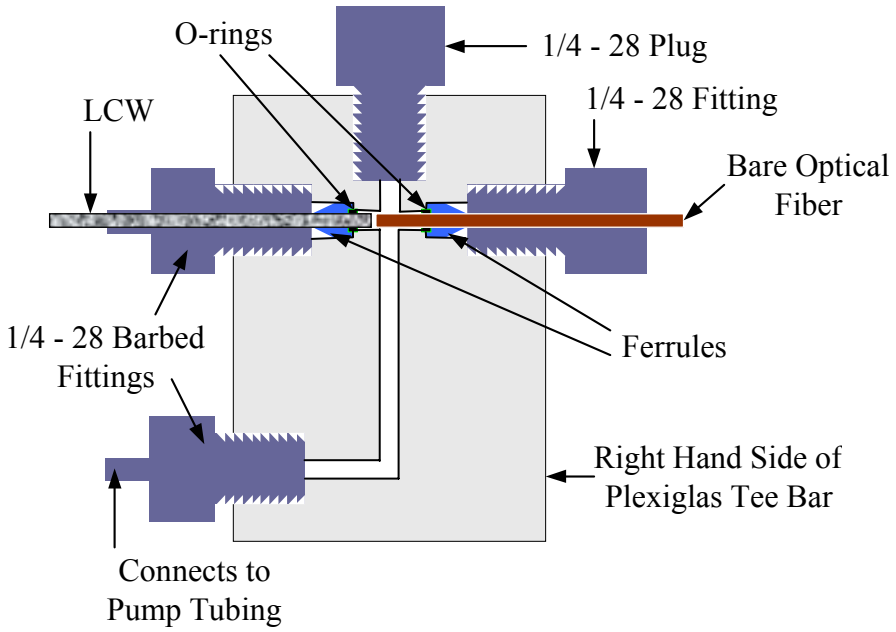

Figure K.3 Coupling tee for version 3 of the LCW spectrometer.

rings (ORV-001-10, Small Parts, Inc.) have dimensions of 1/32” ID, 3/32” OD, and 1/32” thickness. The bare optical fibers are butted as close as possible to the LCW for an efficient light coupling.